PROTECTIVE STRATEGIES AGAINST ACETAMINOPHEN INDUCED HEPATOTOXICITY

BY

Chieko Saito

Submitted to the Graduate Degree Program in Pharmacology, Toxicology, and Therapeutics and the Graduate Faculty of the University of Kansas in partial fulfillment of the requirements for the degree of Doctor of Philosophy

Dissertation Committee

Hartmut Jaeschke, Ph.D. (Chair)

Curtis D. Klaassen, Ph.D.

Bryan L. Copple, Ph.D.

John D. Robertson, Ph.D.

John G. Wood, Ph.D.

Date defended: Janurary 19, 2010

The dissertation committee for Chieko Saito certifies that this is the approved version of the following dissertation:

PROTECTIVE STRATEGIES AGAINST ACETAMINOPHEN INDUCED HEPATOTOXICITY

Dissertation Committee

Hartmut Jaeschke, Ph.D. (Chair)

Curtis D. Klaassen, Ph.D.

Bryan L. Copple, Ph.D.

John D. Robertson, Ph.D.

John G. Wood, Ph.D.

Date approved:

ACKNOWLEDGEMENTS

I would like to thank my mentor, Dr. Hartmut Jaeschke, for his guidance during my graduate training. I would also like to thank the members of my lab, Dr. Mary Lynn Bajt, Dr. Anup Ramachandran, Dr. Min Yang, Huimin Yan, Margitta Lebofsky, Clarence Williams, Mitch McGill, Dr. Ji-Young Hong, Dr. Tadashi Hasegawa, Dr. Jayanthika Wijeweera, and Cathleen Cover for teaching me experimental techniques for correcting my English, and being good partners for discussion. I would like to acknowledge the members of my dissertation committee Dr. Curtis Klaassen, Dr. Bryan Copple, Dr. John Robertson, and Dr. John Wood. I am grateful to you for all your contributions. I would like to thank Dr. Antonio Artigues, Dr. Maria Villar, and Dr. Partha Krishnamurthy at the University of Kansas Medical Center for giving me good advice and helping me with my experiments. I would like to acknowlege Dr. Claudia Zwingmann at the Centre hospitalier de l'Universite de Montreal for helping me with NMR experiments. I would like to thank all other Pharm/Tox faculty members and office staff for their support. I would like to show my gratitude to my colleagues at the University of Kansas Medical Center: Thank you, Noriko Esterly, Kaori Nakamoto, Dr. Masayuki Fukui, Dr. Jennifer (Yukun) Zhang, Dr. Baljit Kaur, Yi Weaver, Dr. Benjamin Weaver, Dr. Mary Shawgo, Shary Shelton, Dr. Chunshan Gui, Emily Zhou, Dr. Bo Kong, Dr. Manimaran Rengasamy, Miyuki Shimizu, and Mariko Nishibe for being good friends and helping me a lot.

I would like to express thanks to faculties and friends at the University of Arizona: Dr. Ronald Lynch, Dr. Heddwen Brooks, Dr. Nathan Cherrington, Dr. Andrew Lickteig, Dr. Adonna Rometo, Gabrielle Halko, David Halko, and Lillie Hansen who encouraged me and with whom I had much fun.

Last, but not least, I appreciate my family for their support.

ABSTRACT

Acetaminophen (APAP) is a widely used analgesic, which is safe at therapeutic levels. APAP is mainly conjugated with glucuronic acid and sulfate to form water-soluble, nontoxic metabolites. Only a small portion of APAP is metabolized by P-450 isoenzymes, thereby forming the reactive metabolite *N*-acetyl-*p*-benzoquinone imine (NAPQI). NAPQI can react with sulfhydryl groups such as GSH. After APAP overdose, hepatic GSH is dramatically reduced, and NAPQI is able to bind to cellular proteins including mitochondrial proteins. This protein binding results in mitochondrial dysfunction and reactive oxygen species formation. This chain of events eventually leads to necrotic cell death of hepatocytes. My goal was to investigate the mechanisms and signaling pathways of APAP-induced cell necrosis in the liver, and to identify therapeutic approaches to prevent liver failure. Three protective strategies were investigated in detail:

1) Glutathione (GSH) and *N*-acetylcysteine (NAC)

2) Metallothionein (MT)

3) C-jun N-terminal kinase (JNK) inhibitor

1) Both in humans and in experimental animals, NAC is used as an antidote against APAP-induced liver injury. The doses of NAC that are being used clinically and experimentally are higher than needed for re-synthesis of hepatic GSH levels. In fact, our laboratory demonstrated that lower doses of GSH are highly effective in protecting against APAP toxicity. Therefore, I

investigated whether there is a difference between the efficacy of NAC and GSH in protecting against APAP hepatotoxicity. Our data indicate that the amino acids supplied with the delayed treatment of the same dose of GSH or NAC are used for the re-synthesis of hepatic glutathione at similar levels, which protect against APAP-induced reactive oxygen species and peroxynitrite in the mitochondria. However, excess amino acids derived from GSH also serve as energy substrates for the Krebs cycle, which results in better protection against APAP hepatotoxicity than NAC treatment. Thus, the optimal protection by delayed GSH or NAC treatment involves the combination of two mechanisms, which are the accelerated recovery of mitochondrial GSH levels and the support of the mitochondrial bioenergetics.

2) Metallothionein (MT) expression attenuates APAP-induced liver injury; however, the mechanism of this protection remains incompletely understood. To address this issue, mice were treated with $ZnCl_2$ for three days to induce MT. Twenty-four hours after the last dose of zinc, the animals received 300 mg/kg APAP. We found that the protective effect of MT *in vivo* was not due to the direct scavenging of reactive oxygen species and peroxynitrite. In addition, zinc treatment had no effect on the early GSH depletion kinetics after APAP administration, which is an indicator of the metabolic activation of APAP to its reactive metabolite NAPQI. MT was able to effectively trap NAPQI by covalent binding. We conclude that MT scavenges some of the excess NAPQI after GSH depletion and prevents covalent binding to cellular proteins,

which is the trigger for the propagation of the cell injury mechanisms through mitochondrial dysfunction and nuclear DNA damage.

3) C-jun N-terminal kinase (JNK) has been suggested to contribute to APAP-induced liver injury. The postulated mechanism of JNK involvement was the promotion of mitochondrial Bax translocation, which triggers mitochondrial outer membrane pore formation and results in the release of intermembrane proteins such as apoptosis inducing factor (AIF) and endonuclease G (EndoG). However, it was reported that Bax-deficient mice were only temporally protected against APAP-induced liver injury (Bajt *et al.*, 2008). In contrast, the protective effect of a JNK inhibitor was observed consistently up to 24 h. Therefore, additional mechanisms of injury involving JNK activation need to be considered. To address this issue, I treated mice with the JNK inhibitor, SP600125 1h before APAP (600 mg/kg). SP600125 reduced peroxynitrite formation; however, it did not have any significant effect on the level of nitrate and nitrite in plasma. Moreover, L-*N*-(1-iminoethyl)lysine (L-Nil), a specific iNOS inhibitor, attenuated neither plasma nitrate and nitrite levels nor hepatic injury after APAP injection. Taken together, SP600125 reduced peroxynitrite formation by decreasing superoxide formation. In summary, my investigation demonstrated that JNK is a critical factor for Bax translocation, which causes mitochondria outer membrane pore formation. In addition, JNK accelerates peroxynitrite generation via induction of superoxide formation.

In conclusion, I demonstrated the efficacy of three protective strategies against APAP-induced hepatotoxicity: Mechanism of protection A: Preventing NAPQI binding to proteins (e.g., induction of MT gene expression); Mechanism of protection B: Scavenging (GSH, NAC) or reducing (JNK inhibition) the formation of reactive oxygen species; and Mechanism of protection C: Supplying mitochondrial energy substrates (GSH, NAC).

TABLE OF CONTENTS

ABBREVIATIONS

℃	Celsius
AIF	Apoptosis inducing factor
ALT	Alanine aminotransferase
AMAP	3'-hydroxyacetanilide
ANT	Adenine nucleotide translocator
Anti-Fas	Agonistic anti-Fas antibody
APAP	Acetaminophen
ASC	Apoptosis-associated speck-like protein containing caspase recruitment domain
Bad	Bcl-2 associated death promoter
Bak	Bcl-2 antagonist/killer 1
Bax	Bcl-2 associated X protein
Bcl-2	B cell lymphoma 2
Bcl-x_L	Bcl-2 like 1
BH3	Bcl-2 homology 3
Bid	BH3 interacting domain
Bik	Bcl-2 interacting killer
Bim	Bcl-2 interacting mediator of cell death
Bok	Bcl-2 related ovarian killer
CAD	Caspse activated DNase
CAMs	Cellular adhesion molecules
CARD	Caspase recruitment domains
CK	Creatine kinase
COX	Cyclooxygenase
CsA	Cyclosporin A
CyD	Cyclophilin D
DMSO	Dimethyl sulfoxide
DNase	Deoxyribonuclease
DTNB	Dithionitrobenzoic acid
ER	Endoplasmic reticulum
Endo G	Endonuclease G
$GdCl_3$	Gadolinium chloride
GPx	Glutathione peroxidase
GSH	Glutathione
h	Hour
HK	Hexokinase
HOCl	Hypochlorous acid
ICAM-1	Intercellular cell adhesion molecules

IFN-γ	Interferon-γ
IgG	Immunoglobulin G
IL-	Interleukins
IL-1 R	IL-1 receptor
IL-1RA	IL-1 receptor antagonist
IM	Inner mitochondrial membrane
JNK	c-Jun N-terminal protein kinase
kDa	Kilodaltons
KO mice	Knockout mice
L-Nil	L-N^6-(1-iminoethyl)-lysine
LPO	Lipid peroxidation
LPS	Lipopolysaccharide
M	Molar
Mcl-1	Myeloid cell leukemia-1
Min	Minute
mL	milliliter
MOMP	Mitochondrial outer membrane permeabilization
MPO	Myeloperoxidase
MPT	Mitochondrial membrane permeability transition
NAC	*N*-acetylcysteine
Nalp3	NACHT, LRR, and pyrin domain-containing protein 3
NAPQI	*N*-acetyl-p-benzoquinone imine
NK	Natural killer
NKT	Natural killer with T-cell receptors
NO	Nitric oxide
OM	Outer mitochondrial membrane
p53	Protein 53
PBR	Peripheral-type benzodiazepine receptor
PC	Pyruvate carboxylase
PDH	Pyruvate dehydrogenase
Prx	Peroxiredoxin
Puma	p53-upregulated modulator of apoptosis
ROS	Reactive oxygen species
Smac	Second mitochondria-derived activator of caspases
SODs	Superoxide dismutases
tBid	Truncated Bid
TLR	Toll-like receptor
TNF R	Tumor necrosis factor receptor
TNF-Rp55	TNF receptor with a molecular weight of 55 kDa
TNF-α	Tumor necrosis factor α
TOM	Translocase of the outer mitochondrial membrane
TUNEL	Terminal deoxynucleotidyl transferase-mediated dUTP nick-ending labeling

U	Unit
VCAM-1	Vascular cell adhesion molecule
VDAC	Voltage-dependent anion chennel
WT	Wild type
ZVAD-FMK	Benzyloxycarbonyl-Val-Ala-Asp-fluoromethylketone
μg	Microgram
μl	Microliter

CHAPTER 1: GENERAL INTRODUCTION

1) APAP-induced cell death: apoptosis versus oncotic necrosis

It has been discussed whether APAP overdose induces apoptotic or necrotic cell death. Apoptosis and necrosis are defined by characteristic morphological changes of the cell (table 1). In apoptotic cell death, a cell undergoes shrinkage, shows chromatin condensation in the nucleus, and eventually breaks down into apoptotic bodies. In contrast, oncotic necrosis is characterized by cell swelling, chromatin flocculation, and absence of vesicle formation. It has been reported that apoptosis has a critical role in APAP-induced liver failure (Ferret *et al.*, 2001; Zhang *et al.*, 2000b). It was observed that after APAP administration, the pro-apoptotic Bcl-2 family member Bax translocated to mitochondria (Bajt *et al.*, 2008), mitochondrial cytochrome c was released (Bajt *et al.*, 2008), and DNA fragments could be detected on an agarose gel (Cover *et al.*, 2005b), all of which occur in apoptotic cell signaling. However, based on morphological evidence, APAP appears to induce oncotic necrosis in the centrilobular area *in vivo* (Gujral *et al.*, 2002). In addition, none of the above mentioned indicators are specific for apoptosis and have been shown to be positive in oncotic necrosis (Bajt *et al.*, 2008).

Apoptosis	Oncotic Necrosis
Membrane blebbing, but no loss of integrity	Loss of membrane integrity
Aggregating of chromatin at the nuclear membrane	Flocculation of chromatin
Cell shrinkage	Swelling of the cell and lysis
Formation of membrane bound vesicles (apoptotic bodies)	No vesicle formation, complete lysis
No disintegration of organelles: organelles remain intact	Disintegration (swelling) of cell organelles

Table 1-1

Morphological characteristics for apoptosis and oncotic necrosis

2) The mechanism of APAP-induced hepatotoxicity

a) APAP metabolism and protein binding

APAP is eliminated mainly as nontoxic conjugates with glucuronic acid via glucuronyltransferase (Nelson, 1990, 1995) and excreted into bile through the canalicular multidrug resistance-associated protein 2 (Mrp2, *Abcc2*) or into blood through Mrp3 (*Abcc3*) (Xiong *et al.*, 2000). APAP is also conjugated with sulfate through sulfotransferases and is eliminated into bile mainly via Mrp2, and to lesser degree via breast cancer resist protein (BCRP, ABCG2) (Zamek-Gliszczynski *et al.*, 2005). A small part of the APAP dose is metabolized to a reactive metabolite NAPQI by CYP2E1, CYP1A2, and CYP3A4 in liver microsomes.

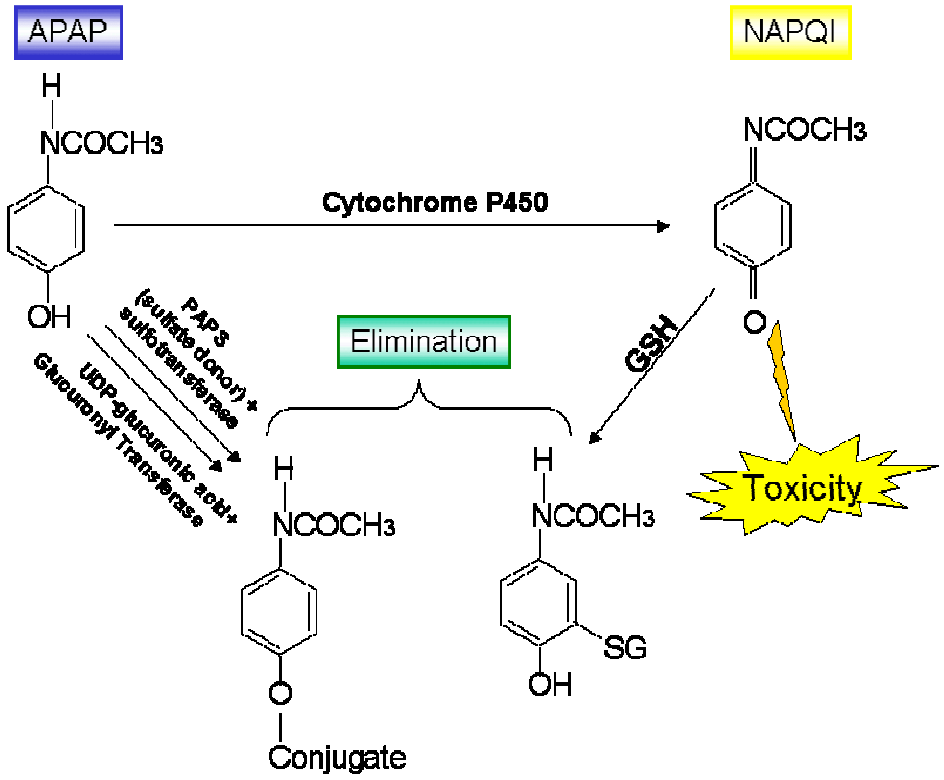

Figure 1.1

Scheme for APAP overdose metabolism. Modified from (James *et al.*, 2003b).

It has been shown that NAPQI reacts very rapidly with GSH (k_1 = 3.2 X 10^4 M^{-1} s^{-1} at pH 7.0) (Coles *et al.*, 1988). Therefore, after NAPQI formation following APAP overdose, the GSH concentration becomes very low in the centrilobular cells (Figure 1.1). Following depletion of GSH, remaining NAPQI reacts with cysteinyl sulfhydryl groups on proteins to produce the corresponding 3-(cystein-S-yl)acetaminophen adduct. No other sites of binding to protein have been identified *in vivo* (Roberts *et al.*, 1987). It has

been demonstrated by mass spectrometry that approximately 40 proteins can react with APAP metabolites (Qiu *et al.*, 1998). The covalent modification of cellular proteins was originally thought to be the cause of necrotic cell death, which is supported by the fact that prevention of covalent binding can reduce cell death (Jollow *et al.*, 1973; Mitchell *et al.*, 1973a; Mitchell *et al.*, 1973b). However, it was reported that total binding to cellular proteins may be less relevant than selective modifications of specific critical targets. The regioisomer of APAP, 3'-hydroxyacetanilide (AMAP) can cause GSH depletion and a similar degree of covalent binding to cellular proteins as APAP; however, AMAP does not cause liver injury (Tirmenstein and Nelson, 1989). Furthermore, APAP administration depleted mitochondrial GSH to a greater extent than AMAP. Moreover, APAP metabolites bound more extensively to mitochondrial proteins than AMAP (Tirmenstein and Nelson, 1989). This indicated that mitochondria are a target for covalent binding of NAPQI, which is a critical event in APAP-induced hepatotoxicity (Gupta *et al.*, 1997; Pumford *et al.*, 1990; Tirmenstein and Nelson, 1989).

b) Mitochondria respiration

Succinate dehydrogenase (associated with respiratory complex II) is very sensitive to NAPQI because it contains a number of cysteine-rich sulfur clusters. In addition, NAPQI inhibits NADH dehydrogenase (complex I) to a lesser extent. However, NAPQI does not have any effect on the activities of either ubiquinol-cytochrome c oxidoreductase (complex III) or cytochrome

oxidase (complex IV) in hepatocytes. (Burcham and Harman, 1991). Moreover, exposure of both rat and mouse liver mitochondria to NAPQI has been shown to result in the irreversible inhibition of mitochondrial respiration (Esterline *et al.*, 1989; Ramsay *et al.*, 1989). Taken together, these data suggest that NAPQI binds to mitochondrial respiration chain complexes and disrupts energy homeostasis, which contributes to APAP-induced hepatotoxicity.

c) Oxidative stress

Inhibition of mitochondrial respiration by NAPQI causes accumulation of reactive oxygen species (ROS). ROS are generated by one electron reduction of molecular oxygen ($^3O_2$). During the spontaneous dismutation of superoxide (O^-_2), singlet oxygen ($^1O_2$) plus hydrogen peroxide are formed.

Superoxide reacts with Cu^{2+}/Zn^{2+} - or Mn^{3+} -superoxide dismutase (SOD) in the cytosol and nucleus or in the mitochondria, respectively (Slot *et al.*, 1986), which produced molecular oxygen ($^3O_2$) and hydrogen peroxide (H_2O_2). H_2O_2 is more stable than O^-_2 and quickly diffuses across membranes. In the presence of ferrous iron (Fe^{2+}), H_2O_2 can be reduced to the highly reactive $OH^{\bullet}$ radical (Fenton reaction), which initiates lipid peroxidation (LPO).

Uchiyama et al demonstrated that ROS induce the release of chelatable iron from lysosomes. The iron is taken up by mitochondria via the calcium uniporter (Uchiyama *et al.*, 2008). Wendel and coworkers showed that APAP metabolism triggers massive LPO, which corresponded with hepatotoxicity in

vitamin E-dificient mice (Wendel and Feuerstein, 1981; Wendel *et al.*, 1979). However, mice fed a normal diet showed only minor LPO (Knight *et al.*, 2003). Moreover, enhancing levels of α-tocopheryl acetate in the liver by either repeated injections of α-tocopherol or by feeding high d-α-tocopheryl acetate diet did not have any effect on APAP-induced liver injury (Knight *et al.*, 2003). Taken together, LPO may not be involved in APAP-induced liver toxicity.

However, if nitric oxide (NO) is present, O^{-}_{2} reacts with NO and forms peroxynitrite ($ONOO^{-}$), which causes nitration of proteins (Belizario *et al.*, 2007; James *et al.*, 2003a). It has been reported that peroxynitirite formation, which can be detected by immunohistochemical staining against anti-nitrotyrosine protein adducts, occurrs in the mitochondria after APAP injection (Cover *et al.*, 2005b). The rate of peroxynitrite formation depends on the concentrations of both NO and superoxide (Koppenol, 1998; Squadrito and Pryor, 1998). The source of NO formation remains unclear. Hepatocytes, stellate cells and Kupffer cells express inducible nitric oxide synthase (iNOS) and endothelial cells constitutively express eNOS (Muriel, 2000). It was reported that APAP-induced liver toxicity was significantly lower in eNOS knockout (KO) and iNOS KO mice compared to wild type (WT) animals. In addition, plasma nitrate and nitrite levels were higher in WT animals than in both KO animals (Salhanick *et al.*, 2006). Although Michael et al. showed that serum ALT levels were lower in iNOS knockout mice, which is consistent with the previous data, there was no significant difference in tissue injury as

assessed by histology (Michael *et al.*, 2001). In terms of NOS inhibitors, a selective iNOS inhibitor, L-N^6-(1-iminoethyl)-lysine (L-Nil) did protect against APAP-induced liver injury; however, a nonselective NOS inhibitor, N^G-nitro-L-arginine methyl ester (L-NAME) did not (Ito *et al.*, 2004). Others did not find protection with various iNOS inhibitors (Hinson *et al.*, 2002). Therefore the source of NO during APAP-induced liver injury needs further investigation.

Mimitochondrial DNA (mtDNA) may be a target of ROS due to close proximity to the electron transport chain and a lack of protective histones (Ott *et al.*, 2007a). mtDNA is essential for electron transport and ATP generation by oxidative phosphorylation. Therefore, mtDNA damage can cause respiratory dysfunction (Anderson *et al.*, 1981). It was shown that mitochondrial oxidant stress can cause depletion of mitochondrial DNA (mtDNA) in several *in vivo* models, such as alcohol binge drinking (Mansouri *et al.*, 1999) and tacrine hepatotoxicity (Mansouri *et al.*, 2003). In the APAP model, there is a significant reduction of mtDNA between 3 and 12h after APAP administration. However, scavenging of peroxynitrite with GSH partially prevented the loss of mDNA, suggesting that peroxynitrite was, at least in part, responsible for the mtDNA loss (Cover *et al.*, 2005b).

d) Antioxidant defense

There are many antioxidant defense systems to handle both the continuous formation of reactive oxygen and reactive nitrogen species in physiological

and pathophysiological conditions. For example, superoxide is removed by superoxide dismutases (SODs). Cu^{2+}/Zn^{2+}-SOD (SOD1) is mainly located in the cytosol and nuclear matrix, and Mn^{3+}-SOD (SOD2) is present in the mitochondria (Slot *et al.*, 1986). The high intracellular SOD levels (approx. 10 μM) keep the steady-state levels of superoxide in the range of 1 to 10 pM (Cadenas and Davies, 2000; Koppenol, 1998). What is the advantage of high SOD expression when superoxide alone is not very toxic? The main reason for the importance of SOD might be to limit peroxynitrite generation (Koppenol, 1998; Squadrito and Pryor, 1998). The rate of depletion for superoxide is 20000/sec with SOD (approx. 10 μM), but only 200/ sec with NO (approx. 10 nM under physiological conditions) (Squadrito and Pryor, 1998). Therefore, SOD prevents peroxynitrite formation under physiological conditions.

Hydrogen peroxide formed by SOD is detoxified by catalase and glutathione peroxidase (GPx). Most of the cellular catalase is located in peroxisomes, and the main function of the enzyme is to metabolize hydrogen peroxide generated by oxidases in the peroxisomes. However, it was reported that catalase may be constitutively expressed in rodent liver mitochondria (Salvi *et al.*, 2007). Further, the 30% reduction of catalase activity has been demonstrated after APAP overdose (Lores Arnaiz *et al.*, 1995), and this might be involved in APAP-induced hepatotoxicity. These results suggested that catalase could be a key antioxidant enzyme during APAP hepatotoxicity. However, whether this small reduction in catalase activity has any

pathophysiological relevance remains unclear because massive catalase induction did not reduce APAP hepatotoxicity (Chen *et al.*, 2002). Another antioxidant enzyme, glutathione peroxidase (GPx-1) is located in the cytosol (75%) and mitochondria (25%), and it was reported that cellular GPx could also reduce peroxynitrite *in vitro* (Sies *et al.*, 1997). In spite of this, APAP-induced peroxynitrite-dependent injury was not increased in GPx-1 knockout mice (Knight *et al.*, 2002). It is known that cellular GPx-1 can reduce peroxides, including hydrogen peroxide and organic peroxides (Brigelius-Flohe, 1999), and this requires GSH as a cofactor, but has a low specificity for peroxide. During the reduction of the peroxide, GSH is oxidized to glutathione disulfide (GSSG). Normally GSSG is reduced back to GSH by glutathione reducatase and NADPH (>95%) or excreted into bile and plasma from hepatocytes (<5%) (Lauterburg *et al.*, 1984). However, extreme oxidative stress can overwhelm these processes leading to accumulation of GSSG, because the glutathione reductase is the rate-limiting step of this cycle. In addition, GSSG can not be exported from mitochondria although mitochondria take up and release GSH (Olafsdottir and Reed, 1988).

GSH is the most important water-soluble antioxidant and it is used as a cofactor for GPxs and GSTs. Other low-molecular-weight antioxidants include ascorbate (vitamin C), α-tocopherol (vitamin E). GSH is not only present in the cytosol, but also in mitochondria, which contain 15% of total cellular GSH (Fernandez-Checa and Kaplowitz, 2005). GSH is a tripeptide of

glutamic acid, glycine and cysteine, which is formed in the cytosol by two ATP-dependent enzymes, γ-glutamylcysteine synthetase and GSH synthetase (Figure 1.2). Because of its γ-glutamyl bond, GSH can be degraded only by γ-glutamyltranspeptidase, which is located on the surface of epithelial cells in the kidney, lung, and intestine and in the biliary tract. It was previously shown that the half-life of intravenously injected GSH in plasma is less than 5 min in starved animals (Wendel and Jaeschke, 1982). Therefore, injected GSH is degraded in the kidney and the amino acids are re-absorbed and then taken up by hepatocytes for GSH synthesis.

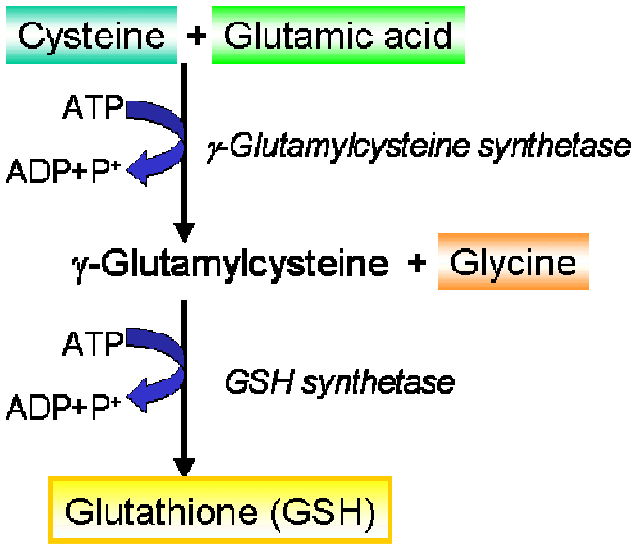

Figure 1.2

GSH synthesis.

e) Innate immunity

The innate immune response is the first line of defense against microbes and toxins (Janeway and Medzhitov, 2002). Kupffer cells, the resident macrophages in the liver, are highly phagocytic and are able to remove microorganisms. In addition, they can produce inflammatory mediators leading to invasion of inflammatory cells, such as neutrophils, monocytes, T and B lymphocytes as well as natural killer (NK) cells in the liver. Neutrophils accumulate within the hepatic microvasculature before they extravasate into liver parenchyma (Ramaiah and Jaeschke, 2007). Many inflammatory mediators, such as tumor necrosis factor α (TNF-α), interleukin-1 (IL-1), CXC chemokine and platelet activating factor (PAF) can cause neutrophil accumulation within the hepatic microvasculature (Jaeschke and Hasegawa, 2006). Chemokines represent a large family of chemotactic peptides that can be produced by hepatocytes, sinusoidal endothelium, cholangiocytes, Kupffer cells and stellate cells (Ramaiah and Jaeschke, 2007). The exposure to inflammatory mediators triggers mobilization of secretory granules and increased adhesion molecule expression on neutrophils, resulting in priming and activation of cells. In general, neutrophil activation/accumulation within sinusoids and postsinusoidal venules typically does not cause liver damage (Ramaiah and Jaeschke, 2007).

Extravasation into the parenchyma is required to fully activate neutrophils, which can generate reactive oxygen species and cause tissue

damage (Chosay *et al.*, 1997). Normally, the adhesion molecules β2 integrin/ intracellular cell adhesion molecules (ICAM)-1 and β1 integrin/vascular cell adhesion molecule (VCAM)-1 interactions are involved in the migration of neutrophils into parenchyma, which is a prerequisite of neutrophil-mediated injury (Chosay *et al.*, 1997; Essani *et al.*, 1997; Essani *et al.*, 1995). However, during extensive endothelial damage resulting from ischemia-reperfusion, neutrophils can extravasate directly into the parenchyma without cellular adhesion molecules (CAMs) (Farhood *et al.*, 1995). Independent of the condition of the endothelial cell barrier, signaling from parenchymal cells or extravasated neutrophils is required for neutrophil migration. It was reported that lipid peroxidation products including lipid aldehydes are potent chemotactic factors for neutrophils (Jaeschke, 2000). In addition, CXC chemokines are chemotactic factors (Okaya and Lentsch, 2003), which have been shown to contribute to the promotion of neutrophilic hepatitis during ischemia-reperfusion injury (Colletti *et al.*, 1996; Lentsch *et al.*, 1998). However, the massive amounts of CXC chemokines generated in parenchymal cells during endotoxemia do not cause neutrophil extravasation when endotoxin is administered alone (Dorman *et al.*, 2005). Moreover, CXC chemokines, MIP-2 and KC, in circulation are much less effective in recruiting neutrophils into the hepatic vasculature and activation of neutrophils *in vivo*, compared to cytokines or complement (Bajt *et al.*, 2001). Therefore, further

studies are necessary to investigate the mechanism of neutrophils activation and extravasation.

Once extravasated, the neutrophils will adhere to the target, i.e. parenchymal cells. Upon activation, neutrophils generate superoxide via NADPH oxidase which is a multicomponent enzyme system that assembles at the cell membrane (El-Benna *et al.*, 2005). Superoxide dismutases converts superoxide to hydrogen peroxide, which can be used by neutrophil-derived myeloperoxidase (MPO) to generate a potent oxidant, hypochlorous acid (HOCl) (El-Benna *et al.*, 2005). Hypochlorous acid also can react with amino groups forming toxic chloramines (Bilzer and Lauterburg, 1991). In addition to ROS, neutrophil-derived serine proteases are known to contribute to hepatocyte damage (Jaeschke and Smith, 1997a, b) (Figure 1.3).

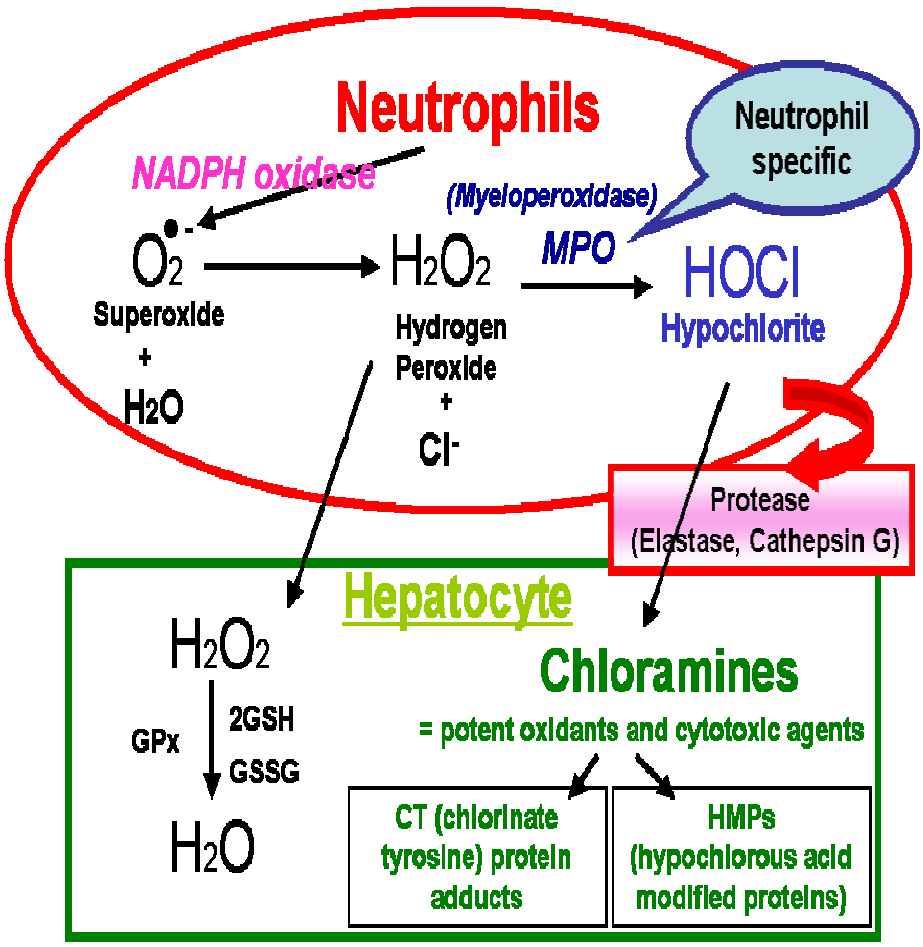

Figure 1.3

Proposed mechanisms for neutrophil-mediated liver pathology. Modified from (Jaeschke, 2006)

The involvement of innate immunity in APAP-induced hepatotoxicity is controversial. It was reported that APAP treatment induced Kupffer cell activation (Laskin and Pilaro, 1986) and migration of neutrophils into the liver (Lawson *et al.*, 2000). Kupffer cells have been implicated in the mechanism of hepatocellular injury and peroxynitrite formation after APAP overdose (Laskin *et al.*, 1995; Michael *et al.*, 1999). Mice treated with APAP plus gadolinium chloride ($GdCl_3$), a macrophage inhibitor, decreased hepatotoxicity as evidenced by lower ALT levels (Michael *et al.*, 1999). In contrast, mice treated with APAP plus liposome-entrapped clodronate, an effective Kupffer cell-depleting agent, increases APAP-induced hepatotoxicity (Ju *et al.*, 2002). Ju et al. showed that the difference between gadolinium chloride treated mice and liposome-entrapped clodronate is IL-10 level in the liver. IL-10, which is produced by macrophages is completely inhibited by the Kupffer cell-depleting agent, liposome-entrapped clodronate treated group (Ju *et al.*, 2002). These results are supported by the fact that IL-10 KO mice are more susceptible after APAP administration via induction of iNOS mRNA expression. Furthermore, serum nitrite-nitrate levels were significantly elevated in IL-10 KO mice after APAP administration (Bourdi *et al.*, 2002). Moreover, it was reported that peroxynitrite formation was increased in sinusoidal endothelial cells during the early phase after APAP administration (Knight *et al.*, 2001). However, $GdCl_3$ treatment had no effect on peroxynitrite

formation in vascular endothelial cells or parenchymal cells (Liu *et al.*, 1995). This suggests an intracellular oxidant stress and peroxynitrite formation in sinusoidal endothelial cells rather than a Kupffer cell-derived oxidant stress. Furthermore, the most active Kupffer cells are located in the periportal area (Bautista *et al.*, 1990; Jaeschke *et al.*, 1991) and activation of these cells in ischemia-reperfusion model results in a periportal to midzonal injury (Jaeschke and Farhood, 1991). In contrast, APAP causes strict centrilobular necrosis. Therefore, overall these results indicate that Kupffer cells are not a relevant source of vascular oxidant stress during APAP hepatotoxicity.

It is controversial whether polymorphonuclear leukocytes (neutrophils) are relevant for APAP-induced liver injury. The presence of neutrophils in the areas of necrosis after APAP overdose injection was first demonstrated by Mitchell et al (Mitchell *et al.*, 1973a), but the pathophysiological relevance of this observation was unclear. Cover et al showed that the location of most neutrophils was outside the area of necrosis, which was in contrast to models where neutrophils caused liver cell injury (Cover *et al.*, 2006). Inflammatory cytokines and CXC chemokines were also increased after APAP administration (Horbach *et al.*, 1997; Lawson *et al.*, 2000; Takada *et al.*, 1995); however, there was no upregulation of Mac-1 (CD11b/CD18) on circulating neutrophils. Moreover, an anti-CD18 antibody had no protective effect against APAP overdose (Lawson *et al.*, 2000). In addition, mice deficient in ICAM-1, a counter receptor for Mac-1, were not

protected against APAP-induced hepatotoxicity (Cover *et al.*, 2006). Taken together, neutrophil migration into the parenchyma might not be relevant to APAP-induced hepatotoxicity. In terms of oxidative stress caused by neutrophils, despite the substantial number of neutrophils transmigrated into hepatocytes, there was no evidence for the generation of relevant amounts of HOCl-modified proteins, which is a specific marker for neutrophil-derived oxidant stress (Cover *et al.*, 2006). Furthermore, animals deficient in gp91 phox, an essential protein of activated NADPH oxidase complex in phagocytes, did not show any protective effect after APAP administration (James *et al.*, 2003b). In support of this finding, a chemical inhibitor of NADPH oxidase, DPI, did not decrease APAP-induced hepatotoxicity (Cover *et al.*, 2006). Together, these data lead to the conclusion that neutrophils do not actively contribute to the injury.

Natural killer (NK) and natural killer T (NKT) cells, which play a role in defense against viral infection and tumor transformation, might be involved in APAP-induced liver toxicity. The liver contains a resident lymphocyte population, composed of 5-10% NK cells and 30-40% NKT cells in mice. (Gao *et al.*, 2008; Gao *et al.*, 2009). Liu et al. showed that depletion of NK, NKT cells by anti-NK1.1 significantly reduced APAP-induced hepatotoxicity by 1) reduction of interferoṇ-γ (IFN-γ) secretion, which modulates inflammatory chemokine formation, 2) reduction of neutrophil accumulation, and 3) reduction of Fas ligand expression on innate immune cells (Liu *et al.*, 2004).

Moreover, it was demonstrated that APAP-induced liver injury was significantly attenuated in IFN-γ-KO mice (Ishida *et al.*, 2002). In addition, Fas deficient *lpr* mice and FasL-deficient *gld* mice showed significantly decreased APAP-induced hepatotoxicity (Liu *et al.*, 2004). However, Masson et al. demonstrated that dimethyl sulfoxide (DMSO) activated hepatic NK and NKT cells *in vivo*, which was shown by induction of intracellular levels of IFN-γ and granzyme B. Importantly, depletion of NK, NKT cells protected against APAP-induced liver injury only with DMSO as vehicle. In the absence of DMSO, NK, NKT cells did not induce IFN-γmRNA expression. In addition, there was no significant difference in liver injury between control and anti-NK1.1 pretreated groups after various doses of APAP in mice (Masson *et al.*, 2008). Therefore, DMSO should be used cautiously in drug hepatotoxicity experiments. NK and NKT cells may only be involved in APAP hepatotoxicity if these cells are activated independently. Although it is known that APAP induces inflammatory gene expression in mice (Cover *et al.*, 2006), the relevance of this for liver injury has not been determined.

The production of tumor necrosis factor-α (TNF-α) is one of the earliest events in the hepatic inflammatory response, and TNF-α is mainly released by activated liver macrophages (Decker, 1990). Ishida et al. reported that liver injury in mice deficient in the 55 KDa TNF receptor (TNF-Rp55) was attenuated after APAP challenge. In addition, APAP-induced mortality was reduced in TNF-Rp55 KO mice (Ishida *et al.*, 2004). Moreover, post-treatment

of anti-TNF-α Ab at 2 hours and 8 hours after APAP administration reduced hepatotoxicity significantly, which was shown by serum ALT levels (Ishida *et al.*, 2004). However, a reduction in TNF-α by pre-treatment with anti-TNF-α antibodies did not decrease APAP-induced liver injury (Simpson *et al.*, 2000; Yee *et al.*, 2007). In addition, TNF-α and lymphotoxin-α double KO mice did not show any protection against APAP overdose (Boess *et al.*, 1998). The reason for using these double knockout mice is that these two closely related cytokines may cross-compete for binding at the TNF receptors on target cells (Vandenabeele *et al.*, 1995). In contrast, it was reported that TNF-Rp55 KO mice exaggerate APAP-induced hepatotoxicity (Gardner *et al.*, 2003). Therefore, further studies need to be conducted to elucidate how TNF signaling is involved in APAP-induced liver injury.

It has been recently discussed whether another proinflammatory cytokine, IL-1, is involved in APAP-induced hepatotoxicity. There are two distinct types of IL-1, IL-1 α and IL-1 β, both of which signal through IL-1 receptor (IL-1 R). IL-1β is a very potent proinflammatory cytokine, which requires processing by activated caspase-1 (Mariathasan *et al.*, 2004; Martinon *et al.*, 2002; Ogura *et al.*, 2006). It is known that the combination of two distinct signaling pathways triggers caspase 1 activation. One is the activation of a cytosolic protein complex called the inflammasome. Three types of inflammasomes are reported based on biochemical analysis of three Apaf-1-like proteins, NALP1, NALP2, NALP3 (Agostini *et al.*, 2004). The

NALP3 inflammasome is composed of NALP3, apoptosis-associated speck-like protein containing a caspase recruitment domain (ASC) which is the adaptor protein, and caspase 1 (Trendelenburg, 2008). The other pathway involves activation of immune cells, such as macrophages, via Toll-like receptor (TLR) agonists, which induces the synthesis of pro-IL-1-β via NF-*k*B and certain inducible components of the inflammasome (Mariathasan and Monack, 2007). In the APAP model, it was reported that TLR9 and the NALP3 inflammasome play critical roles in the induction of hepatotoxicity in mice (Imaeda *et al.*, 2009). In addition, C3H/HeJ mice, which have a mutated TLR4, showed significant reduction of APAP-induced injury compared to controls without changing hepatic GSH level (Yohe *et al.*, 2006). Furthermore, IL-1 receptor KO mice showed a dramatic reduction of APAP-induced liver injury and MPO activity (Chen *et al.*, 2007). In addition, pretreatment with a combination of antibodies to IL-1-α, IL-1-β, and IL-1 R also decreased APAP-induced hepatotoxicity (Chen *et al.*, 2007). In spite of that, the genetic disruption of IL-1-receptor antagonist (IL-1RA), which binds the IL-1 R at the same sites with similar affinity as IL-1 but fails to induce effective signaling (Dinarello, 1996; Dripps *et al.*, 1991), reduced hepatotoxicity in the APAP model (Ishibe *et al.*, 2009). It was reported that the reason for this protection was inhibition of APAP metabolism in IL-RA KO mice. These data are supported by the observation that IL-1 signaling suppresses CYP gene

transcription via activation of NF-*k*B (Cao *et al.*, 1999; Riddick *et al.*, 2004; Zhou *et al.*, 2006).

In terms of other cytokines, it was demonstrated that APAP-induced hepatotoxicity is increased in IL-13 deficient mice, as well as by IL-13 neutralizing antibody pretreatment (Yee *et al.*, 2007). The mechanism has not been investigated yet, but IL-13 may have a regulatory role in modulating the infiltration of neutrophils into hepatocytes following APAP.

Previously, it was shown that IL-10 and IL-4 synergistically inhibit macrophage cytotoxic activity (Oswald *et al.*, 1992). Recently, it was reported that IL-10/ 4 double knockout mice are highly sensitive to APAP-induced hepatotoxicity without disturbance of its metabolism (Bourdi *et al.*, 2007). In addition, pretreatment with an IL-6 neutralizing antibody 1hour prior to APAP reduced liver injury in IL-10/4 KO mice (Bourdi *et al.*, 2007), suggesting that in IL-10/4 KO mice, IL-6 promoted hepatotoxicity.

Taken together, whether innate immunity is relevant for APAP-induced hepatotoxicity is still highly controversial, and it is necessary to do more and better mechanistic studies to resolve these issues.

f) Mitochondrial outer membrane permeabilization (MOMP) and Mitochondrial permeability transition (MPT)

The mitochondrial permeability transition (MPT) is characterized by mitochondrial swelling, and inner membrane permeabilization to solutes of molecular mass up to 1500 Da (Waldmeier *et al.*, 2003).

MPT pore consists of cyclophilin D (CyD) in the matrix, the adenine nucleotide translocase (ANT) in the inner mitochondrial membrane (IM), the voltage-dependent anion channel (VDAC) in the outer mitochondrial membrane (OM) and a number of accessory proteins (Orrenius *et al.*, 2007). Direct interactions have been shown for ANT and CyD, as well as between ANT and VDAC (Crompton, 1999; Woodfield *et al.*, 1998).

CyD in the matrix is thought to be involved in the regulation of MPT pore formation because it can interact with the immunosuppressant, cyclosporin A (CsA), which prevents MPT pore opening. Moreover, CyD knockout mice showed resistance to ischemia/reperfusion induced cardiac injury (Lim *et al.*, 2007) (Figure. 1.4).

In healthy cells, the inner mitochondrial membrane (IM) is nearly impermeable to all ions, including protons. This allows complexes I-IV of the respiratory chain to build up, across the IM, the proton gradient that is required for ATP synthesis (Mitchell and Moyle, 1965a, b). Therefore, the transport of all metabolites that cross the IM is tightly regulated by highly selective channels and transport proteins. The ANT has been proposed to be a main component of the IM. The function of ANT is exchanging of ATP and ADP across the IM (Zamzami and Kroemer, 2001). The ANT-mediated exchange (antiport) of ATP and ADP across the inner mitochondrial membrane is a function that is essential for generation of ATP through oxidative phosphorylation (Klingenberg, 1980). It is reported that mitochondria

isolated from ANT1/ANT2 double KO hepatocytes are relatively resistant against Ca^{2+} -induced swelling, which indicates that ANT is involved in MPT regulation (Kokoszka *et al.*, 2004). Interestingly, the formation of ANT pores is stimulated by Bax (Brenner *et al.*, 2000; Marzo *et al.*, 1998; Zamzami *et al.*, 2000) as well as reactive oxygen species (Vieira *et al.*, 2001).

The permeability of the OM is also regulated. It was shown that the OM is normally permeable to metabolites but not to proteins, which means that OM permeabilization results in the release of intermembrane proteins into the cytosol (Kroemer *et al.*, 2007). The VDAC is the most abundant protein of the OM and it is known as a nonspecific pore, allowing diffusion of solutes up to 5 kDa (Gottlieb, 2000; Zamzami and Kroemer, 2001). It was demonstrated that overexpression of VDAC1 induces apoptosis in a variety of cells (Zaid *et al.*, 2005).

A number of accessory proteins, such as hexokinase (HK), creatine kinase (CK), and peripheral-type benzodiazepine receptor (PBR) have been identified (Figure 1.4) (Kroemer *et al.*, 2007). HK interacts with VDAC from the cytosol. The interaction between HK and VDAC might cause a conformational change which may prevent mitochondrial breakdown during cell stress and injury (Mathupala *et al.*, 2006). However, this interaction can be disrupted by glycogen synthase kinase-3 beta (GSK-3β)-dependent phosphorylation of VDAC and can be promoted by Akt, which inhibits GSK-3β (Pastorino *et al.*, 2005). Creatine kinase (CK) interacts with MPT pore complex from the IM

(Kroemer *et al.*, 2007) and peripheral-type benzodiazepine receptor (PBR) is interacting with MPT pore complex from the OM (Kroemer *et al.*, 2007). The exact functions of these proteins have not been identified yet (Zamzami and Kroemer, 2001).

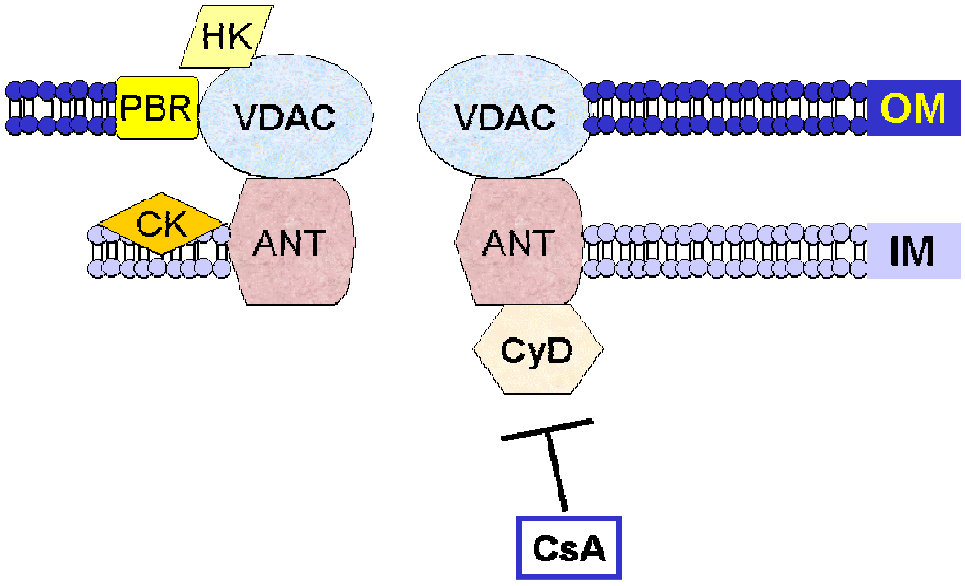

Figure 1.4

Mitochondrial permeability transition pore formation.
Modified from (Orrenius *et al.*, 2007) Voltage-dependent anion channel (VDAC), Cyclophilin D (CyD), Adenine nucleotide translocase (ANT), Inner mitochondrial membrane (IM), Outer mitochondrial membrane (OM), Cyclosporin A (CsA), Hexokinase (HK), Creatine kinase (CK), Peripheral-type benzodiazepine receptor (PBR)

MPT pore formation is regulated in many ways. 1) MPT pore is closed at neutral or acidic pH. Alkalinization is permissive for pore opening with a maximum effect at a matrix pH of ~7.3 (Zamzami and Kroemer, 2001). 2) It was reported that mitochondrial ROS accumulation causes MPT (Kowaltowski *et al.*, 2001). Thiol groups of inner membrane proteins are

oxidized. This causes conformational changes, which lead to formation of a large non-selective pore (Kowaltowski *et al.*, 2001). In particular, the oxidation of a critical residue (Cys56) of the ADP/ATP transporter leads to MPT pore opening in isolated mitochondria (Costantini *et al.*, 2000). 3) An increase in matrix Ca^{2+} enhances the probability of pore opening, while matrix Mg^{2+} or Mn^{2+} decrease it (Zamzami and Kroemer, 2001). In terms of calcium, high concentrations stimulate MPT via a decreased transmembrane electrical potential (Hunter and Haworth, 1979; Jurkowitz *et al.*, 1983; Vercesi, 1987; Zago *et al.*, 2000). In the APAP model, it was demonstrated that 1 h pretreatment with calcium channel blocking agents, e.g. diltiazem, verapamil, and gallopamil, protected primary cultures of rat hepatocytes. In addition, it has been shown that verapamil prevents APAP-induced hepatotoxicity *in vivo* (Ray *et al.*, 1993). Moreover, calcium can activate calpains, which are intracellular cysteine proteases that can cleave Bid and induce MPT and cell death. It has been shown that the specific calpain inhibitor, calpeptin, reduced AIF release in isolated mouse liver mitochondria (Polster *et al.*, 2005). In addition, when N-CBZ-VAL-PHE methyl ester (CBZ), which is a calpain inhibitor, was administered 1 hour before APAP, liver injury was significantly reduced (Limaye *et al.*, 2003). Furthermore, overexpression of calpastatin, which is an endogenous inhibitor of calpain, attenuated APAP-induced hepatotoxicity (Limaye *et al.*, 2006).

4) Members of the Bcl-2 family have either anti-apoptotic or pro-apoptotic function (Ranger *et al.*, 2001). The members are classified by sequence homology in four α-helical segments, which are called BH1-BH4 (Gross *et al.*, 1999). The highly conserved anti-apoptotic family members (Bcl-2, Bcl-xL, Mcl-1 and A1) contain all 4 BH domains. The pro-apoptotic members can be divided into 2 groups, multi-domain pro-apoptotic members (Bax, Bak, and Bok) and BH3 only members (Bid, Bad, Bim, Bik, Noxa and Puma) (Ranger *et al.*, 2001) (Figure 1.5). It has been demonstrated that overexpression of the anti-apoptotic protein Bcl-2 increases the transmembrane electrical potential, which prevents MPT (Kowaltowski *et al.*, 2000). Also, it has been reported that Bcl-2 and Bax can interact directly or indirectly with VDAC in the OM (Shimizu *et al.*, 1999), whereas Bcl-2, Bcl-xL, Bax, and Bak interact directly with ANT (Marzo *et al.*, 1998). Therefore, it is likely that the Bcl-2 family can regulate MPT to some extent.

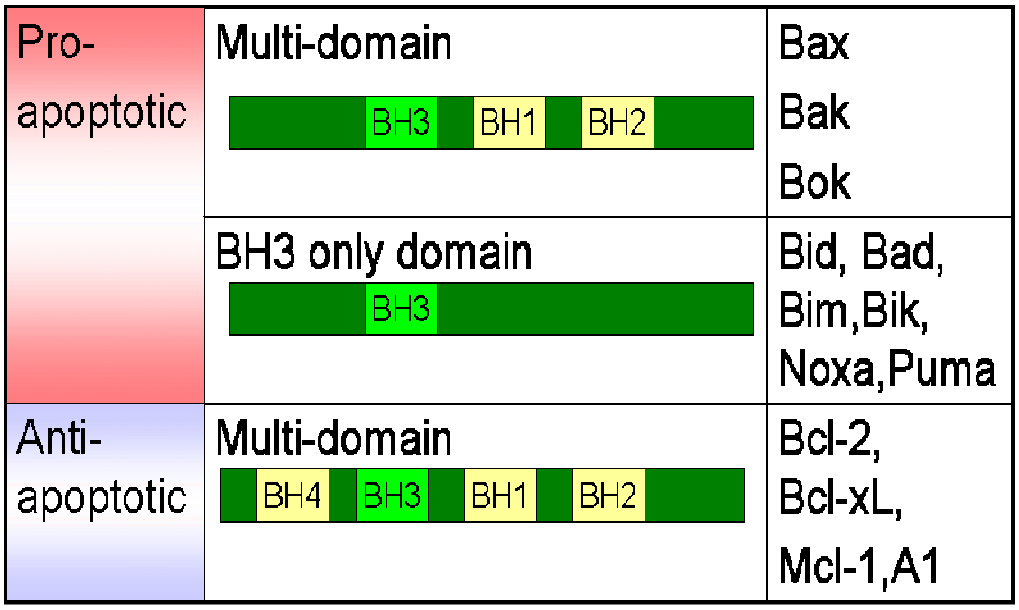

Figure 1.5

Bcl-2 family of proteins. Modified from (Ronger *et al*. 2001)

Mitochondrial outer membrane permeabilization (MOMP) is also regulated by Bcl-2 family members (Orrenius *et al.*, 2007) (Figure 1.6). Permeabilization of the OM is caused by the oligomeric form of Bax (Antonsson *et al.*, 2000), which follows binding to the truncated form of the BH3-domain-only pro-apoptotic protein, Bid (Eskes *et al.*, 2000). Anti-apoptotic proteins, such as Bcl-2 and Bcl-xL, interact with the pro-apoptotic proteins Bax or Bak, which prevents their oligomerization. It has been suggested that the ratio of Bcl-2 to Bax determines the amount of Bcl-2/Bax heterodimers versus Bax/Bax homodimers, which is important in determining the susceptibility to apoptosis (Yang and Korsmeyer, 1996).

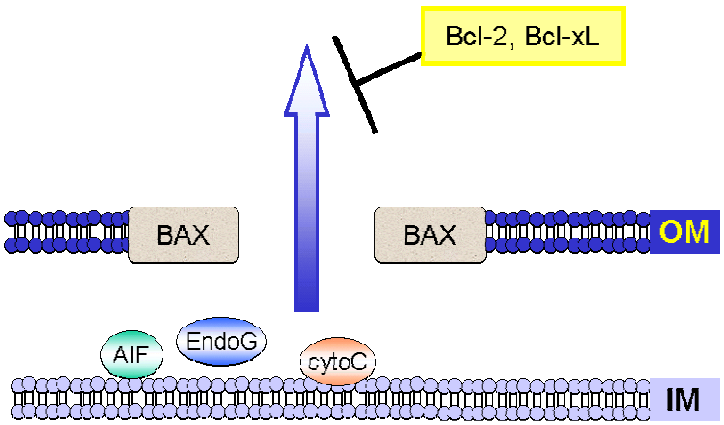

Figure 1.6

Mitochondrial outer membrane permeabilization (MOMP) formation. Modified from (Orrenius *et al.* 2007).

Li, *et al.* showed that ROS can stimulate phosphorylation and ubiquitination of Bcl-2 family proteins, thereby controlling their expression (Li *et al.*, 2004a). In addition, it was shown that activated c-Jun N-terminal protein kinase (JNK) can phosphorylate the anti-apoptotic proteins Bcl-2 and Bcl-xL resulting in inactivation. At the same time, JNK can phosphorylate Bax, which causes activation of Bax after APAP overdose (Latchoumycandane *et al.*, 2007).

How does Bax recognize the proper membrane in which to insert itself? Several possible Bax receptors have been suggested. The first candidate for a mitochondrial Bax receptor was VDAC, which is also known as mitochondrial porin. Tsujimoto and colleagues showed that Bax enhances VDAC activity which regulates the mitochondrial membrane potential and the release of cytochrome c during apoptosis (Shimizu *et al.*, 1999). However, absence of VDAC isoforms 1, 2 and 3 did not affect apoptosis signaling in fibroblasts isolated from VDAC 1-3 knockout mice (Baines *et al.*, 2007). Other potential Bax receptors include various components of the translocase of the outer mitochondrial membrane (TOM complex). Tom 22 was found to interact with the N-terminal of Bax (Bellot *et al.*, 2007). In addition, it was reported that antibodies against Tom 22 inhibit the association of truncated Bid (tBid) /Bax with rat liver mitochondria (Bellot *et al.*, 2007; Cartron *et al.*, 2008). In contrast, proteolytic removal of Tom22 did not prevent against tBid/Bax-induced cytochrome c release in yeast (Ott *et al.*, 2007b). Another target of Bax is

cardiolipin, which binds to cytochrome c in the IM and limits cytochrome c release during apoptosis (Ott *et al.*, 2002). However, there is very little cardiolipin in the OM, representing around 0.3% of the total phospholipids in mitochondria from rat liver (de Kroon *et al.*, 1997). Therefore, it is not known yet how Bax receptors are involved in MOMP formation.

g) Intermembrane proteins and DNA damage

After outer mitochondrial membrane permeabilization, intermembrane proteins, such as EndoG, AIF, cytochrome c, Smac/Diablo, HtrA2/Omi, AIF,and EndoG are released (Er *et al.*, 2006). Cytochrome c, Smac/Diablo and HtrA2/Omi are released into the cytosol, which is necessary for the activation of caspases in the mitochondrial apoptotic pathyway (Wang, 2001). Despite inducing cytochrome c release, APAP does not induce caspase-3 activation (Knight and Jaeschke, 2002; Lawson *et al.*, 1999). Furthermore, it was shown that post-treatment with a pancaspase inhibitor, ZVAD-FMK (benzyloxycarbonyl-Val-Ala-Asp-fluoromethylketone) did not protect against APAP hepatotoxicity (Lawson *et al.*, 1999). However, a subsequent report showed a protective effect with pre-treatment of ZVAD-FMK (El-Hassan *et al.*, 2003). Most likely, the solvent dimethyl sulfoxide (DMSO) used to dissolve the inhibitor attenuated the APAP metabolism (Jaeschke *et al.*, 2006). Thus, DNA fragmentation observed after APAP overdose is independent of the caspase-activated DNase (CAD).

EndoG and AIF are involved in DNA damage after translocation from mitochondria to the nucleus in APAP overdose (Bajt *et al.*, 2006). AIF is thought to trigger chromatin condensation and can induce large scale DNA fragmentation (50-300 kb) (Susin *et al.*, 1999). EndoG and Mn^{2+} dependent endonuclease can produce oligonucleosomal DNA fragments (Li *et al.*, 2001). Subsequent studies also demonstrated that EndoG catalyzes both high-molecular-weight DNA cleavage and oligonucleosomal DNA breakdown in a sequential fashion (Widlak *et al.*, 2001). It was observed that AIF KO mice have reduced APAP-induced DNA fragmentation and liver injury (Jaeschke, 2007), indicating that AIF could be a key target for protection against APAP hepatotoxicity.

Another nuclease is deoxyribonuclease 1 (DNase 1). DNase 1 is a Ca^{2+}/Mg^{2+}-dependent endonuclease, which cleaves double-stranded DNA into 3'-OH/5'-phospho tri-and/or tetra-oligonucleotides (Napirei *et al.*, 2005). DNase1 gene expression has been demonstrated in many different organs, including the murine liver (Napirei *et al.*, 2004a). Extracellular DNase1 diffuses into necrotic cells and, together with the plasminogen system, induces necrotic chromatin breakdown *in vitro* (Napirei *et al.*, 2004b). A recent study showed that DNase 1 KO mice suffered less liver injury after APAP overdose (Napirei *et al.*, 2006). It was concluded that DNase 1 caused some of the DNA damage and aggravated energy depletion via stimulation of DNA repair mechanisms, such as poly-adenosine diphosphate-ribose polymerase

(PARP) activation during APAP-induced hepatotoxicity (Jacob *et al.*, 2007; Napirei *et al.*, 2006). In addition, it was reported that excessive PARP-1 activation leads to depletion of nicotinamide adenine dinucleotide (NAD^+) and ATP content that causes oncotic necrosis (Charron and Bonner-Weir, 1999; Ha and Snyder, 1999; Szabo and Dawson, 1998; Virag and Szabo, 2002). These data are supported by the fact that nicotinamide supplementation also decreases APAP-induced hepatotoxicity (Ray *et al.*, 2001). However, neither PARP-1 KO mice (Cover *et al.*, 2005a) nor cultured hepatocytes treated with a PARP inhibitor (Shen *et al.*, 1992) were protected against APAP-induced liver injury. Therefore PARP activation does not appear to be critical for APAP hepatotoxicity. However, DNase 1 may contribute to nuclear DNA damage, especially at later time-points.

3) Summary

Acetaminophen (APAP) is only used as analgesic and antipyretic agent in therapeutic doses (15 mg/kg, three to four times per day). However, APAP overdose (a single dose of 150 mg/kg) causes hepatotoxicity (Brok *et al.*, 2006). APAP is eliminated by sulfation and glucuronidation. A small portion of APAP is metabolized by cytochrome P450 isoenzymes that produce *N*-acetyl-*p*-benzoquinone imine (NAPQI). NAPQI is detoxified by glutathione (GSH), resulting in the depletion of this sulfhydryl compound. Subsequently, NAPQI covalently binds to cellular proteins (Nelson, 1990), including mitochondrial proteins. Mitochondrial proteins appear to be the most critical

targets of NAPQI leading to inhibition of mitochondrial respiration and causing oxidative stress, which eventually triggers the mitochondrial membrane permeability transition (MPT) (Kon *et al.*, 2004). In addition, mitochondrial and nuclear DNA fragmentation is induced. These series of events results in extensive centrilobular liver necrosis (Figure 1.7).

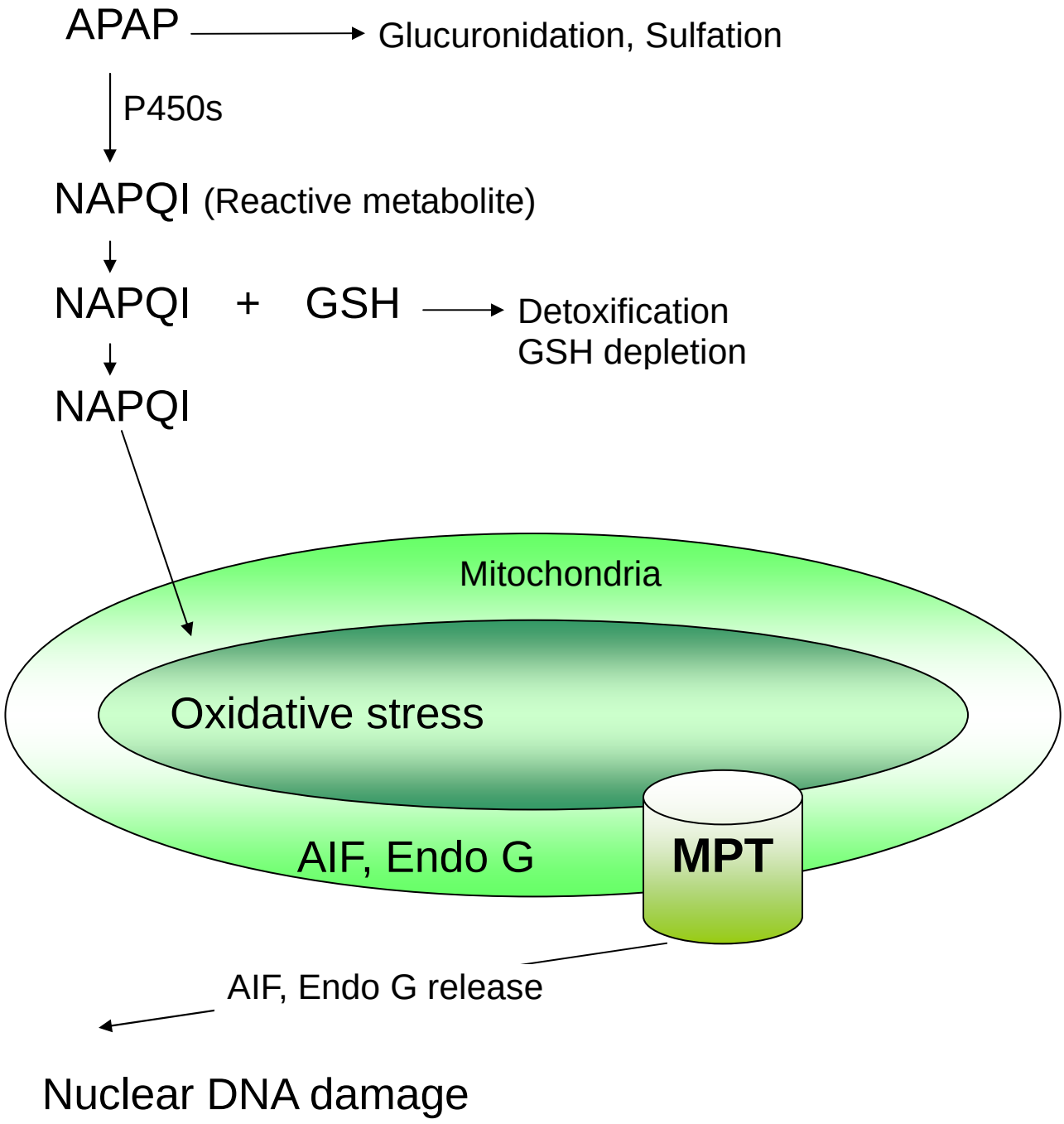

Figure 1.7
Mechanism of acetaminophen-induced hepatotoxicity.

CHAPTER 2 : HYPOTHESIS AND AIMS

Acetaminophen (APAP) is a commonly used drug for the relief of fever and pain. However, an overdose of APAP is hepatotoxic. The mechanisms of APAP-induced liver injury have been studied extensively. Based on these findings, three protective strategies were investigated in detail:

Aim 1) Glutathione (GSH) and *N*-acetylcysteine (NAC)

Aim 2) Metallothionein (MT)

Aim 3) JNK inhibitor

Aim 1

NAC is used at very high doses both in humans and in experimental animals. These doses are higher than needed for the re-synthesis of hepatic GSH levels. However, our lab demonstrated that a moderate dose of GSH is highly effective in protecting against APAP toxicity. Therefore, I investigated whether there is a difference between the efficacy of NAC and GSH in protecting against APAP hepatotoxicity.

Aim 2

Metallothionein (MT) has been suggested to react with free radicals. APAP-induced hepatotoxicity studies showed a protective effect by MT. The modulation of APAP toxicity was independent of P450 levels and the metabolic activation of APAP. In contrast, the protection appeared to be correlated with the antioxidant function of MT. However, it remains unclear whether MT can actually scavenge reactive oxygen species (ROS) of APAP.

Thus, the objective of this study was to investigate the mechanism by which induction of MT expression protects against APAP-induced hepatotoxicity *in vivo*.

Aim3

C-jun N-terminal kinase (JNK) has been suggested to contribute to APAP-induced liver injury. The postulated mechanism of JNK involvement was the promotion of mitochondrial Bax translocation, which triggers mitochondrial outer membrane pore formation resulting in the release of intermembrane proteins such as apoptosis inducing factor (AIF) and endonuclease G (EndoG). However, our laboratory reported that Bax-deficient mice were only temporally protected against APAP-induced liver injury (Bajt *et al.*, 2008). In contrast, the protective effect of JNK inhibitor was observed consistently up to 12 h. Therefore, additional mechanisms of injury need to be triggered by JNK activation, and tested the hypothesis that JNK promotes iNOS induction and mitochondrial oxidant stress.

CHAPTER 3: MATERIALS AND METHODS

3.1 Common methods

3.1.1 Experimental Protocols.

At selected times after APAP treatment, groups of animals were killed by cervical dislocation under isoflurane anesthesia. Blood was drawn from the vena cava into heparinized syringes and centrifuged. The plasma was used for determination of alanine aminotransferase (ALT) activities. Immediately after collecting the blood, the livers were excised and rinsed in saline. A small section from each liver was placed in 10% phosphate buffered formalin. The remaining liver was frozen in liquid nitrogen and stored at -80℃.

3.1.2. ALT.

Plasma ALT activities were determined with the kinetic test kit 68-B (Biotron Diagnostics, Inc., Hernet, CA) and expressed as IU/liter.

3.1.3 Subcellular fraction and protein concentrations.

The method is described in the manufacturer's instructions (Pierce, Rockford, IL). Mitochondria and cytosol were isolated using the mitochondria isolation kit for tissue (Pierce, Rockford, IL).

Protein in cytosol and mitochondria fraction was measured using the bicinchoninic acid kit (Pierce, Rockford, IL).

3.1.4 Western blotting.

Liver tissue was homogenized in 25 mM HEPES

(4-(2-hydroxyethyl)-1-piperazineethanesulfonic acid) (pH 7.5) containing 5 mM EDTA, 2 mM DTT (dithiothreitol), 0.1% CHAPS (3-[(3-cholamidopropyl)dimethylammonio]-1-propanesulfonate), 1 mg/ml pepstatin, leupeptin, and aprotinin. Homogenates were centrifuged at 14,000 g at 4℃ for 20 min. Cytosolic extracts (10 μg per lane) were resolved by 4–20% SDS–polyacrylamide gel electrophoresis under reducing conditions. Separated proteins were transferred to polyvinylidine difluoride membranes (PVDF, Immobilin-P, Millipore, Bedford, MA). For metallothionein, separated proteins were transferred to a polyvinylidine difluoride membrane (PVDF, Immobilon-PSQ Millipore, Bedford, MA), which is a special membrane for smaller molecular weight proteins. The membranes were first blocked with 5% milk in TBS (20 mM Tris, 154 mM NaCl, 0.1% Tween 20, and 0.1% BSA) overnight at 4℃, followed by incubation with primar y antibody, e.g., a rabbit anti-Bax polyclonal antibody (Cell signaling Technology, Danvers, MA), a rabbit anti-AIF monoclonal antibody (Epitomics, Burlingame, CA), rabbit anti-Cytochrome c polyclonal antibody (Santa Cruz Biotechnology, Santa Cruz, CA), a monoclonal mouse anti-Metallothionein antibody (DAKO Corp., Carpinteria, CA) for 2 h at room temperature. The membranes were washed and then incubated with the secondary antibody with horseradish peroxidase (Santa Cruz Biotechnology). Proteins were visualized by enhanced chemiluminescence (Amersham Pharmacia Biotech. Inc., Piscataway, NJ), according to the manufacturer’s instructions. Densitometric analysis of the

gels was performed with a GS170 Calibrated Imaging Densitometer (Biorad, Hercules, CA) using Quantity One 4.0.3 software (Biorad).

3.1.5 Total GSH and GSSG measurements.

Total soluble GSH and GSSG were measured in the liver homogenate and in isolated mitochondria with a modified method of Tietze as described (Jaeschke and Mitchell, 1990; Knight *et al.*, 2002). Frozen tissues (or isolated mitochondria) were homogenized at 0° C in 3% sulfosal icylic acid containing 0.1 mM EDTA (Jaeschke and Mitchell, 1990). An aliquot of the homogenate was added to 10 mM *N*-ethylmaleimide (NEM) in potassium phosphate buffer (KPP), and another aliquot was added to 0.01 N HCl. The NEM-KPP sample was centrifuged, and the supernatant was passed through a C_{18} cartridge to remove free NEM and NEM-GSH adducts (Sep-Pak; Waters, Milford, MA). The HCl sample was centrifuged, and the supernatant was diluted with KPP. All samples were assayed using dithionitrobenzoic acid (DTNB). All data are expressed in GSH-equivalents.

3.1.6 Histology, TUNEL assay, immunohistochemistry for nitrotyrosine.

Formalin-fixed tissue samples were embedded in paraffin and 5 µm sections were cut. Replicate sections were stained with hematoxylin and eosin (H&E) for evaluation of necrosis (Gujral *et al.*, 2002). For the terminal deoxynucleotidyl transferase-mediated dUTP nick-end labeling (TUNEL) assay, sections of liver were stained with the In Situ Cell Death Detection Kit,

AP (Roche Diagnostics, Indianapolis, IN) as described in the manufacturer's instructions (Gujral *et al.*, 2002). Nitrotyrosine protein adducts were detected with standard immunohistochemical methods using an anti-nitrotyrosine antibody (Molecular Probes, Eugene, OR) (Knight *et al.*, 2002).

3.1.7 Quantitative real-time polymerase chain reaction (qRT-PCR).

Total RNA was reversed transcribed with M-MLV reverse transcriptase (Invitrogen, Carlsbad, CA) and oligo-dT primers (ABI Primer Express software, Foster City, CA).

The primer sequences for the genes examined are as follows:

β-actin:

Forward, 5'-GTATGACTCCACTCACGGCAAA-3',

Reverse, 5'-GGTCTCGCTCCTGGAAGATG-3',

MT-1:

Forward 5'-AATGTGCCCAGGGCTGTGT-3',

Reverse, 5'-GCTGGGTTGGTCCGATACTATT,

MT-2:

Forward, CCTCACTGGCAGGAAATCATC,

Reverse, 5'-CCTCGTGGAGACGCTTTACATA,

iNOS:

Forward, 5'-ACATCAGGTCGGCCATCACT3',

Reverse, 5'-CGTACCGGATGAGCTGTGAATT-3'.

The SYBR green PCR Master Mix (Applied Biosystems, Foster City, CA) was used for real-time PCR analysis. The relative differences in gene expression between groups were expressed using cycle time (Ct) values. Ct values for the various genes were first normalized with that of β-actin in the same sample, and then relative differences between groups were expressed as relative increases setting control as 1.

3.1.8 Statistics.

Data are expressed as means ± S.E. Comparison between two groups were performed with Student's t-test or one-way ANOVA followed by Bonferroni t-test for multiple groups. If the data were not normally distributed, the Mann-Whitney test was applied for comparison of two groups and the Kruskal-Wallis Test (nonparametric ANOVA) followed by Dunn's Multiple Comparisons Test for multiple groups. $P<0.05$ was considered significant.

3.2 Specific methods for Aim 1

3.2.1 Animals.

Male C3HeB/FeJ mice (8-10 weeks old) were purchased from Jackson Laboratories (Bar Harbor, ME). Animals received humane care according to the criteria outlined in the "Guide for the Care and Use of Laboratory Animals". The experimental protocol was approved by the Institutional Animal Care and Use Committee of Kansas University Medical Center. The animals were fasted overnight and then received 300 mg/kg

APAP (Sigma Chemical Co., St. Louis, MO) dissolved in warm saline (15 mg/ml) (i.p.). Some animals received a single intravenous bolus dose of glutathione (200 mg/kg GSH; 0.65 mmol/kg) dissolved in phosphate-buffered saline (PBS), 106 mg/kg (0.65 mmol/kg) or 318 mg/kg (1.95 mmol/kg) *N*-acetyl cysteine, a mixture of 3 amino acids [49 mg/kg (0.65 mmol/kg) glycine, 96.4 mg/kg (0.65 mmol/kg) glutamic acid, and 106 mg/kg (0.65 mmol/kg) NAC] or a mixture of 2 amino acids [73.5 mg/kg (0.98 mmol/kg) glycine and 144.6 mg/kg (0.98 mmol/kg) glutamic acid]. All compounds were administered intravenously through the penile vein 1.5 h after APAP injection (Bajt *et al.*, 2003; Cover *et al.*, 2005b; Knight *et al.*, 2002). The rationale for the treatment at 1.5 h is based on the assumption that by that time most of the administered APAP has been metabolized and most of the protein binding of NAPQI is completed.

3.2.2 NMR experiments.

For NMR experiments, further groups of mice were treated with APAP and the study substances at t = 1.5 h as mentioned above [GSH, NAC, a mixture of 3 amino acids (glycine, glutamate, cysteine), a mixture of 2 amino acids, or cysteine]. At t = 1.5 h or t = 6 h, all mice received [U-13C]glucose (500 mg/kg; 2.78 mmol/kg) (Cambridge Isotopes, Andover, MA), which was injected intraperitoneally in bolus to study metabolic changes in awake mice. Using 500 mg/kg [U-13C]glucose, plasma glucose was <10 mM in all experiments. The mice were killed by cervical dislocation and the livers

freeze-clamped immediately. Blood was taken after severing of the carotid artery and put into tubes containing heparin. Water-soluble metabolites were extracted from blood or tissue with perchloric acid and analyzed by NMR spectroscopy (Zwingmann and Bilodeau 2006).

3.3 Specific methods for Aim 2

3.3.1 Animals.

Male C57BL/6J mice (8-10 weeks old), male age-matched wildtype 129S1/SvImJ and male MT-1/MT-2 deficient mice (129S7/SvEvBrd-Mt1tm1Bri Mt2tm1Bri/J) were purchased from Jackson Laboratories (Bar Harbor, ME). Animals received humane care according to the criteria outlined in the “Guide for the Care and Use of Laboratory Animals”. The experimental protocol was approved by the Institutional Animal Care and Use Committee of Kansas University Medical Center. Some animals received a non-toxic dose of 100 μmol/kg zinc chloride (Fluka Chemical Corp., Milwaukee, WI) dissolved in saline (9.9 μmol/ml) subcutaneously once a day for 3 days (Liu et al., 2009). All animals were fasted overnight and on the 4th day, they received 300 mg/kg APAP (Sigma Chemical Co., St. Louis, MO) dissolved in warm saline (15 mg/ml) by intraperitoneal injection.

3.3.2 Mouse hepatocyte isolation.

Primary hepatocytes were isolated from overnight fasted mice with a standard collagenase procedure as previously described in detail (Bajt et al.,

2004). Untreated and $ZnCl_2$-treated animals were used. Some of the animals were treated with 100 mg/kg phorone i.p. (Sigma) to deplete hepatic GSH levels 90 min before cell isolation. The GSH-depleted cells were then incubated in the presence of the GSH synthesis inhibitor buthionine sulfoximine (1 mM) (Sigma). From the isolation of one mouse liver, a typical yield was about 50–60 $x10^6$ hepatocytes. Cell viability, as determined by trypan blue exclusion, was generally >90%, and cell purity was >95% hepatocytes. Cells were plated in six-well plates (6×10^5 cells/well) (Biocoat collagen I cellware plates; Becton Dickinson) in Williams' Medium E (Gibco) containing 10% fetal bovine serum (Gibco), 100 U/ml penicillin/streptomycin, and 1×10^{-7} M insulin and cultured at 37 ℃ in room air with 5% CO_2. After an initial 4 h attachment period, cultures were washed with phosphate-buffered saline (PBS) and then plain culture medium (controls) or media containing various concentrations of hydrogen peroxide were added. Cell injury was assessed by lactate dehydrogenase (LDH) release into the medium. LDH activities were measured as described (Bajt et al., 2004).

3.3.3 Analysis of MT-NAPQI interactions by mass spectrometry.

MT from rabbit liver was purchased from Sigma (M5269) as a lyophilized powder. The protein was suspended in deionized water to a protein concentration of 1 mg/ml. NAPQI was purchased from Sigma (A7300) and diluted in water to a final concentration of 12 µg/ml. For mass spectrometric measurements, protein samples were desalted on a C18

reverse phase column (Zorbax C18SB Wide pore guard Column, MicroTech Scientific, 1 cm x 0.32 mm), which was connected online to a valve to direct the flow either to waste or to the mass spectrometer (MS). After washing the column with 0.1% (v/v) TFA at a flow of 100 µl/min, the flow was directed to the mass spectrometer and the protein eluted using a 0-60% (v/v) acetonitrile gradient in 0.1% TFA at a flow rate of 20 µl/min. Electrospray ionization (ESI) MS data were acquired in the m/z range 800-2000 on a ThermoFinnigan LTQ FT. The mass spectrometer was under manual control to facilitate switching between two modes of data acquisition, on the Ion Trap (IT) and on the Ion Cyclotron Resonance Fourier Transform cell (ICR FT). Final optimized settings for detection of MT were: ion spray voltage 2.1 kV, capillary temperature 250 °C, capillary voltage 34V. The two modes of operation have different sensitivity and mass resolution. The charge state of all protein species detected was calculated from the isotopic distribution of the high resolution spectrum obtained in the ICR FT. However, due to the higher sensitivity of the IT, data reported here are for the acquisition on the IT. Masses of the different protein variants were calculated from the multiple charged protein ions using the deconvolution software included in BioworksBrowser V. 3.1 (ThermoFinningan). The resulting masses were measured with an experimental precision of ± 1.5 dalton.

3.4 Specific methods for Aim 3

3.4.1 Animals.

Male C57BL/6J mice (8-10 weeks old), JNK2-deficient mice (B6.129S2-Mapl9$^{tm1Flv/J}$ or age-matched wild type (C57Bl/6J) mice were purchased from Jackson Laboratories (Bar Harbor, ME). Animals received humane care according to the criteria outlined in the "Guide for the Care and Use of Laboratory Animals". The experimental protocol was approved by the Institutional Animal Care and Use Committee of the Kansas University Medical Center.

3.4.2 Experimental Protocols.

All animals were fasted overnight and some animals received a JNK inhibitor, 10 mg/kg SP600125 (LC Laboratories) dissolved in 8.3 % DMSO in PBS (1 mg in 125 μl of DMSO diluted with 1375 μl of PBS) (Hanawa *et al.*, 2008). JNK inhibitor and DMSO, unless noted otherwise, were injected intraperitoneally 1 h prior to 600 mg/kg APAP injection (Sigma Chemical Co., St. Louis, MO). Some animals received 300 mg/kg APAP with either 0.65 mmol/ kg GSH (i.v.) administration at 1.5h after APAP or 100 μmol/kg $ZnCl_2$ administration for 3 days. APAP was dissolved in warm saline (15 mg/ml). Some animals received 2 mg/kg ip lipopolysaccharide (Sigma), with/without 3.3 mg/kg ip L-*N*-(1-iminoethyl)lysine (L-Nil) (Cayman) at 0 and 3 h.

3.4.3 Measurement of Nitrite/nitrate in plasma.

The plasma concentrations of nitrite/nitrate were determined with a kit

(Cayman) by means of the Griess reaction.

CHAPTER 4: NOVEL MECHANISMS OF PROTECTION AGAINST ACETAMINOPHEN HEPATOTOXICITY IN MICE BY GLUTATHIONE AND N-ACETYLCYSTEINE

4.1 Abstract.

Acetaminophen (APAP) overdose is a major cause of acute liver failure. The glutathione (GSH) precursor *N*-acetylcysteine (NAC) is used to treat patients with APAP overdose for up to 48 h. Although it is well established that early treatment with NAC can improve the scavenging of the reactive metabolite *N*-acetyl-*p*-benzoquinone imine (NAPQI), protective mechanisms at later times remain unclear. To address this issue, fasted C3Heb/FeJ mice were treated with 300 mg/kg APAP and then received intravenously 0.65 mmol/kg GSH or NAC at 1.5 h after APAP. The animals were sacrificed at 6 h. APAP alone caused severe liver injury with peroxynitrite formation and DNA fragmentation, all of which were attenuated by both treatments. However, GSH (-82%) was more effective than NAC (-46%) in preventing liver injury. Using nuclear magnetic resonance spectroscopy to measure tissue ATP levels and the substrate flux through the mitochondrial Krebs cycle, it was observed that the reduced liver injury correlated with accelerated recovery of mitochondrial GSH content, maintenance of ATP levels and an increased substrate supply for the mitochondrial Krebs cycle compared to APAP alone. NAC treatment was less

effective in recovering ATP and mitochondrial GSH levels and showed reduced substrate flux through the Krebs cycle, compared to GSH. However, increasing the dose of NAC improved the protective effect similar to GSH suggesting that the amino acids not used for GSH synthesis were used as mitochondrial energy substrates. Taken together, delayed treatment with GSH and NAC protect against APAP overdose by dual mechanisms, i.e. by enhancing hepatic and mitochondrial GSH levels (scavenging of reactive oxygen species and peroxynitrite) and by supporting the mitochondrial energy metabolism.

4.2 Introduction.

Acetaminophen (APAP) is a safe analgesic at therapeutic levels. However, an overdose can cause severe liver injury and even acute liver failure. During the last decade, APAP became the most frequent cause of acute liver failure in the US and many other countries (Larson *et al.*, 2005). Early animal studies established the formation of the reactive metabolite *N*-acetyl-*p*-benzoquinone imine (NAPQI), which first depletes glutathione and subsequently binds to proteins, critical events in APAP toxicity (Jollow *et al.*, 1973; Mitchell *et al.*, 1973a; Mitchell *et al.*, 1973b). Based on this mechanistic insight, *N*-acetylcysteine (NAC) was introduced to treat patients with APAP overdose in the 1970s (Prescott *et al.*, 1977). Even today, NAC therapy is still the best therapeutic option for the overdosed patient (Polson and Lee, 2005).

NAC is most effective when given as early as possible after APAP intoxication. The main mechanism of action of NAC is to promote hepatic GSH synthesis (Corcoran and Wong, 1986; Lauterburg *et al.*, 1983), which supports the detoxification of NAPQI and reduces protein binding (Corcoran *et al.*, 1985). However, NAC therapy is clinically effective even when initiated 24 h after APAP overdosing, i.e. at a time when there is no relevant amount of drug left to be metabolized (Harrison *et al.*, 1990; Smilkstein *et al.*, 1988). These observations suggest that there might be other, yet unknown mechanisms of protection. This hypothesis is also supported by the fact that NAC can protect in models without GSH depletion (Zwingmann and Bilodeau, 2006). Recent insight into the molecular mechanisms of APAP-induced hepatotoxicity in a mouse model indicated that the early protein binding is an essential initiating event, which requires intracellular propagation and amplification (Jaeschke and Bajt, 2006; Jaeschke *et al.*, 2003). Key to this propagation mechanism is mitochondrial dysfunction and oxidant stress (Jaeschke and Bajt, 2006). Intravenous administration of GSH after APAP treatment resulted in the accelerated recovery of GSH in the mitochondria (Knight and Jaeschke, 2002). The elevated levels of mitochondrial GSH effectively scavenged reactive oxygen and peroxynitrite, which reduced APAP-induced liver injury and promoted regeneration (Bajt *et al.*, 2003; Cover *et al.*, 2005b; Knight and Jaeschke, 2002). Delayed treatment with NAC had a similar protective effect (James *et al.*, 2003c). These findings support the hypothesis that the delayed

supply of cysteine can be involved in a second mechanism of protection, i.e. the scavenging of reactive oxygen species and peroxynitrite (Jaeschke and Bajt, 2006; Jaeschke *et al.*, 2003). The dose of GSH we used in our recent experiments (Bajt *et al.*, 2003; Cover *et al.*, 2005b; Knight and Jaeschke, 2002) was based on previous data showing its efficacy in supporting the recovery of hepatic GSH levels after starvation (Wendel and Jaeschke, 1982). This dose provides enough cysteine to re-synthesize twice the entire GSH content of a mouse liver. However, in most studies with NAC, generally much higher doses are used, e.g. 300 – 1200 mg/kg of NAC (Corcoran *et al.*, 1985; James *et al.*, 2003c; McConnachie *et al.*, 2007; Salminen *et al.*, 1998; Whitehouse *et al.*, 1985), which is sufficient to synthesize the hepatic GSH content between 6 and 23 times. For treatment of acute APAP poisoning in patients, the recommended dose for NAC is a 150 mg/kg loading dose followed by maintenance doses of 50 mg/kg every 4 h (Polson and Lee, 2005). Again, even the loading dose alone would be sufficient cysteine to synthesize several times the entire hepatic GSH content. This raises the question whether GSH is more effective than NAC, or if there are additional benefits of high doses of NAC that have not been considered. To address this important question, we compared the efficacy and mechanisms of protection of equimolar doses of GSH and NAC in a murine model of APAP hepatotoxicity.

4.3 Results.

GSH treatment was most effective in preventing APAP-induced liver injury. Male C3Heb/FeJ mice treated with an overdose of APAP (300 mg/kg) showed evidence of severe liver injury at 6 h as indicated by increases in plasma ALT values (Figure 4.1.A). In addition, there was only a partial recovery of the hepatic GSH content and evidence of oxidant stress, as indicated by the elevated levels of hepatic GSSG and increased GSSG-to-GSH ratio (Figure 4.1 B-D). Treatment of mice with equimolar doses of GSH or NAC (0.65 mmol/kg) at 1.5 h after APAP resulted in reduced increases in plasma ALT. (Figure 4.1 A). However, GSH treatment was more effective in preventing APAP-induced liver injury as indicated by the 82% lower ALT values compared to the 46% reduction with NAC. However, both treatments resulted in a complete recovery of hepatic GSH levels (Figure 4.1 B). The hepatic GSSG content was further increased in the GSH and NAC treated mice, compared to APAP alone. However, the GSSG-to-GSH ratio was similar in all APAP-treated groups (Figure 4.1 D). These results suggest that ROS are still being formed after GSH or NAC treatment but this oxidant stress is more efficiently detoxified due to the higher GSH levels. The biochemical data was confirmed by histological findings. H&E staining of liver sections indicated the substantial centrilobular necrosis 6 h after APAP administration (Figure 4.2). The loss of basophilic staining, vacuolization, cell swelling and karyolysis around the centrilobular veins documents that the

cells undergoing oncotic necrosis (Figure 4.7). The extent of necrosis correlated with massive DNA fragmentation, as demonstrated by the TUNEL assay and peroxynitrite formation, as indicated by the presence of nitrotyrosine protein adducts in the centrilobular areas (Figure 4.2). Delayed treatment with GSH markedly reduced the area of necrosis, nitrotyrosine protein adducts as well as the number of TUNEL-positive cells (Figure 4.2; Figure 4.7). Treatment with NAC also attenuated the areas of necrosis, nitrotyrosine staining and the extent of DNA damage (Figure 4.2). However, the protective effect of NAC was less pronounced compared than GSH. Together, these results suggest that treatment with GSH 1.5 h after APAP administration was more effective in protecting the liver compared to an equimolar dose of NAC. Because hepatic GSSG levels further increased after GSH or NAC treatment compared to APAP alone, this indicates that ROS are more effectively detoxified but are still being formed. Thus, both delayed treatments did not affect the oxidant stress induced by APAP overdose (Figure 4.1C,D).

GSH and NAC treatment had similar effects on early GSH recovery.

Although there was a clear difference in tissue injury between the GSH- and the NAC-treated groups, based on the GSH and GSSG data of the 6 h time point (Figure 4.1), it appears that the efficacy in supplying cysteine for recovery of hepatic GSH levels and scavenging reactive oxygen was similar between the 2 treatment groups. To verify that this conclusion is justified, a

more detailed time course of the depletion and recovery of hepatic GSH levels was studied (Figure 4.3 A). Treatment with APAP resulted in an 86% depletion of hepatic GSH levels within 30 min and no further decline thereafter (Figure 4.3 A). When saline was injected 1.5 h after APAP, there was no immediate recovery of the GSH content. However, between 2.5 and 4 h, GSH levels spontaneously recovered to about 70% of baseline, with no further improvement thereafter (Figure 4.3 A). In contrast, injection of GSH or NAC resulted in a rapid and complete recovery of hepatic GSH levels within 1 h and an additional increase over the next 1.5 h (Figure 4.3 A). Despite the similar recovery of the hepatic GSH content, plasma ALT values indicated improved protection in the GSH-treated animals compared to NAC (Figure 4.3 B). Because our previous studies identified the mitochondria as the main source of oxidant stress and peroxynitrite formation (Cover *et al.*, 2005b; Jaeschke, 1990; Knight *et al.*, 2001; Tirmenstein and Nelson, 1990), the mitochondrial GSH content was evaluated 45 min after the injection of GSH or NAC (Figure 4.3 C). Compared to an untreated control, mitochondrial GSH levels are still 90% depleted 2.25 h after APAP exposure. Injection of GSH resulted in a complete recovery of mitochondrial GSH levels (Figure 4.3 C). However, injection of an equimolar dose of NAC caused only a partial recovery of the mitochondrial GSH content to levels 34% below controls or GSH-treated animals (Figure 4.3 C). These results indicate that the supply of cysteine through GSH or NAC is sufficient to re-synthesize GSH in the cytosol

but there is a delay of the energy-dependent transport of GSH into the mitochondria with NAC.

Hepatic energy status and metabolism.

It is well established that APAP-induced hepatotoxicity causes mitochondrial dysfunction with depletion of hepatic ATP levels (Jaeschke, 1990; Kon *et al.*, 2004; Tirmenstein and Nelson, 1990). In addition, it was recently shown that high levels of NAC can improve mitochondrial energy metabolism (Zwingmann and Bilodeau, 2006). Therefore, we hypothesized that the difference between GSH and NAC treatment might be caused by differential effects on mitochondrial energy metabolism. Using NMR, we compared changes in ATP levels with alterations in mitochondrial energy metabolism. We chose to evaluate these parameters at two time points, an early time (2.25 h) during the initiation of the injury and a late time (6.75 h) when substantial necrosis was evident. As a measure of the hepatocellular energy state, the concentrations of ATP were determined from ^{31}P-NMR spectra of liver extracts (Figure 4.4). ATP levels in the livers of mice treated with APAP were reduced to 66% and 42% of saline-treated controls at the early and late time point, respectively. Whereas ATP levels were not significantly different from controls after administration of GSH at both time-points, treatment with NAC did not result in an early ATP recovery, and improved the energy status only partially (to 70% of controls) at the late time point.

GSH causes early and late upregulation of mitochondrial energy

metabolism.

Two pathways mediate the entry of carbon from [U-^{13}C]glucose into the Krebs cycle after conversion to [U-^{13}C]pyruvate (Figure 4.5 A): 1) Pyruvate dehydrogenase (PDH), which converts pyruvate into acetyl-CoA and is considered the key enzyme for mitochondrial energy metabolism. 2) Pyruvate carboxylase (PC) converts pyruvate into the Krebs cycle intermediate oxaloacetate, which needs to combine with acetyl-CoA to allow for synthesis of amino acids such as glutamate. Oxaloacetate can also be replenished after anaplerotic entry of other substrates to the Krebs cycle, such as the glutamate residue in GSH. Therefore, we administered GSH or NAC together with [U-^{13}C]glucose 1.5 h after APAP treatment. Additional GSH/NAC treated animals were injected with [U-^{13}C]glucose at 6 h. Figure 4.5 shows the amounts of ^{13}C-labelled glutamate (C-4 position), formed through PDH from [U-^{13}C]glucose (Figure 4.5 D,E), as well as of the Krebs cycle intermediate succinate (Figure 4.5 B,C). Despite ATP depletion, treatment of mice with APAP did not result in a diminished flux through PDH with reduced succinate or glutamate formation at both time points (Figure 4.5 B-E). However, administration of GSH to APAP-treated mice caused a significantly augmented formation of both ^{13}C-labelled glutamate and succinate (more than 4-fold and 2-fold elevation at 2.25 h, respectively), which supports early mitochondrial ATP formation (Figure 4.5 B,D). The stimulating effects on glutamate and succinate formation could still be observed 6.75 h after APAP

administration (Figure 4.5 C,E). The effects of NAC were much less pronounced compared to GSH at 2.25 h (Figure 4.5 B,D) and disappeared at 6.75 h (Figure 4.5 C,E).

High doses of NAC effectively protect against APAP hepatotoxicity.

To evaluate if the difference between GSH and NAC in protecting against APAP toxicity is caused by the different amount of amino acids administered, 3 times higher doses of NAC were injected and the efficacy compared to the 3 individual amino acids of GSH (glutamate, glycine and cysteine) and to a similar dose of only 2 amino acids (glutamate, glycine). Both, the high dose of NAC and the 3 amino acids were more effective than the low NAC group in protecting against APAP-induced toxicity (Figure 4.6 A) and in maintaining liver ATP levels at early and later time points (Figure 4.6 C,D). All three treatments were equally effective in restoring total hepatic GSH levels (Figure 4.6 B). In contrast, treatment with 2 amino acids (lack of cysteine) did not improve the recovery of hepatic GSH levels and failed to protect despite the partial improvement of hepatic ATP levels (Figure 4.6 A-D). The substrate flux through the Krebs cycle correlated with ATP formation in the different treatment groups (Figure 4.8).

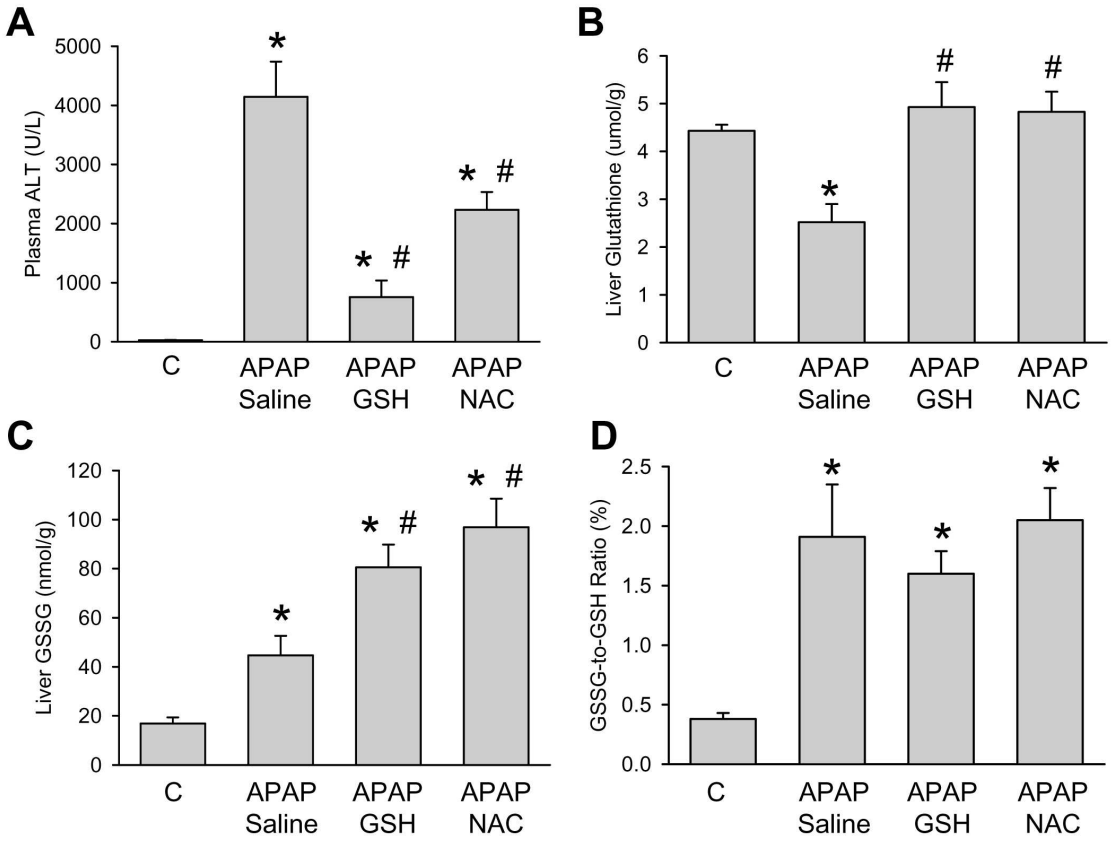
A
Plasma ALT (U/L)
5000
4000
3000
2000
1000
0
C
APAP Saline
APAP GSH
APAP NAC
B
Liver Glutathione (umol/g)
6
5
4
3
2
1
0
C
APAP Saline
APAP GSH
APAP NAC
C
Liver GSSG (nmol/g)
120
100
80
60
40
20
0
C
APAP Saline
APAP GSH
APAP NAC
D
GSSG-to-GSH Ratio (%)
2.5
2.0
1.5
1.0
0.5
0.0
C
APAP Saline
APAP GSH
APAP NAC

Figure 4.1

Figure 4.1

Plasma alanine aminotransferase (ALT) activities (A) and the hepatic content of glutathione (GSH+GSSG) (B) and glutathione disulfide (GSSG) (C) were quantified in control animals or mice treated with 300 mg/kg acetaminophen (APAP) for 6 h. The ratio between GSSG and total glutathione was calculated (D). Some of the animals received additionally 10 ml/kg saline, 0.65 mmol/kg GSH or 0.65 mmol/kg *N*-acetylcysteine (NAC) iv 1.5 h after APAP. Data represent means ± SE of n = 5 animals per group. *P<0.05 (compared to controls); #P<0.05 (compared to APAP/saline)

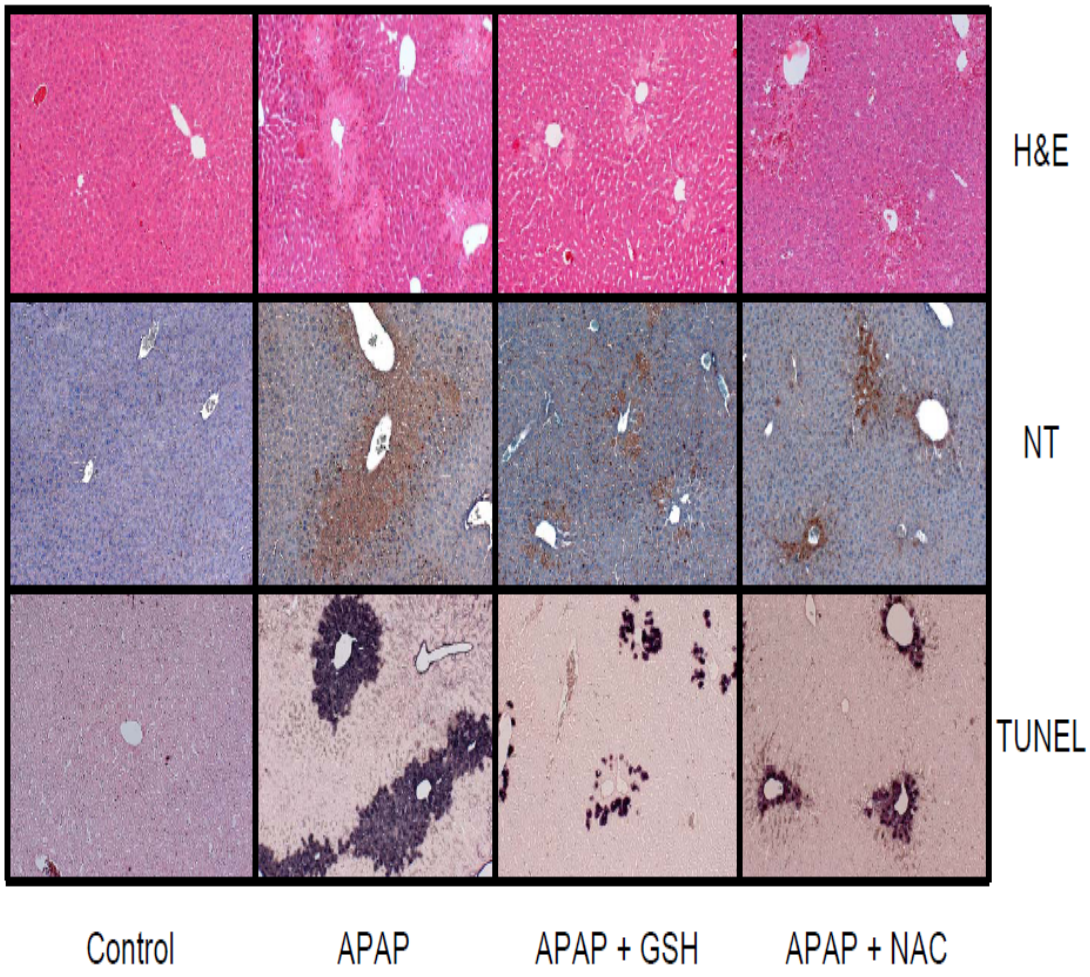

Figure 4.2

Figure 4.2

Histological assessment of liver injury (hematoxilin & eosin, H&E), peroxynitrite formation (nitrotyrosine staining) and DNA fragmentation (TUNEL assay) in control animals or mice treated with 300 mg/kg acetaminophen (APAP) for 6 h. Some of the animals received additionally 10 ml/kg saline, 0.65 mmol/kg GSH or 0.65 mmol/kg *N*-acetylcysteine (NAC) iv 1.5 h after APAP. The representative pictures show extensive centrilobular necrosis, which correlated with the areas of nitrotyrosine staining and TUNEL-positive cells in APAP-treated animals. Both, GSH and NAC treatment improved all parameters with GSH being more effective than NAC. (x100 for all panels)

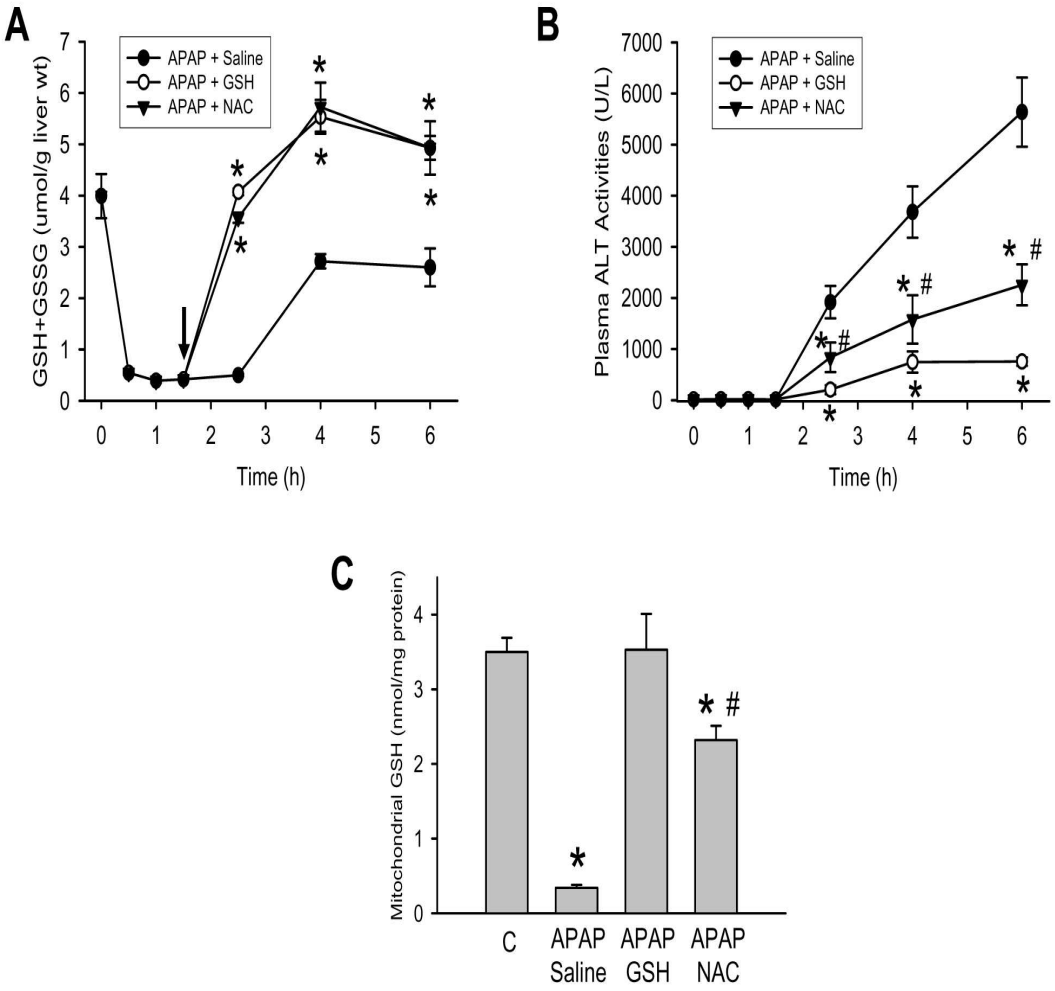
A
GSH+GSSG (umol/g liver wt)
APAP + Saline
APAP + GSH
APAP + NAC
Time (h)
B
Plasma ALT Activities (U/L)
APAP + Saline
APAP + GSH
APAP + NAC
Time (h)
C
Mitochondrial GSH (nmol/mg protein)
C
APAP Saline
APAP GSH
APAP NAC

Figure 4.3

Figure 4.3

Time course of hepatic glutathione (GSH+GSSG) levels (A) and plasma ALT activities (B) after treatment with 300 mg/kg APAP. Some animals received additionally 10 ml/kg saline, 0.65 mmol/kg GSH or 0.65 mmol/kg *N*-acetylcysteine (NAC) iv 1.5 h after APAP. Data represent means ± SE of n = 4 animals per time point. *P<0.05 (compared to APAP/saline); #P<0.05 (compared to APAP/GSH). Mitochondrial glutathione content in controls or 2.5 h after injection of APAP alone or in combination with GSH and NAC (C). Data represent means ± SE of n = 4 animals per group or time point. *P<0.05 (compared to controls, C); #P<0.05 (compared to APAP/GSH)

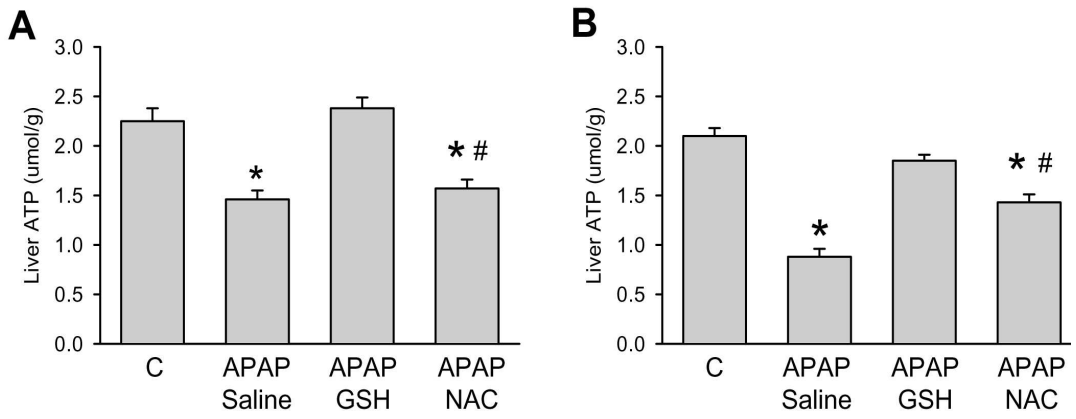
A
B
Liver ATP (umol/g)
3.0
2.5
2.0
1.5
1.0
0.5
0.0
*
* #
C
APAP Saline
APAP GSH
APAP NAC

Figure 4.4

Figure 4.4

Tissue concentrations of ATP (µmol/g wet weight), as calculated from its resonances in ^{31}P-NMR spectra of liver extracts. The mice were treated with 300 mg/kg APAP and some subsequently received 0.65 mmol/kg GSH or NAC at 1.5 h after APAP. ATP levels were measured 2.25 h (A) or 6.75 h (B) after treatment with APAP. Data represent means ± SE of n = 4 animals per group. *P<0.05 (compared to controls, C); #P<0.05 (compared to APAP/GSH)

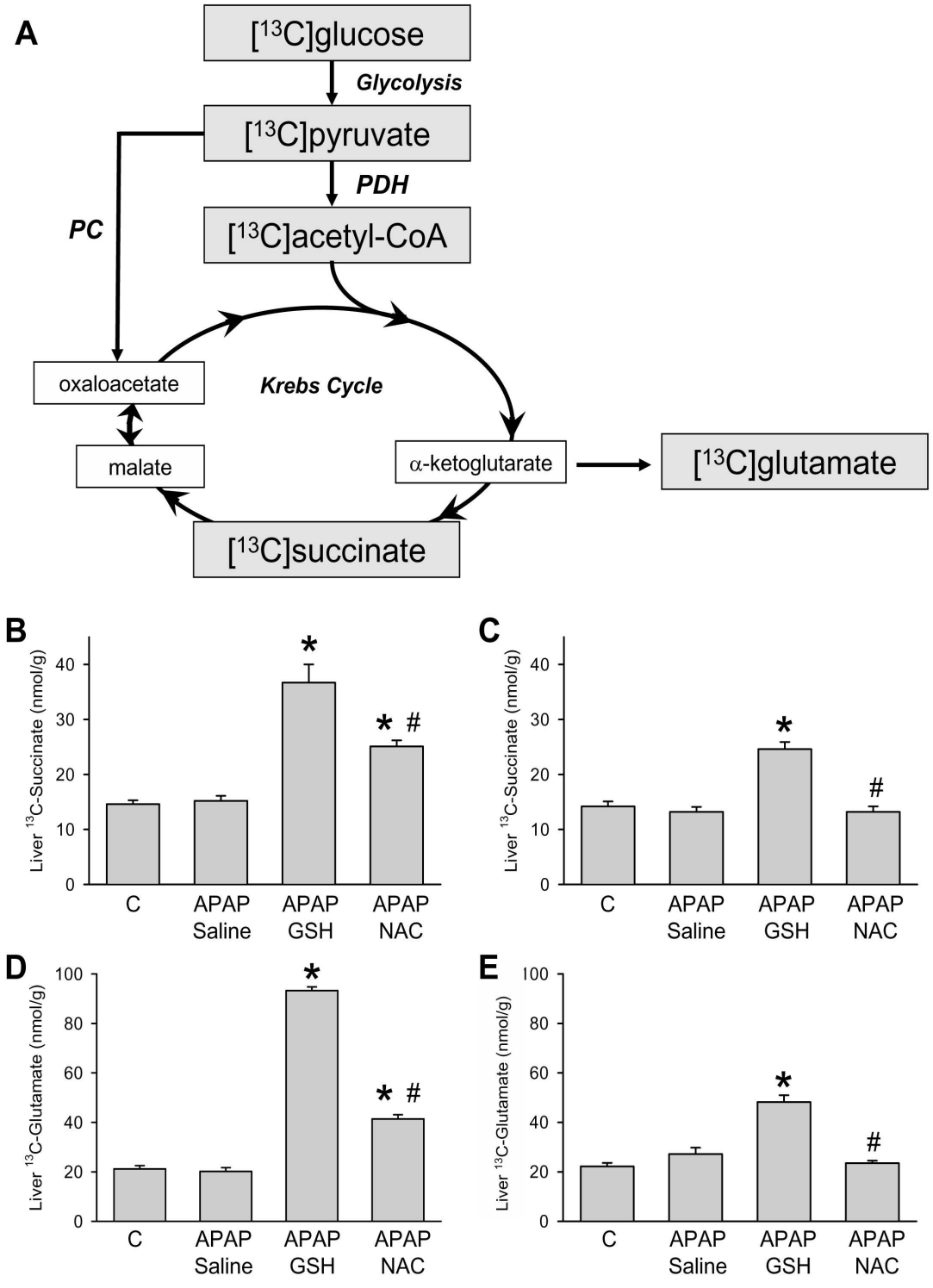
A
[13C]glucose
Glycolysis
[13C]pyruvate
PDH
PC
[13C]acetyl-CoA
oxaloacetate
Krebs Cycle
malate
α-ketoglutarate
[13C]glutamate
[13C]succinate
B
Liver 13C-Succinate (nmol/g)
C
APAP Saline
APAP GSH
APAP NAC
C
Liver 13C-Succinate (nmol/g)
D
Liver 13C-Glutamate (nmol/g)
E
Liver 13C-Glutamate (nmol/g)

Figure 4.5

Figure 4.5

Labeling of glutamate from [U-^{13}C]glucose. [U-^{13}C]glucose is first metabolized to [3-^{13}C]pyruvate, which is converted via pyruvate dehydrogenase (PDH) and pyruvate carboxylase (PC) to [2-13C]acetyl-CoA and [3-^{13}C]oxaloacetate, respectively. The fluxes through PDH and PC lead to a different ^{13}C-labeling pattern in the Krebs cycle intermediate citrate, and are finally measured by the isotopomer pattern of glutamate in ^{13}C-NMR spectra (A). Concentrations of ^{13}C-labelled [4,5-^{13}C]glutamate and the Krebs cycle intermediate [2,3-^{13}C]succinate (nmol/g wet weight), as calculated from their resonances in 1H- and 13C-NMR spectra of liver extracts. The mice were treated with 300 mg/kg APAP and some subsequently received 0.65 mmol/kg GSH or NAC at 1.5 h after APAP. Glutamate (D,E) and succinate (B,C) levels were measured 45 min after injection of [U-^{13}C]glucose, i.e. at 2.25 h after APAP (B,D) or 45 min after injection of [U-^{13}C]glucose , i.e. 6.75 h after APAP (C,E). Data represent means ± SE of n = 4 animals per group. *P<0.05 (compared to controls, C); #P<0.05 (compared to APAP/GSH)

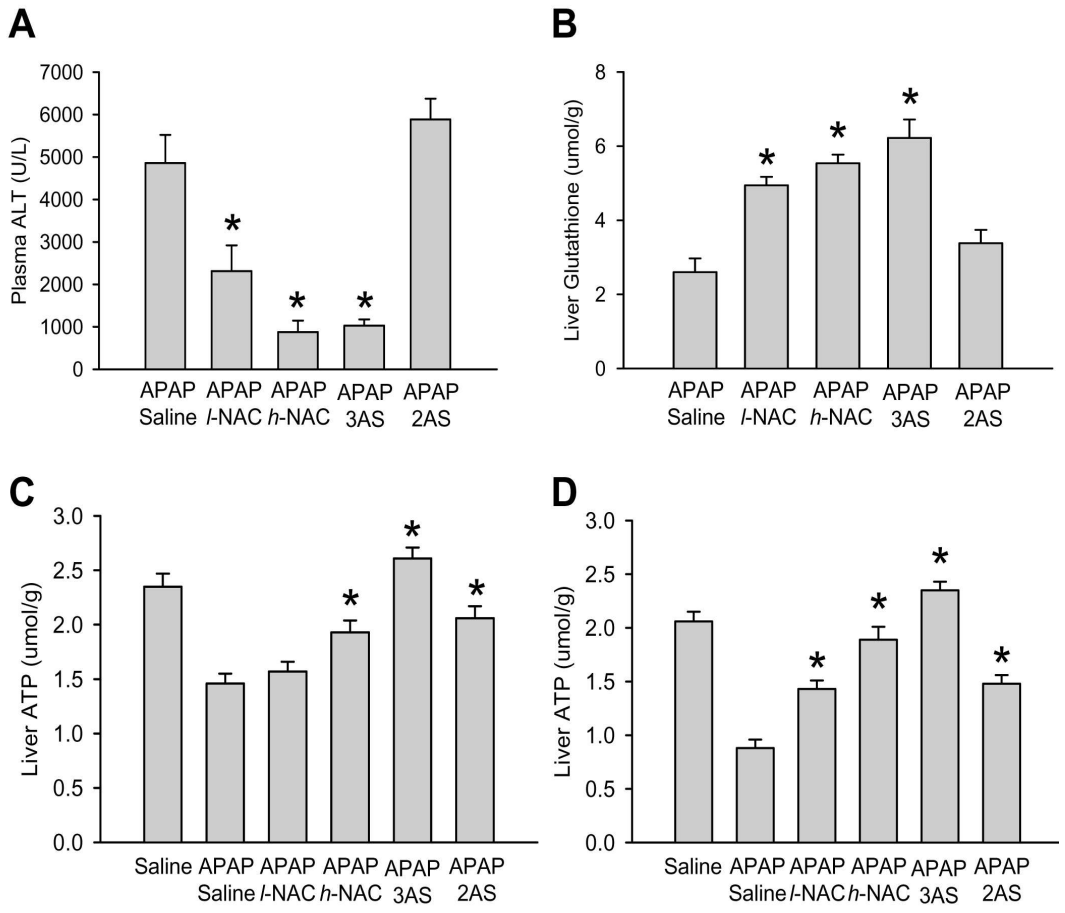
A
Plasma ALT (U/L)
7000
6000
5000
4000
3000
2000
1000
0
APAP Saline
APAP l-NAC
APAP h-NAC
APAP 3AS
APAP 2AS
B
Liver Glutathione (umol/g)
8
6
4
2
0
APAP Saline
APAP l-NAC
APAP h-NAC
APAP 3AS
APAP 2AS
C
Liver ATP (umol/g)
3.0
2.5
2.0
1.5
1.0
0.5
0.0
Saline
APAP Saline
APAP l-NAC
APAP h-NAC
APAP 3AS
APAP 2AS
D
Liver ATP (umol/g)
3.0
2.5
2.0
1.5
1.0
0.5
0.0
Saline
APAP Saline
APAP l-NAC
APAP h-NAC
APAP 3AS
APAP 2AS

Figure 4.6

Figure 4.6

Plasma alanine aminotransferase (ALT) activities (A) and the hepatic content of glutathione (GSH+GSSG) (B) were measured in mice treated with 300 mg/kg acetaminophen (APAP) for 6 h. Some of the animals received additionally 10 ml/kg saline, 0.65 mmol/kg *N*-acetylcysteine (*l*-NAC), 1.95 mmol/kg NAC (*h*-NAC), a mixture of 3 amino acids (0.65 mmol/kg of glycine, glutamic acid and NAC) (3AS) or a mixture of 2 amino acids (0.98 mmol/kg glycine and glutamic acid) (2AS) iv 1.5 h after APAP. Data represent means ± SE of n = 5 animals per group. *P<0.05 (compared to controls); #P<0.05 (compared to APAP/saline). Tissue concentrations of ATP (µmol/g wet weight) (C, D), as calculated from its resonances in ^{31}P-NMR spectra of liver extracts. The mice were treated as under A-B and ATP levels were measured 2.25 h (C) or 6.75 h (D) after treatment with APAP. Data represent means ± SE of n = 4 animals per group. *P<0.05 (compared to APAP/saline)

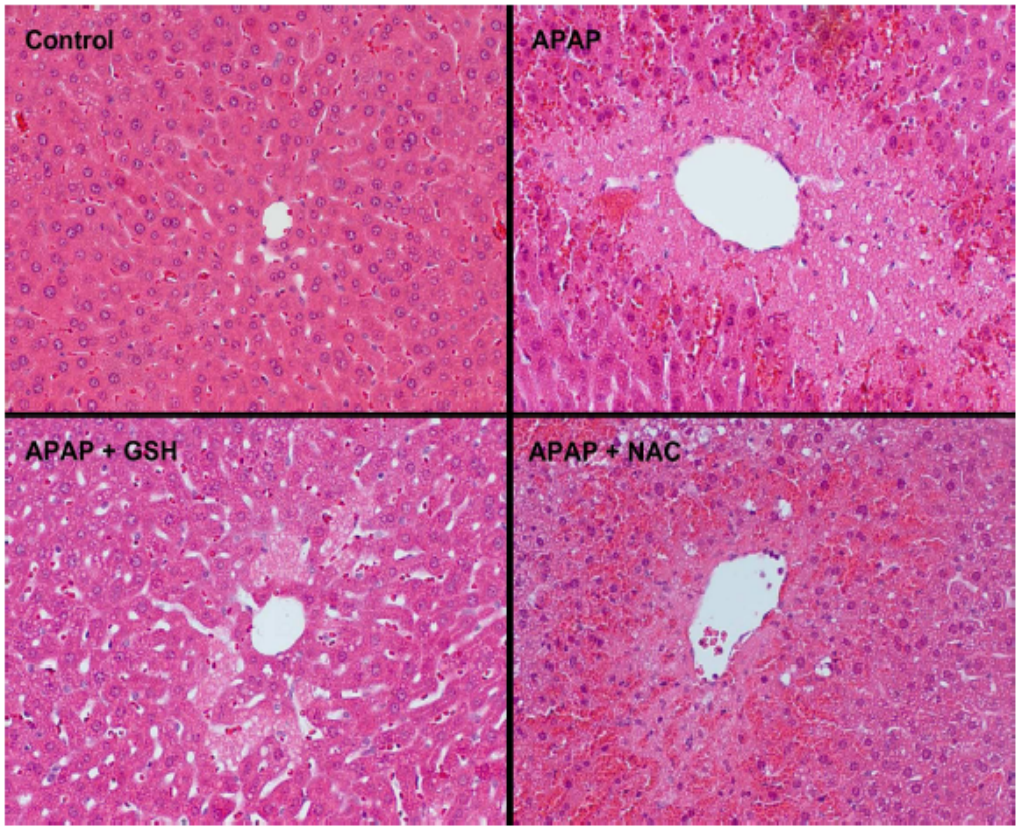

Figure 4.7

Figure 4.7

Histological assessment of liver injury (hematoxilin & eosin, H&E) in control animals or mice treated with 300 mg/kg acetaminophen (APAP) for 6 h. Some of the animals received additionally 10 ml/kg saline, 0.65 mmol/kg GSH or 0.65 mmol/kg *N*acetylcysteine (NAC) iv 1.5 h after APAP. The representative pictures show extensive centrilobular necrosis as indicated by the loss of basophilic staining, vacuolization, cell swelling and karyolysis in APAP-treated animals. Both, GSH and NAC treatment improved the area of necrosis with GSH being more effective than NAC. (x200 for all panels)

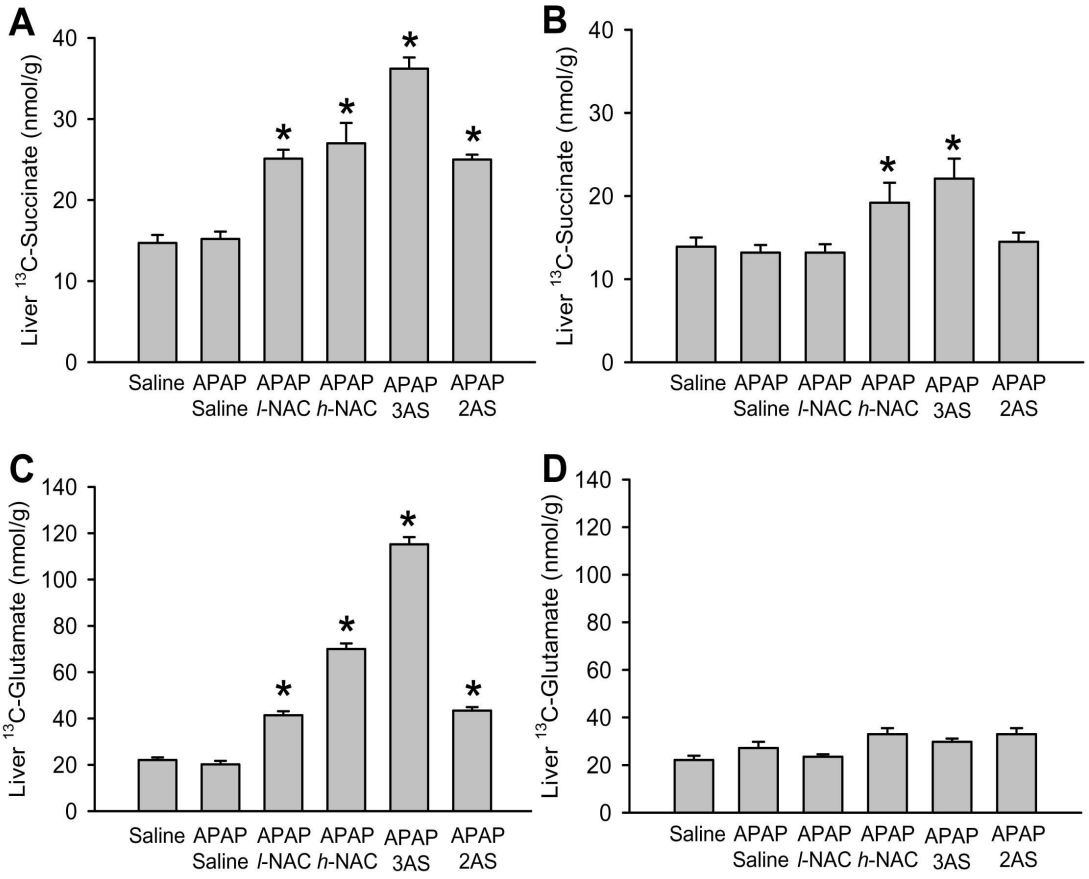
A
B
C
D
Liver ^{13}C-Succinate (nmol/g)
Liver ^{13}C-Glutamate (nmol/g)
0
10
20
30
40
60
80
100
120
140
*
Saline
APAP Saline
APAP l-NAC
APAP h-NAC
APAP 3AS
APAP 2AS

Figure 4.8

Figure 4.8

Concentrations of ^{13}C-labelled [4,5-^{13}C]glutamate and the Krebs cycle intermediate [2,3-^{13}C]succinate (nmol/g wet weight), as calculated from their resonances in ^{1}H- and ^{13}CNMR spectra of liver extracts. The mice were treated with 300 mg/kg APAP and some subsequently received additionally 10 ml/kg saline, 0.65 mmol/kg *N*-acetylcysteine (*l*-NAC), 1.95 mmol/kg NAC (*h*-NAC), a mixture of 3 amino acids (0.65 mmol/kg of glycine, glutamic acid and NAC) (3AS) or a mixture of 2 amino acids (0.98 mmol/kg glycine and glutamic acid) (2AS) iv 1.5 h after APAP. Data represent means ± SE of n =5 animals per group. *P<0.05 (compared to controls)

4.4 Discussion

The objectives of this investigation were to evaluate whether there is a difference in the efficacy to protect against APAP hepatotoxicity between GSH and clinically relevant doses of NAC, and to assess the mechanisms of this protection. The present data indicate that when animals are treated with low equimolar doses of GSH or NAC, GSH is more effective due to the higher amounts of amino acids, which are not only used to re-synthesize hepatic GSH but are also metabolized to serve as energy substrates in the Krebs cycle. This difference in protection between GSH and NAC can be eliminated if higher doses of NAC are used.

***Mechanisms of protection I: preventing covalent binding*.**

The best established and most effective mechanism of protection by GSH or NAC is to enhance the scavenging capacity for NAPQI in hepatocytes. This prevents covalent modification of cellular proteins and thereby blocks the initiation of APAP toxicity (Corcoran *et al.*, 1985; Lauterburg *et al.*, 1983). Intravenously administered GSH is rapidly degraded in the kidney with a half-life in plasma of <2 min and the individual amino acids are re-absorbed (Wendel and Jaeschke, 1982). NAC or the amino acids of GSH are taken up into hepatocytes and are being used for re-synthesis of hepatocellular GSH, which is consumed by conjugation with NAPQI (Corcoran *et al.*, 1985; Corcoran and Wong, 1986; Lauterburg *et al.*, 1983). Despite the capacity of NAC to directly react with NAPQI, it has been clearly demonstrated that the

protection of NAC or GSH against APAP overdose requires the synthesis of GSH (Corcoran *et al.*, 1985; Corcoran and Wong, 1986; Lauterburg *et al.*, 1983; Wendel and Jaeschke, 1982). However, in order to be effective through this mechanism, GSH or NAC has to be administered during the metabolism phase of APAP toxicity. The delayed presentation of overdose patients to the emergency room can limit the efficacy of NAC through this mechanism.

***Mechanisms of protection II: scavenging of reactive oxygen species and peroxynitrite*.** Covalent binding of NAPQI to mitochondrial proteins is a critical step that links the metabolic activation of APAP to the mitochondrial dysfunction (Nelson, 1990). This leads to inhibition of mitochondrial respiration with enhanced formation of reactive oxygen species and peroxynitrite in mitochondria (Cover *et al.*, 2005b; Jaeschke, 1990; Knight *et al.*, 2001; Tirmenstein and Nelson, 1990). The oxidant stress can directly trigger the mitochondrial membrane permeability transition pore opening with collapse of the mitochondrial membrane potential (Kon *et al.*, 2004). In addition, the oxidant stress can activate the cjun N-terminal kinase, which can translocate to the mitochondria and facilitate the mitochondrial membrane permeability transition pore opening (Hanawa *et al.*, 2008). Either mechanism assumes a critical role of mitochondrial reactive oxygen species and peroxynitrite formation in the pathophysiology. The toxicity of these reactive oxygen and reactive nitrogen species is potentiated by the fact that mitochondrial GSH levels are severely depleted during APAP metabolism,

which leaves these cell organelles highly vulnerable (Knight *et al.*, 2001). Thus, delayed treatment with GSH or NAC can accelerate the recovery of mitochondrial GSH levels and scavenge reactive oxygen and reactive nitrogen species (James *et al.*, 2003c; Knight *et al.*, 2002). Despite the initial covalent binding, this treatment limits cellular necrosis, improves survival and facilitates repair of the damaged tissue (Bajt *et al.*, 2003). Thus, a critical second mechanism of protection by NAC and GSH is the protection against oxidant stress and peroxynitrite specifically in mitochondria.

Mechanisms of protection III: mitochondrial energy substrates. The higher efficacy of GSH versus an equimolar dose of NAC in protecting against APAP suggests the involvement of a third mechanism. As was shown, both GSH and NAC provide enough cysteine to allow for an effective re-synthesis of the depleted cellular GSH levels. However, two critical differences between GSH- and NAC-treated animals emerged. First, cellular ATP levels were significantly better preserved with GSH treatment than with NAC. Based on the higher substrate supply for the Krebs cycle, this was most likely caused by the use of the excess amino acids not needed for GSH synthesis as energy substrates. The higher ATP levels support energy-requiring cellular functions including the maintenance of ion gradients by Na^+/K^+-ATPase and Ca^{2+}-ATPase. Dysfunction of these enzymes has been implicated in necrotic cell death (Carini *et al.*, 1995; Tsokos-Kuhn *et al.*, 1988). Although the Km of ATP for transporters and enzymes is lower than the declining tissue ATP

levels after APAP treatment, it needs to be kept in mind that these concentrations represent the average in tissue homogenates, which includes healthy as well as dying cells. Thus, one would expect that ATP levels in cells of the centrilobular area are much lower than the average, and may well be in the range of the Km for ATP-dependent transporters and enzymes. In addition, the improved energy supply to mitochondria may be responsible for the accelerated uptake of cytosolic GSH into mitochondria, as was observed after GSH treatment. GSH is transported into mitochondria by the dicarboxylate carrier and the oxoglutarate carrier, which mediate electroneutral exchange of dicarboxylates for inorganic phosphate and 2-oxoglutarate for other dicarboxylates, respectively (Fernandez-Checa and Kaplowitz, 2005; Lash, 2006; Zhong *et al.*, 2008). During the post-metabolism phase of APAP toxicity, mitochondrial GSH is most critical for the effective scavenging of reactive oxygen species and specifically peroxynitrite (Knight *et al.*, 2002). The higher mitochondrial GSH levels and the reduced areas of nitrotyrosine staining correlated with the reduced areas of necrosis after GSH compared to NAC treatment. Supply of cysteine without providing additional energy substrates leads to sub-optimal protection as was observed with NAC treatment. However, supply of excess amino acids without cysteine leads to a partial recovery of ATP levels without GSH synthesis, but fails to prevent liver cell necrosis. This indicates that just supporting mitochondrial energy metabolism alone is insufficient to prevent cell death. These data extend previous data

obtained on the effects of NAC and GSH in non-acetaminophen toxicity in mice. In particular, NAC significantly increased the flux through PDH, an effect which has been shown to be uncoupled from GSH synthesis, and was associated with the prevention of liver injury induced by tert-butylhydroperoxide and 3-nitropropionic acid. This study also showed that NAC has a limited capacity to increase GSH de novo synthesis, but that the administration of the GSH precursor cysteine alone in equimolar concentrations to NAC does not protect from a disturbed mitochondrial energy metabolism (Zwingmann and Bilodeau, 2006). The present study provides evidence that injection of GSH itself or of excess amino acids in APAP-treated animals clearly results in a better recovery of ATP levels. It further suggests a dual role of GSH supplementation in prevention of mitochondrial energy failure together with cellular GSH supply. This would also explain the higher efficiency when increasing the NAC doses and therefore of the amino acid cysteine. Thus, based on these observations it can be concluded that a combination of cysteine supply for glutathione synthesis and excess amino acids for metabolism in the Krebs cycle provides the most effective protection against APAP-induced mitochondrial dysfunction and necrotic cell death during the later, postmetabolism phase of the injury. This effect can be achieved by injection of either GSH or NAC in sufficient quantities. Although the present data show that at a dose of 0.65 mmol/kg GSH is more effective than NAC, the effect is clearly caused by the 3-fold

higher amount of amino acids injected with GSH compared to an equimolar dose of NAC. In fact, a 3-fold higher dose of NAC shows equally effective protection as with GSH or the mixture of the individual amino acids of GSH. Because the practice guidelines for the use of NAC recommend much higher doses than would be needed for the re-synthesis of hepatic GSH levels alone (Polson and Lee, 2005), our data suggest that the reason for the efficacy of high doses of NAC at these later time points is caused by recovery of hepatic and in particular mitochondrial GSH levels, and the improved mitochondrial bioenergetics.

In summary, our data indicate that the amino acids supplied with the delayed treatment of GSH or NAC are being used for the re-synthesis of hepatic glutathione levels, which protect against cell injury by scavenging reactive oxygen species and peroxynitrite in mitochondria. However, excess amino acids, i.e. amino acids not used for GSH synthesis, serve as energy substrates for the Krebs cycle and support the improved maintenance of hepatic ATP levels. Thus, the optimal protection by delayed GSH or NAC treatment involves the combination of two mechanisms, i.e., the accelerated recovery of mitochondrial GSH levels and support of the mitochondrial bioenergetics. These new findings provide the rationale for the clinical use of high doses of NAC well beyond the metabolism of APAP. In addition, these data suggest that more effective substrates for the mitochondrial energy metabolism than excess NAC may further limit cell death and improve

regeneration after APAP overdose.

CHAPTER 5: MECHANISM OF PROTECTION BY METALLOTHIONEIN AGAINST ACETAMINOPHEN HEPATOTOXICITY

5.1 Abstract.

Acetaminophen (APAP) overdose is the most frequent cause of drug-induced liver failure in the US. Metallothionein (MT) expression attenuates APAP-induced liver injury. However, the mechanism of this protection remains incompletely understood. To address this issue, C57BL/6 mice were treated with 100 μmol/kg $ZnCl_2$ for 3 days to induce MT. Twenty-four hours after the last dose of zinc, the animals received 300 mg/kg APAP. Liver injury (plasma ALT activities, area of necrosis), DNA fragmentation, peroxynitrite formation (nitrotyrosine staining), MT expression, hepatic glutathione (GSH) and glutathione disulfide (GSSG) levels were determined 6 h after APAP alone caused severe liver injury with oxidant stress (increased GSSG levels), peroxynitrite formation and DNA fragmentation, all of which were attenuated by zinc-induced MT expression. In contrast, MT knockout mice were not protected by zinc. Hydrogen peroxide-induced cell injury in primary hepatocytes was dependent only on the intracellular GSH levels but not on MT expression. Thus, the protective effect of MT *in vivo* was not due to the direct scavenging of reactive oxygen species and peroxynitrite. Zinc treatment had no effect on the early GSH depletion kinetics after APAP administration, which is an indicator of the metabolic activation of APAP to its reactive metabolite

N-acetyl-*p*-benzoquinoneimine (NAPQI). However, MT was able to effectively trap NAPQI by covalent binding. We conclude that MT scavenges some of the excess NAPQI after GSH depletion and prevents covalent binding to cellular proteins, which is the trigger for the propagation of the cell injury mechanisms through mitochondrial dysfunction and nuclear DNA damage.

5.2 Introduction.

Acetaminophen (APAP) is a widely used analgesic and antipyretic drug. Although safe at therapeutic levels, an overdose can cause severe liver injury in animals and in humans (Larson *et al.*, 2005). The toxicity is dependent on the metabolic activation of APAP via cytochrome P-450, which results in the formation of an electrophilic reactive metabolite, *N*-acetyl-*p*-benzoquinone imine (NAPQI) (Nelson, 1990). NAPQI is rapidly conjugated with glutathione (GSH) and the GSH-APAP adduct is excreted mainly into bile (Nelson, 1990). However, after the cellular GSH content is exhausted, NAPQI covalently binds to cellular proteins (Cohen and Khairallah, 1997; Jollow *et al.*, 1973) including mitochondrial proteins (Qiu *et al.*, 2001; Tirmenstein and Nelson, 1989). This covalent binding is thought to be responsible for the mitochondrial dysfunction observed after APAP overdose, including inhibition of mitochondrial respiration, ATP depletion, release of intermembrane proteins, and mitochondrial oxidant stress and peroxynitrite formation (Jaeschke and Bajt, 2006). The characteristic nuclear DNA damage

after APAP overdose (Ray *et al.*, 1990) is initially linked to mitochondrial Bax translocation (Bajt *et al.*, 2008) and later to oxidant stress/peroxynitrite formation and mitochondrial dysfunction (Cover *et al.*, 2005b). The opening of mitochondrial membrane permeability transition (MPT) pores with collapse of the membrane potential and declining ATP levels (Kon *et al.*, 2004) together with the extensive nuclear DNA damage (Shen *et al.*, 1991) are the main reasons for the massive oncotic necrotic cell death after APAP overdose (Gujral *et al.*, 2002). In addition to the intracellular signaling pathways of APAP-induced liver injury, a potential contribution of inflammatory cells is extensively but controversially discussed (Jaeschke, 2005, 2008; Liu *et al.*, 2006). For example, investigations into the role of neutrophils yielded opposite results using the same neutropenia-inducing antibody (Cover *et al.*, 2006; Liu *et al.*, 2006). We suggested that the different results were caused by the prolonged pretreatment regimen in one of the studies that lead to a preconditioning effect with induction of several acute phase genes, in particular metallothionein (MT) (Jaeschke and Liu, 2007). Upregulation of any of these genes rather than neutropenia could have been the reason for the protection of the anti-neutrophil antibody. However, in order to address this complex problem, it is necessary to understand the mechanism by which some of these individual genes including MT could protect against APAP-induced hepatotoxicity.

MT, a ubiquitous heavy metal binding and cysteine-rich protein (Klaassen *et al.*, 1999), has been suggested to react with free radicals and organic electrophiles (Cagen and Klaassen, 1980). Studies of APAP hepatotoxicity demonstrated enhanced liver injury and mortality in metallothionein-deficient mice (Liu *et al.*, 1999; Rofe *et al.*, 1998). In addition, induction of MT attenuated APAP-induced liver injury (Chengelis *et al.*, 1986; Szymanska *et al.*, 1991). The modulation of toxicity was independent of the P450 levels and the metabolic activation of APAP (Liu *et al.*, 1999; Rofe *et al.*, 1998). In contrast, the protection appeared to be correlated with an antioxidant function of MT (Liu *et al.*, 1999). However, no direct evidence for this mechanism exists *in vivo*. In particular, it remains unclear whether MT can actually scavenge reactive oxygen species (ROS) and peroxynitrite, which are critical mediators of MPT and cell death (Jaeschke *et al.*, 2003). Thus, the main objective of this investigation was to investigate the mechanism by which induction of MT gene expression may protect against APAP hepatotoxicity *in vivo*.

5.3 Results.

Hepatic MT induction by $ZnCl_2$.

Treatment with a non-toxic dose of $ZnCl_2$ for 3 days resulted in a 100-fold increase of MT-1 mRNA expression and a 190-fold increase in MT-2 (Figure 5.1 A). No other gene quantified showed a significant change including

CuZnSOD, MnSOD, GPx1, catalase, HO-1, HSP70, TNF-α, IL-1β, IL-10, KC, MIP-2, iNOS or ICAM-1 (data not shown). Similar gene expression profiles were recently reported for the same dose of $ZnCl_2$ given over 4 days (Liu *et al.*, 2009). The increase in MT mRNA translated into extensive MT protein expression, as indicated by western blot analysis (Figure 5.1 B) and immunohistochemical staining of liver sections (Figure 5.1 C).

Hepatic MT induction protects against APAP toxicity.

A dose of 300 mg/kg of APAP-induced severe liver injury at 6 h as indicated by the increase in plasma ALT activities and extensive liver necrosis (Figure 5.2, 5.3). Pretreatment with $ZnCl_2$ attenuated the increase in plasma ALT levels by 68% and reduced the area of necrosis by 62% compared to APAP alone (Figure 5.2, 5.3). A similar protective effect was observed at 24 h (data not shown). To investigate the mechanism of protection, liver sections were stained for nitrotyrosine protein adducts, which is an indicator of peroxynitrite formation, and the TUNEL assay, an indicator for nuclear DNA fragmentation. Whereas there was no nitrotyrosine or TUNEL staining in untreated controls (data not shown), extensive centrilobular areas stained positive for both nitrotyrosine and DNA fragmentation 6 h after APAP treatment (Figure 5.3). The staining correlated with the area of necrosis as assessed in H&E stained sections (Figure 5.3). Pretreatment with $ZnCl_2$ substantially reduced both nitrotyrosine staining and the number of TUNEL-positive cells (Figure 5. 3). Because most peroxynitrite is being formed in mitochondria (Cover *et al.*,

2005b), these data suggest that MT induction either prevented the mitochondrial oxidant stress or scavenged peroxynitrite.

MT induction prevents against APAP-induced oxidant stress.

In a previous study, we demonstrated that ROS (mainly hydrogen peroxide) but not peroxynitrite was responsible for GSSG formation in the liver after APAP overdose (Knight *et al.*, 2002). To assess whether MT can scavenge hydrogen peroxide *in vivo*, hepatic GSH and GSSG levels were measured in the liver (Figure 5.4). At 6 h after APAP treatment, total glutathione (GSH+GSSG) levels only partially recovered (Figure 5.4 A), the GSSG content was significantly increased (Figure 5.4 B) and the GSSG-to-GSH ratio was increased from 0.5% to 2.5% (Figure 5.4 C). The data indicate a significant oxidant stress in these livers consistent with previous reports that identified this GSSG increase as being predominantly in mitochondria (Jaeschke, 1990; Knight *et al.*, 2001). Induction of MT with $ZnCl_2$ improved the recovery of hepatic GSH levels, attenuated the increase in GSSG content and significantly reduced the GSSG-to-GSH ratio (Figure 5.4 A-C). These results suggest that MT induction attenuated the formation of reactive oxygen species *in vivo* rather than scavenged them. To directly assess whether MT is able to scavenge reactive oxygen species in intact cells, isolated mouse hepatocytes were exposed to various concentrations of hydrogen peroxide (H_2O_2), the ROS most likely responsible for the elevated GSSG levels. H_2O_2 dose-dependently caused cell injury as indicated by LDH release (Figure 5.5

A,B). However, pretreatment with $ZnCl_2$ did not affect the injury in normal cells. In contrast, prior depletion of GSH substantially aggravated H_2O_2 – induced cell death (Figure 5.5 A,B). In agreement with these results, $ZnCl_2$ – pretreatment did not affect cell injury in GSH-depleted hepatocytes (data not shown). Together these data suggest that intracellular GSH was able to detoxify H_2O_2 diffusing into the cell. However, intracellular MT expression did not impact ROS-mediated toxicity indicating that MT, in contrast to GSH, did not detoxify H_2O_2. Overall, the combined *in vitro* and *in vivo* data suggest that MT prevented APAP-induced ROS formation rather than scavenged ROS.

MT induction did not affect NAPQI formation.

The fact that MT induction prevented the oxidant stress indicates that MT must have acted upstream of mitochondria. To evaluate whether $ZnCl_2$ treatment affected NAPQI formation, the initial depletion kinetics of GSH was measured. During the first 20 min after APAP injection, the rapid decline of hepatic GSH levels is caused almost exclusively by NAPQI formation (Jaeschke, 1990). Controls and $ZnCl_2$ – treated animals showed a similar rate of GSH loss during the first 20 min (Figure 5.6). However, livers from $ZnCl_2$ – treated mice had significantly higher basal GSH levels than livers from control animals (Figure 5.6). The difference was maintained during the first 20 min and disappeared when GSH depletion in controls slowed down more rapidly compared to the $ZnCl_2$ - treated animals (Figure 5.6). Together, these data suggest that NAPQI formation was not impaired by MT induction, but the

livers from $ZnCl_2$ - treated animals had a higher capacity to detoxify NAPQI. The slightly higher GSH level may have been a contributing factor but was unlikely the only reason for the effective protection against APAP-induced liver injury.

MT can scavenge and covalently bind NAPQI.

Because MT induction did not reduce NAPQI formation but prevented the mitochondrial oxidant stress, which is assumed to be caused by NAPQI binding to mitochondrial proteins, the only remaining intervention point could be the direct scavenging of NAPQI by MT. To test this hypothesis, a solution of purified MT (1 mg/ml) was mixed with NAPQI solution (12 µg/ml) at 4^oC and transferred immediately or after 2 h of incubation at 4^oC to the loop of an HPLC connected online to a mass spectrometer and analyzed as indicated in material and methods (Figure 5.7). As a control sample, an aliquot of MT kept under the same conditions, but without the addition of NAPQI, was analyzed under the identical conditions. This control sample showed multiple ions in the m/z range 1537-1566, corresponding to the +4 charge state of the protein (Figure 5.7 A). This is consistent with the presence of several isoforms of MT in the commercially available form of the protein. Mixing of MT with NAPQI resulted in the immediate disappearance of the ions at m/z range 1537-1566 with a time-dependent formation of a series of ions at a higher m/z range (1592-1644) (Figure 5.7 B). Four of these ions, at m/z at 1637.6, 1643.7, 1666.4 and 1671.7, are clearly newly formed. Other ions, at m/z at 1592.7,

1611.6 and 1618.3, appear on top of small ions present in the commercial preparation of MT. However, their relative change in intensity indicates that these ions are also the result of the reaction of NAPQI with MT. The dead time between the addition of NAQPI and the injection on the loop of the HPLC to start the chromatographic separation was 20 sec. This reaction is complete following 2 h incubation at 4^{o}C (Figure 5.7 C). Because of the complexity of the resulting mass spectra, the exact pair of shifts in mass can not be determined with absolute certainty. However, given the accuracy of the mass measurement and the fact that the reaction of NAPQI with proteins results in an increase in mass of 149.1 Dalton (Hoos *et al.*, 2007), it is possible to assume that most of the isoforms of MT reacted with one, two or three molecules of NAPQI, resulting in a shift of 149 Dalton (from m/z 1554.6 to m/z 1592.8), 298 Dalton (from m/z 1537.1, 1545.2, 1561.2 to 1565.6 to 1611.6, 1683.3, 1637.6 and 1643.7, respectively) or 447 Dalton (from m/z 1554.7 and 1561.2 to 1565.4 and 1671.6, respectively).

MT induction is responsible for $ZnCl_2$-induced protection against APAP-induced hepatotoxicity.

To verify that MT gene expression was indeed the mechanism by which Zn reduced APAP-induced liver injury, 129S1/SvImJ wildtype and MT-deficient mice were treated with APAP for 6 h. Based on plasma ALT activities and the area of necrosis, APAP caused severe liver injury, which was significantly attenuated in Zn-treated wildtype animals but not in MT-deficient mice (Figure

5.8). These data support the conclusion that MT gene expression is the main mechanism of protection of the Zn treatment regimen employed in this study.

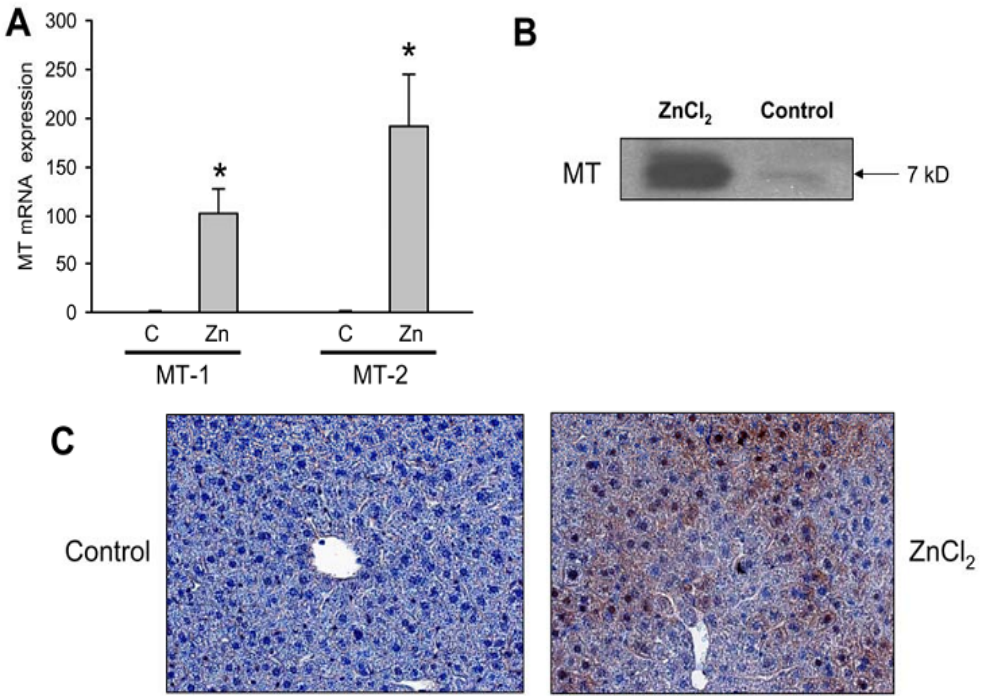
A
300
250
200
150
100
50
0
MT mRNA expression
*
*
C
Zn
C
Zn
MT-1
MT-2
B
ZnCl2
Control
MT
7 kD
C
Control
ZnCl2

Figure 5.1

Figure 5.1

Quantitative real-time PCR was used to analyze for MT-1 and MT-2 mRNA expression in livers of animals treated with saline (6 ml/kg) (controls, C) or 100 µmol/kg $ZnCl_2$ for 3 days. MT mRNA is expressed as the MT-to-actin ratio (A). Data represent mean $\pm$ SE of n = 4 animals *P<0.05 (compared to C). Western blot analysis of MT protein in controls and $ZnCl_2$-treated animals (B). Immunohistochemical analysis of MT expression in control liver compared to the liver of a $ZnCl_2$-treated animal (C).

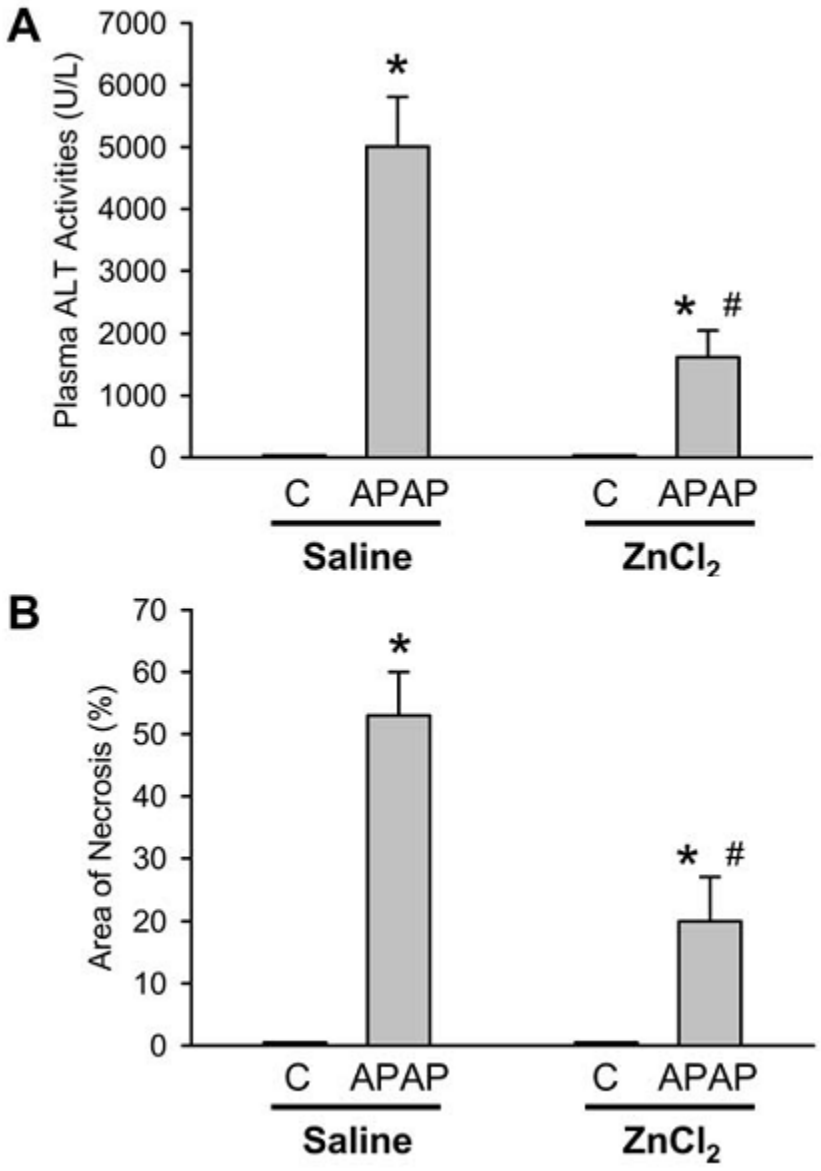
A
Plasma ALT Activities (U/L)
7000
6000
5000
4000
3000
2000
1000
0
*
* #
C
APAP
C
APAP
Saline
ZnCl2
B
Area of Necrosis (%)
70
60
50
40
30
20
10
0
*
* #
C
APAP
C
APAP
Saline
ZnCl2

Figure 5.2

Figure 5.2

Liver injury was evaluated by measuring plasma alanine aminotransferase (ALT) activities (panel A) and quantitating the area of necrosis (panel B) in untreated animals (C) and 6 h after injection of 300 mg/kg acetaminophen (APAP). Animals were either treated with saline (6 ml/kg) or 100 µmol/kg $ZnCl_2$ for 3 days. APAP was injected 24 h after the last dose of Zn/saline. Data represent means ± SE of n = 5 animals per group. *P<0.05 (compared to C) #P<0.05 (compared to APAP/saline)

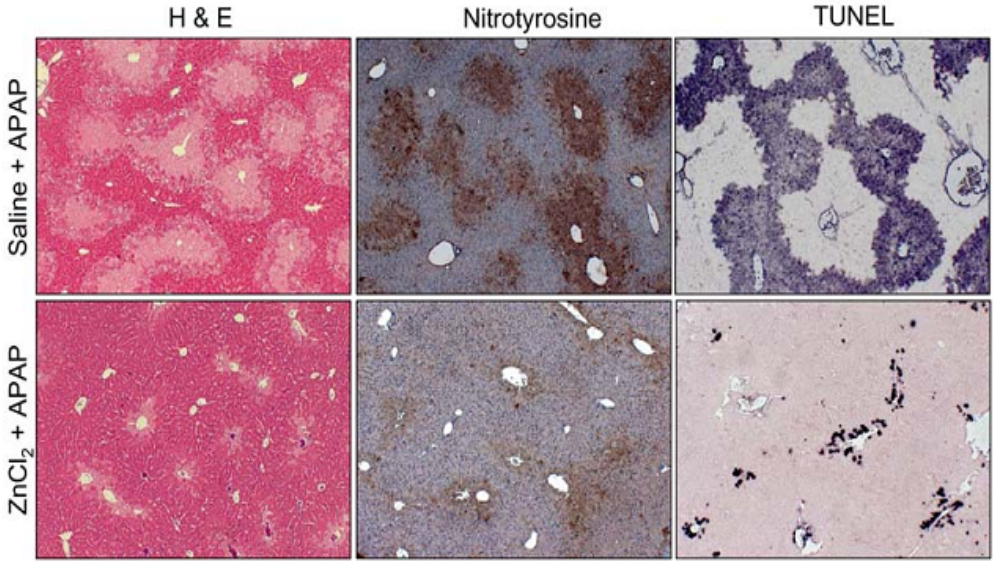

Figure 5.3

Figure 5.3

Representative liver sections of animals treated for 6 h with 300 mg/kg acetaminophen were stained with H&E (assess area of necrosis), a nitrotyrosine antibody (marker of peroxynitrite formation) and the TUNEL assay (marker for DNA strandbreaks). Animals were either treated with saline (6 ml/kg) or 100 µmol/kg ZnCl2 for 3 days. APAP was injected 24 h after the last dose of Zn/saline. (magnification of all graphs: x50)

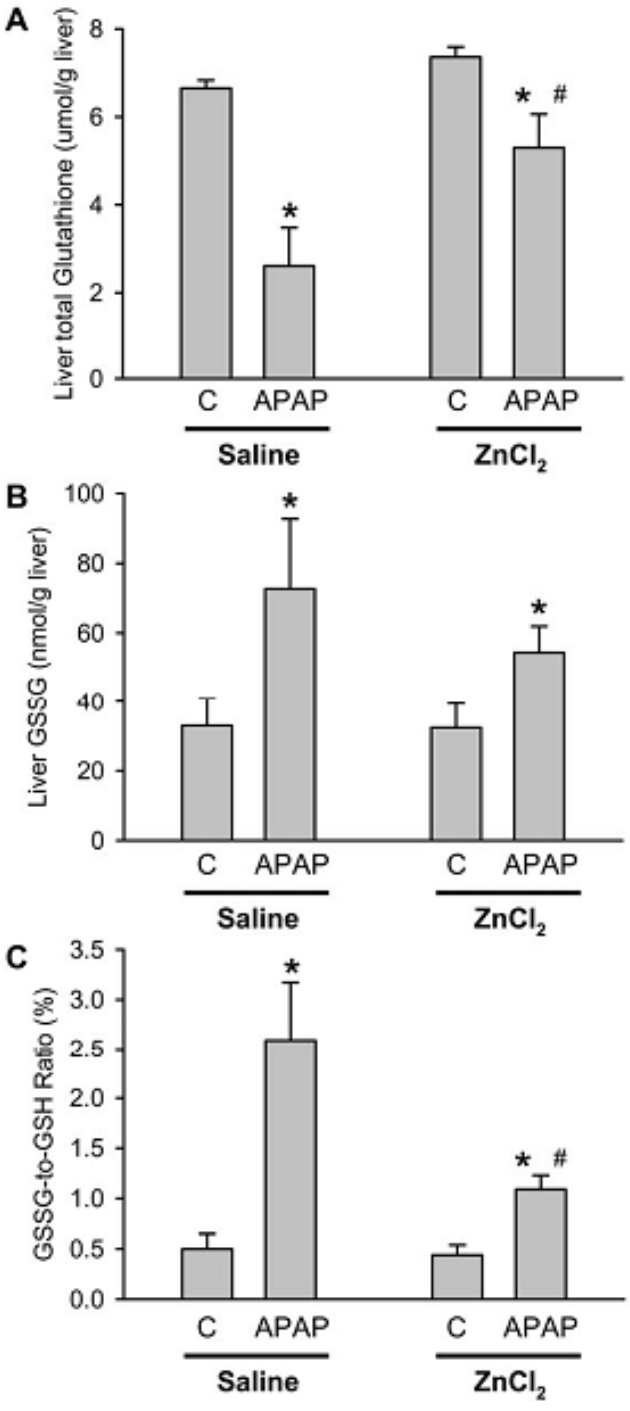
A
Liver total Glutathione (umol/g liver)
0
2
4
6
8
*
* #
C
APAP
C
APAP
Saline
ZnCl2
B
Liver GSSG (nmol/g liver)
0
20
40
60
80
100
*
*
C
APAP
C
APAP
Saline
ZnCl2
C
GSSG-to-GSH Ratio (%)
0.0
0.5
1.0
1.5
2.0
2.5
3.0
3.5
*
* #
C
APAP
C
APAP
Saline
ZnCl2

Figure 5.4

Figure 5.4

Total glutathione (GSH+GSSG) (panel A) and glutathione disulfide (GSSG) (panel B) levels were measured and the GSSG-to-GSH ratio (panel C) was calculated 6 h after treatment with 300 mg/kg APAP. Animals were either treated with saline (6 ml/kg) or 100 µmol/kg $ZnCl_2$ for 3 days. APAP was injected 24 h after the last dose of Zn/saline. Data represent means ± SE of n = 5 animals per group. *P<0.05 (Compared to APAP)

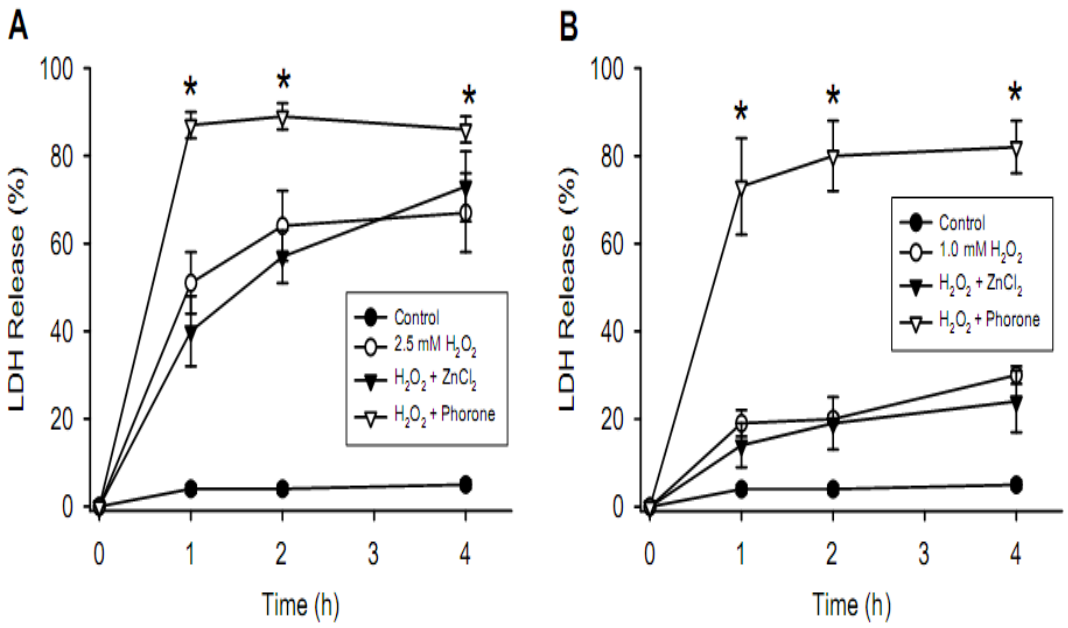
A
B
LDH Release (%)
Time (h)
Control
2.5 mM H_2O_2
1.0 mM H_2O_2
H_2O_2 + $ZnCl_2$
H_2O_2 + Phorone
*

Figure 5.5

Figure 5.5

Primary cultured murine hepatocytes were exposed to various concentrations of hydrogen peroxide (H_2O_2) or vehicle (culture medium) for up to 4 h and cell injury was measured as % of released lactate dehydrogenase (LDH). Animals used for cell isolation were either untreated or received 100 µmol/kg $ZnCl_2$ for 3 days or 100 mg/kg phorone 90 min before isolation. All cells isolated from phorone-treated animals were cultured in the presence of 1 mM buthionine sulfoximine to inhibit GSH synthesis. All data represent means ± SE of 4 independent time course experiments. *$P<0.05$ (compared to H_2O_2 alone)

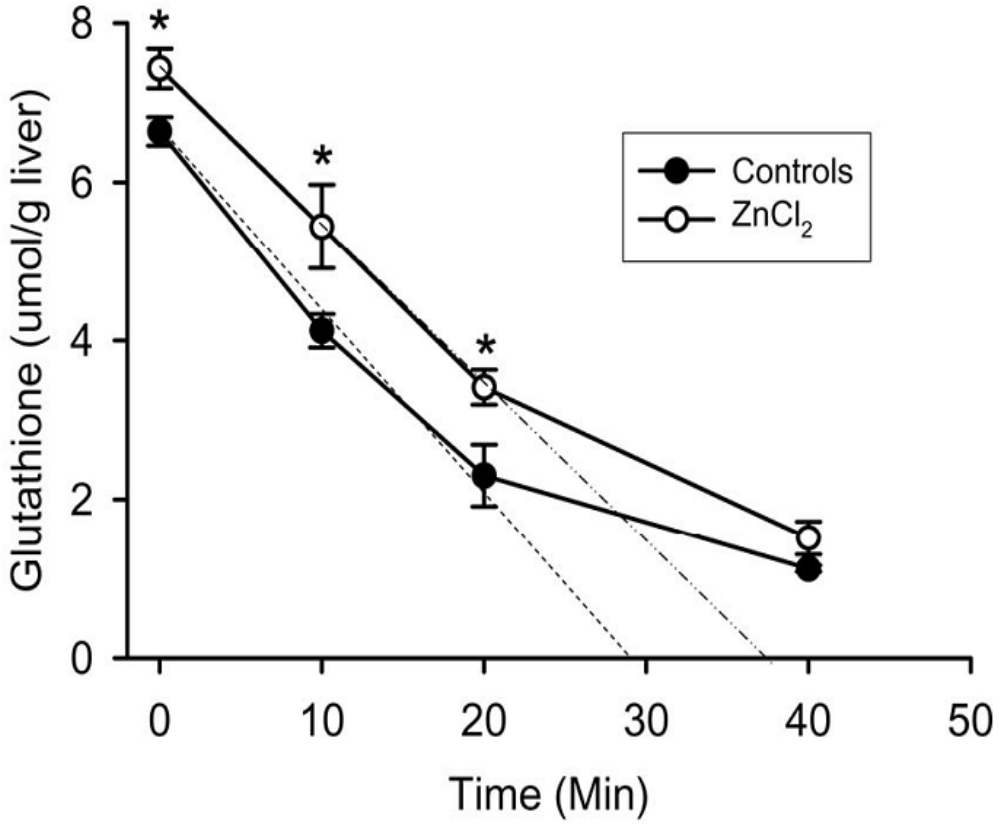
Glutathione (umol/g liver)
Time (Min)
Controls
ZnCl2
0
2
4
6
8
0
10
20
30
40
50
*
*
*

Figure 5.6

Figure 5.6

Hepatic glutathione levels (GSH+GSSG) were measured at early time points (0 – 40 min) after administration of 300 mg/kg acetaminophen. Animals were either treated with saline (6 ml/kg) or 100 µmol/kg $ZnCl_2$ for 3 days. APAP was injected 24 h after the last dose of Zn/saline. Data represent means ± SE of n = 5 animals per group. *P<0.05 (compared to controls)

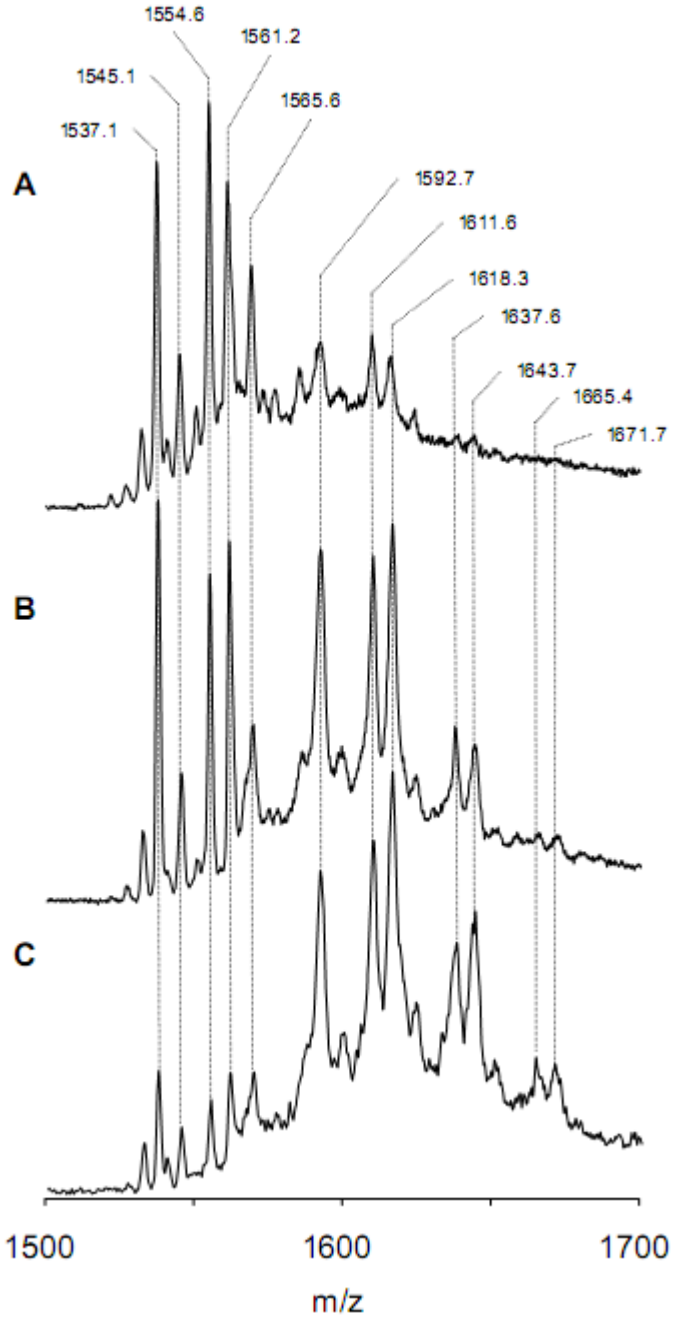
1554.6
1561.2
1545.1
1565.6
1537.1
A
1592.7
1611.6
1618.3
1637.6
1643.7
1665.4
1671.7
B
C
1500
1600
1700
m/z

Figure 5.7

Figure 5.7

Rabbit liver MT was analyzed by reverse phase chromatography/mass spectrometry as described in the experimental procedures. The figure shows the +4 charge state protein ions obtained on the IT of the control sample. An aliquot of MT that was not reacted with NAPQI (A), or following the addition of NAPQI and incubation at 4 °C for 20 sec (B) or 2h (C). For each panel, data are reported as percentage relative to the most intense ion. Thus, the progress of the reaction is indicated by a change in the relative intensities of the ions present at each experimental time. There is a decrease of the intensity of the ions in the m/z range 1537-1565 with a concomitant increase of the ions in the m/z range 1592-1671.

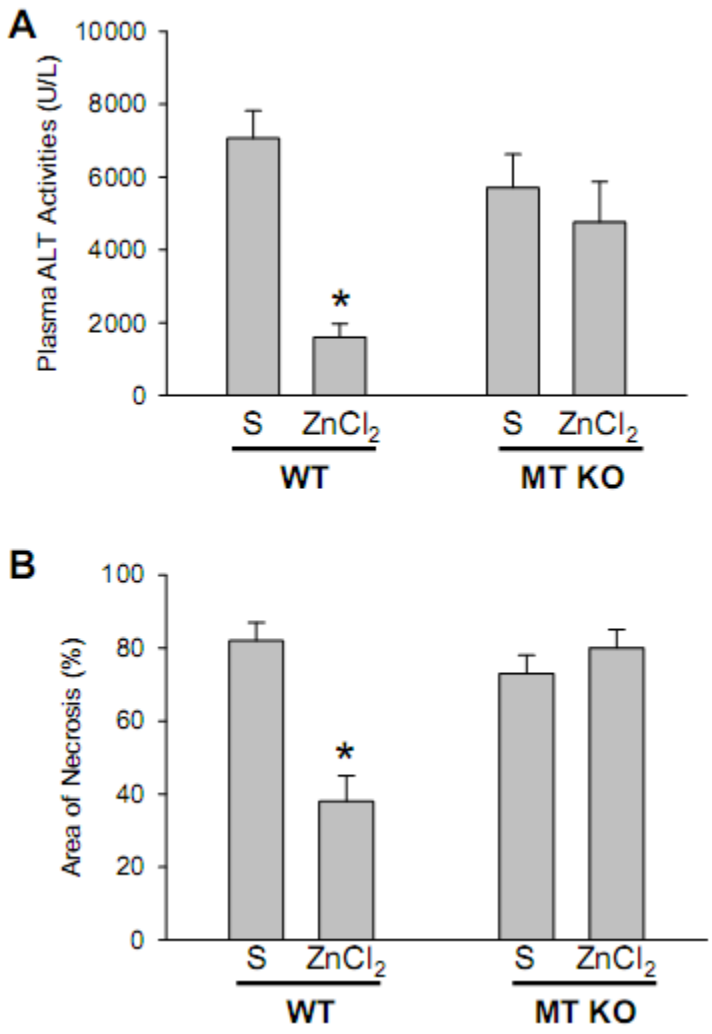
A
Plasma ALT Activities (U/L)
10000
8000
6000
4000
2000
0
*
S
ZnCl2
S
ZnCl2
WT
MT KO
B
Area of Necrosis (%)
100
80
60
40
20
0
*
S
ZnCl2
S
ZnCl2
WT
MT KO

Figure 5.8

Figure 5.8

Liver injury was evaluated by measuring plasma alanine aminotransferase (ALT) activities (panel A) and quantitating the area of necrosis (panel B) in wildtype and MT-1/MT-2-deficient (MT KO) mice 6 h after injection of 300 mg/kg acetaminophen (APAP). Animals were either treated with saline (6 ml/kg) (S) or 100 µmol/kg $ZnCl_2$ for 3 days. APAP was injected 24 h after the last dose of Zn/saline. Data represent means ± SE of n = 4-6 animals per group. *P<0.05 (compared to APAP/saline)

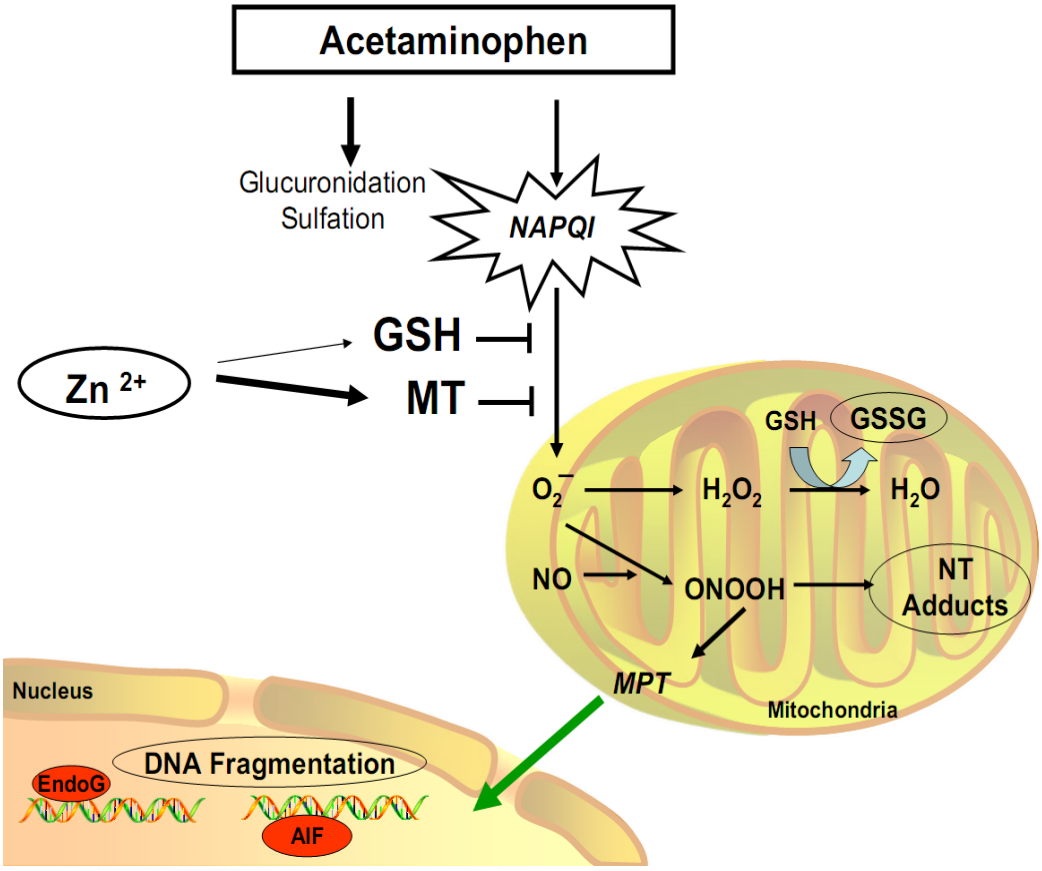
Acetaminophen
Glucuronidation
Sulfation
NAPQI
GSH
MT
Zn 2+
GSH
GSSG
O_2^-
H_2O_2
H_2O
NO
ONOOH
NT
Adducts
MPT
Mitochondria
Nucleus
DNA Fragmentation
EndoG
AIF

Figure 5.9

Figure 5.9

See text for details. Abbreviations: AIF, apoptosis-inducing factor; EndoG, endonuclease G; GSSG, glutathione disulfide; MPT, mitochondrial membrane permeability transition pore; MT, metallothionein; NAPQI, N-acetyl-p-benzoquinone imine; NT adducts, nitrotyrosine protein adducts; ONOOH, peroxynitrite;

5.4 Discussion.

The objective of this investigation was to evaluate the mechanism(s) of protection of MT induction by $ZnCl_2$ against APAP hepatotoxicity. Our data support the conclusion that $ZnCl_2$ selectively induced MT gene expression, which did not scavenge reactive oxygen species but appeared to prevent the oxidant stress by scavenging the reactive metabolite NAPQI.

It is well established that heavy metals including Zn can induce MT gene expression in the liver (Klaassen *et al.*, 1999; Liu *et al.*, 2009). The present data confirmed this observation and showed that both MT-1 and MT-2 mRNA levels were induced in the liver and that this translated into a substantial increase in MT protein expression in hepatocytes. Despite the effective induction of MT by Zn, there is some controversy whether this is the main mechanism by which Zn can protect against drug-induced liver injury. For example, Zn supplementation in the diet attenuated alcoholic liver injury in MT-deficient mice during a 12-week study suggesting that the protection was independent of MT (Zhou *et al.*, 2005). However, the average oral Zn intake was calculated to be 33 mg/kg/day (505 µmol/kg/day), which is about 5 times higher than the subcutaneous dose used in the present investigation for 3 days. A similar s.c. treatment of Zn did not protect MT-deficient mice against APAP-induced liver injury (Liu *et al.*, 2009). We could confirm these findings (Figure 5.8) suggesting that MT induction was the principle mechanism of

protection. In addition, we showed that 100 µmol/kg/day $ZnCl_2$ selectively induced MT but did not affect a number of other genes, whose upregulation has been shown to be beneficial against APAP-induced liver injury. This includes HO-1 (Chiu *et al.*, 2002), HSP70 (Tolson *et al.*, 2006) and MnSOD (Fujimoto *et al.*, 2009). A recent genomic study using the same dose of Zn reported similar findings (Liu *et al.*, 2009). These data together suggest that the protective effect of $ZnCl_2$ treatment was mainly caused by MT induction in hepatocytes. However, the slightly higher hepatic GSH levels in $ZnCl_2$-treated animals may have also contributed to the protection. This effect of Zn could have been caused by the moderate upregulation of nuclear factor-erythroid 2-related factor 2 (Nrf2) (Liu *et al.*, 2009), which positively regulates GSH synthesizing enzymes (Lu, 2009).

It has been extensively postulated that MT can scavenge reactive oxygen species (Kumari *et al.*, 1998; Sato and Bremner, 1993; Thornalley and Vasak, 1985). However, most studies were done with isolated proteins in a test tube. In an *in vivo* study where it was concluded that MT protected against APAP toxicity by acting as ROS scavenger it remained unclear whether MT prevented formation of ROS or scavenged them (Liu *et al.*, 1999). Our *in vivo* data demonstrated that MT induction reduced nitrotyrosine staining and prevented DNA fragmentation, which is dependent on mitochondrial peroxynitrite formation and dysfunction (Bajt *et al.*, 2008; Cover *et al.*, 2005b).

These results can be interpreted as if MT acted as an effective scavenger of peroxynitrite in the mitochondria or that MT acted upstream and prevented the formation of ROS. The fact that MT induction reduced hepatic GSSG levels and the GSSG-to-GSH ratio after APAP, suggestes that the formation of ROS, especially hydrogen peroxide, was prevented. This conclusion is supported by previous findings showing that GSSG levels remained elevated when only peroxynitrite is scavenged, but ROS formation is unaffected (Knight *et al.*, 2002). In addition, the experiments with isolated hepatocytes exposed to various concentrations of hydrogen peroxide did not indicate that MT was able to effectively scavenge ROS in the presence or absence of GSH. In contrast, GSH was the critical antioxidant controlling ROS-induced cell death in hepatocytes. This shows that hydrogen peroxide entered the cells and a competent scavenger (GSH) was able to intercept this oxidant in the cytosol. In general, peroxides diffuse into the cell, trigger mitochondrial dysfunction and ultimately cause MPT pore formation and cell necrosis (Nieminen *et al.*, 1995). Although most MT is expressed in the cytosol after induction, MT did not affect cell injury. This indicates that MT is not a relevant scavenger of hydrogen peroxide, which suggests that the reduced hepatic GSSG levels and the reduced GSSG-to-GSH ratio in APAP-treated animals are unlikely to be caused by the scavenging of ROS, especially not in the presence of GSH. Thus, our findings indicate that MT acted upstream of the initiation of the mitochondrial oxidant stress.

The main event upstream of mitochondrial protein binding is the formation of the reactive metabolite NAPQI. Inhibition of the metabolic activation is most effective in preventing APAP toxicity. Because NAPQI is detoxified by GSH, the initial decline of the hepatic GSH levels reflects the formation of NAPQI (Jaeschke, 1990). Based on the GSH depletion kinetics, there was no relevant difference between controls and $ZnCl_2$-treated animals, suggesting that there was no difference in NAPQI formation. However, it was observed that the basal GSH levels after $ZnCl_2$ were higher than in controls. Although the difference was only 11%, the data indicate a slightly higher capacity to detoxify NAPQI in the $ZnCl_2$-treated livers. This effect may have contributed to the protective effect of $ZnCl_2$ treatment against APAP toxicity. Nevertheless, it is unlikely that this limited amount of additional GSH could have been entirely responsible for the protection against APAP toxicity.

The only remaining explanation for the protective effect of MT after NAPQI formation, but before mitochondrial protein binding, would be a direct scavenging of NAPQI by MT. Due to its high content of cysteine residues, MT can react with organic electrophiles (Cagen and Klaassen, 1980) including NAPQI (Roberts *et al.*, 1987). Our mass spectrometric data confirm these findings and demonstrate directly a time-dependent covalent binding of 1-3 NAPQI molecules to each MT protein. Because the depletion kinetics of GSH is not affected, these data suggest that MT reacts with NAPQI only when GSH

levels are very low. A higher affinity of NAPQI to GSH as compared to the sulfhydryl groups of MT has also been observed with other electrophiles (Cagen and Klaassen, 1980). These findings indicate that MT induction is not a primary detoxification mechanism for organic electrophiles, but MT can become important once GSH is depleted as it is after APAP overdose.

In summary, we demonstrated that $ZnCl_2$ treatment effectively attenuated the APAP-induced mitochondrial oxidant stress and peroxynitrite formation, nuclear DNA damage and necrotic cell death (Figure 9). Because MT-deficient mice were not affected by Zn treatment, the protective effect was mainly caused by the induction of MT protein expression in hepatocytes. The slightly higher GSH levels observed in $ZnCl_2$-treated animals may have also contributed to the protection. The induction of MT did not affect the metabolic activation of APAP but attenuated the oxidant stress. However, lower hepatic GSSG levels after APAP and no evidence that MT was able to scavenge ROS *in vitro* suggested a target upstream of mitochondria. MT was able to effectively react with NAPQI once GSH was depleted. Thus, our data are consistent with the conclusion that MT acts as a second line of defense behind GSH to scavenge NAPQI and prevent the binding to cellular proteins including mitochondrial proteins. This will attenuate the mitochondrial oxidant stress and peroxynitrite formation, which are critical mediators of APAP-induced liver injury. Because MT can be induced by various cellular

stresses it could be target for drug toxicity prophylaxis. As such, MT expression could also be an unrecognized mechanism of protection of certain interventions such as a neutropenia antibody (Jaeschke and Liu, 2007).

CHAPTER 6: ROLE OF C-JUN-N-TERMINAL KINASE IN ACETAMINOPHEN-INDUCED LIVER INJURY

6.1 Abstract

Acetaminophen (APAP) overdose, which causes liver injury in animals and humans, activates c-jun N-terminal kinase (JNK). Although it was shown that the JNK inhibitor SP600125 effectively reduced APAP-induced hepatotoxicity, the mechanisms of protection remain unclear. C57Bl/6 mice were treated with 10 mg/kg SP600125 or vehicle (8% dimethylsulfoxide) 1h before 600 mg/kg APAP administration. APAP time-dependently induced JNK activation (detected by JNK phosphorylation). SP600125, but not the vehicle, reduced JNK activation, attenuated mitochondrial Bax translocation and prevented the mitochondrial release of apoptosis-inducing factor at 4–12 h. Nuclear DNA fragmentation, nitrotyrosine staining, tissue GSSG levels and liver injury (plasma ALT release and necrosis) were partially attenuated by the vehicle (-65%) and completely eliminated by SP600125 (-98%) at 6 and 12h. Furthermore, SP600125 attenuated the increase of inducible nitric oxide synthase (iNOS) mRNA and protein. However, APAP did not enhance plasma nitrite+nitrate levels (NO formation); SP600125 had no effect on this parameter. The iNOS inhibitor L-Nil did not reduce NO formation or injury after APAP but prevented NO formation caused by endotoxin. Since SP600125 completely eliminated the increase in hepatic GSSG levels, an indicator of

mitochondrial oxidant stress, it is concluded that the inhibition of peroxynitrite was mainly caused by reduced superoxide formation. Our data suggest that the JNK inhibitor SP600125 protects against APAP-induced liver injury in part by attenuation of mitochondrial Bax translocation but mainly by preventing mitochondrial oxidant stress and peroxynitrite formation and thereby preventing the mitochondrial permeability transition pore opening, a key event in APAP-induced cell necrosis.

6.2 Introduction

An overdose of acetaminophen (APAP), a commonly used analgesic drug, can cause hepatic necrosis and even liver failure in humans and animals. APAP overdose is currently the most frequent cause of drug-induced liver failure in the US (Larson *et al.*, 2005). APAP-induced liver cell injury is initiated by the formation of a reactive metabolite, *N*-acetyl-*p*-benzoquinone imine (NAPQI), which can be generated by several cytochrome P-450 isoenzymes, especially cyp2E1 (Nelson, 1990). NAPQI is detoxified by glutathione (GSH), resulting in the depletion of this sulfhydryl reagent (Mitchell et al., 1973). Once cellular GSH is consumed, NAPQI covalently binds to cellular proteins (Cohen *et al.*, 1997). However, cell injury correlates less with total protein binding but more with the capacity to bind to mitochondrial proteins (Tirmenstein and Nelson, 1989). These findings support the hypothesis that covalent binding to mitochondrial proteins may be

responsible for mitochondrial dysfunction (Jaeschke and Bajt, 2006; Jaeschke *et al.*, 2003). The well established effects of an APAP overdose on mitochondria include inhibition of mitochondrial respiration, enhanced formation of reactive oxygen species and peroxynitrite, mitochondrial DNA damage, release of mitochondrial intermembrane proteins, which translocate to the nucleus and cause nuclear DNA degradation, and ultimately opening of the mitochondrial membrane permeability transition pore with collapse of the membrane potential (Jaeschke and Bajt, 2006; Jaeschke *et al.*, 2003).

C-jun-*N*-terminal kinase (JNK) is a member of the mitogen-activated protein kinase (MAPK) superfamily (Hibi *et al.*, 1993). JNK can activate a variety of signal cascades through its phosphorylation of not only transcription factors such as c-jun (Li *et al.*, 2004b), p53 (Cheng *et al.*, 2003), and ATF-2 (Hayakawa *et al.*, 2003), but also members of the Bcl-2 family (Latchoumycandane *et al.*, 2007). JNK has 2 ubiquitously expressed isoforms (JNK1, JNK2) and a tissue-specific isoform (JNK3), which is predominately located in neurons of the central nervous system (Resnick and Fennell, 2004). JNK1 mediates the majority of c-jun phosphorylation and JNK2 mainly regulates c-jun stability (Sabapathy *et al.*, 2004).

Studies with APAP overdose clearly demonstrated prolonged activation of JNK before cell death. Furthermore, pharmacological inhibition of JNK or

the silencing of JNK gene expression resulted in reduced liver injury after APAP overdose (Gunawan *et al.*, 2006; Hanawa *et al.*, 2008; Henderson *et al.*, 2007). However, the use of JNK-deficient mice yielded mixed results. One study showed a partial protection with JNK2- but not JNK1-deficient mice (Gunawan *et al.*, 2006). Other studies did not find a protection with either JNK knockout mice (Bourdi *et al.*, 2008; Henderson *et al.*, 2007). In contrast, one report suggested a beneficial role of JNK2 in tissue repair after APAP (Bourdi *et al.*, 2008). Although apoptosis signal-regulating kinase 1 (ASK1), a member of the mitogen-activated protein kinase kinase kinase family, has been identified as the upstream activator of JNK (Nakagawa *et al.*, 2008a), the downstream mechanisms by which JNK affects APAP hepatotoxicity are less clear. It was suggested that JNK may act by triggering Bax activation and translocation to the mitochondria (Gunawan *et al.*, 2006). However, Bax-deficient mice are only temporarily protected against APAP-induced hepatotoxicity (Bajt *et al.*, 2008) suggesting that additional mechanisms may be operative. More recently it was proposed that JNK is activated by reactive oxygen species generated by GSH-depleted mitochondria, which triggers the translocation of activated JNK to mitochondria resulting in the induction of the mitochondrial permeability transition (Hanawa *et al.*, 2008). A caveat of this hypothesis is that reactive oxygen species have not been detected outside the mitochondria (Jaeschke, 1990) and that the more aggressive oxidant peroxynitrite, generated in mitochondria, was identified as a critical mediator

of the injury process (Cover *et al.*, 2005b; Knight *et al.*, 2002). A third mechanism, JNK-mediated activation of inducible nitric oxide synthase (iNOS), was also suggested (Latchoumycandane *et al.*, 2007). However, inhibition of iNOS was not consistently beneficial in APAP hepatotoxicity (Gardner *et al.*, 2003; Hinson *et al.*, 2002). Therefore, our goal was to assess all three mechanisms simultaneously and evaluate by which mechanism the pharmacological and genetic inhibition of JNK protects in an *in vivo* murine model of APAP hepatotoxicity.

6.3 Results

Functional significance of JNK activation after APAP overdose: JNK2 KO Mice

For studying mechanisms of APAP-induced liver injury, the most frequently used dose by us and others is 300 mg/kg in overnight fasted animals (Cover *et al.*, 2005a; Gardner *et al.*, 2003; Hinson *et al.*, 1998; Knight *et al.*, 2002; Knight *et al.*, 2001). This dose consistently causes severe liver injury in almost all mouse strains. Administration of 300 mg/kg APAP resulted in the activation of JNK in the livers of C57Bl/6 mice as indicated by the appearance of the phosphorylated form (P-JNK) with an early peak at 2 h and second peak at 6 h (Figure 1A). At 24 h, no P-JNK was detectable. The phosphorylation of both JNK isoforms (JNK1, 46 kDa; JNK2, 54 kDa) observed after APAP is consistent with previous reports (Bourdi *et al.*, 2008; Hanawa *et al.*, 2008; Henderson *et al.*, 2007; Latchoumycandane *et al.*, 2007; Nakagawa *et al.*, 2008b). Delayed treatment with GSH, which effectively scavenged peroxynitrite and hydrogen peroxide (Knight *et al.*, 2002) or treatment with $ZnCl_2$, which induced metallothionein and partially prevented the mitochondrial oxidant stress (Saito *et al.*) also prevented JNK activation (Figure 6.1B). These data suggest that JNK activation is linked to the formation of oxidant stress in this model. Both, the scavenging of reactive oxygen species by GSH administration and the partial prevention of mitochondrial oxidant stress by Zn pretreatment together with the inhibition of

JNK activation resulted in significantly reduced liver injury (Figure 6.2A). To directly evaluate the pathophysiological role of JNK, wild type and JNK2 KO mice were treated with 300 mg/kg APAP. At 6 h, plasma ALT levels increased to a similar degree in both WT and JNK2 KO mice (Figure 6.2B) reflecting severe centrilobular necrosis (Figure 6.2C). To confirm the findings with JNK2 KO mice, C57Bl/6 mice were treated with the general JNK inhibitor SP600125 or the vehicle DMSO/PBS. Although 300 mg/kg APAP alone caused severe liver injury at 6 h (plasma ALT: 5220 ± 1085 U/L), treatment with the vehicle alone or with SP600125 completely prevented any liver injury (data not shown). The reason for the complete protection by the vehicle alone is that the dose of DMSO (1.2 ml/kg) necessary to dissolve the inhibitor effectively blocks the metabolic activation of APAP (Jaeschke *et al.*, 2006). Thus, a higher dose of APAP (600 mg/kg) had to be used to overcome this block (Hanawa *et al.*, 2008).

Functional significance of JNK activation after APAP overdose: SP600125

Treatment of C57Bl/6 mice with 600 mg/kg APAP resulted in a rapid loss of hepatic GSH content due to NAPQI formation (Figure 6.3). Within 20 min GSH levels decreased by 62% and within 2 h 92% was lost. However, pretreatment with SP600125 or its vehicle substantially delayed the initial decline, but GSH levels had fallen by 81-88% by 2 h (Figure 6.3). These data

indicate that the high dose of APAP overcame some of the inhibition of the metabolic activation in the presence of DMSO. To evaluate the functional significance of JNK, the effect of SP600125 on liver injury was evaluated at 6 and 12 h after APAP (Figure 6.4 A,B). Compared to PBS-treated animals, the DMSO-containing vehicle substantially attenuated liver injury at both time-points as reflected by the approximately 65% reduction in ALT release at both time points (Figure 6.4A) and the reduced area of necrosis at 12 h (Figure 6.4B). However, liver injury was essentially completely prevented by pretreatment with SP600125 (Figure 6.4A,B). These findings were confirmed by using the TUNEL assay to evaluate nuclear DNA damage (Figure 6.4C). Previous reports from our laboratory provided evidence for the translocation of mitochondrial intermembrane proteins such as apoptosis-inducing factor (AIF) and endonuclease G to the nucleus as the main cause of the nuclear DNA damage after APAP overdose (Bajt *et al.*, 2006). This effect was caused initially by formation of Bax pores in the outer membrane and subsequently by mitochondrial swelling and rupture of the outer membrane due to MPT (Bajt *et al.*, 2008). In support of these events, JNK activation, release of AIF into the cytosol and translocation of Bax to the mitochondria was observed 12 h after APAP (Figure 6.5). Although the vehicle was without effect on these parameters, SP600125 effectively reduced JNK activation, mitochondrial AIF release and mitochondrial Bax translocation (Figure 6.5). To confirm that these events are not just consequences of the protection observed at 12 h,

the same parameters were also measured at an earlier time point (4 h) where only minimal injury occurred (Figure 6.6). Again, APAP caused JNK activation, mitochondrial Bax translocation and release of AIF, all of which were effectively attenuated by SP600125 (Figure 6.6). The vehicle DMSO partially prevented mitochondrial AIF release but had no relevant effect on JNK activation and mitochondrial Bax translocation (Figure 6.6). Together these data support the conclusion that JNK activation causes mitochondrial Bax translocation, which is responsible for the initial AIF and endonuclease G release from the mitochondria and early nuclear DNA damage. However, studies with Bax-deficient mice showed no effect of Bax on the mitochondrial oxidant stress and peroxynitrite formation, which ultimately were responsible for the later release of AIF and endonuclease G and the resulting DNA degradation and cell death (Bajt *et al.*, 2008). Since SP600125 effectively prevented cell death even at later time points, these data suggest that JNK has additional, more critical effects than just causing Bax activation.

Effect of SP600125 on iNOS expression and peroxynitrite formation

It is well established that APAP overdose causes peroxynitrite formation in cells undergoing necrotic cell death (Hinson *et al.*, 1998; Knight *et al.*, 2001). To evaluate if JNK activation is associated with peroxynitrite formation, liver tissue was stained for nitrotyrosine protein adducts (Figure 6.7). APAP overdose caused substantial peroxynitrite formation in centrilobular

hepatocytes at 6 h (Figure 6.7) and at 12 h (data not shown). Pretreatment with the vehicle DMSO partially reduced, whereas treatment with SP600125 completely eliminated, nitrotyrosine staining at both 4 and 12 h (Figure 6.7). These data suggest that JNK activation is involved in peroxynitrite formation. Since it was previously hypothesized that JNK activation may enhance liver injury by promoting peroxynitrite formation through iNOS induction (Latchoumycandane *et al.*, 2007), the effect of APAP and JNK on iNOS was investigated. APAP overdose caused a 3.5-fold and a 7-fold increase of iNOS mRNA at 4 and 12h, respectively (Figure 6.8A). This translated into a minor increase in iNOS protein expression at 6 h (Figure 6.8B) and at 12 h (data not shown). However, plasma nitrite + nitrate levels as indicators of NO formation did not change significantly (Figure 6.8C). Although SP600125 attenuated iNOS mRNA and protein levels, there was no significant effect on plasma nitrite + nitrate concentrations (Figure 6.8). In addition, the iNOS inhibitor L-Nil, affected neither plasma nitrite + nitrate levels (Figure 6.8C) nor APAP-induced liver injury (Figure 6.8D). As a positive control, LPS treatment substantially enhanced plasma nitrite + nitrate concentrations, which where reduced to baseline by L-Nil treatment (Figure 6.8C). Although these data confirm that JNK was involved in a minor transcriptional induction of iNOS after APAP overdose, the beneficial effect of inhibiting JNK activation on peroxynitrite formation and liver injury was independent of iNOS.

Role of JNK in APAP-induced mitochondrial oxidant stress

Since APAP-induced peroxynitrite formation did not appear to be caused by JNK-mediated enhanced NO generation, especially from iNOS, formation of reactive oxygen was assessed. It was previously demonstrated that increased tissue levels of GSSG after APAP reflect mainly mitochondrial superoxide/hydrogen peroxide but not peroxynitrite formation (Jaeschke, 1990; Knight and Jaeschke, 2004; Knight *et al.*, 2001). Thus, GSH and GSSG levels were measured at 12 h after APAP (Figure 6.9). The total hepatic glutathione content (GSH+GSSG) was still partially depleted after treatment with APAP alone but GSSG levels were significantly elevated above controls (Figure 6.9A,B). This resulted in an increased GSSG-to-GSH ratio from less than 0.5 to more than 2.5 (Figure 6.9C). The vehicle-treated group, which was partially protected against APAP-induced liver injury (Figure 6.4), showed higher total glutathione and GSSG levels resulting in a significantly elevated GSSG-to-GSH ratio (Figure 6.9). These data indicate that the vehicle DMSO accelerated the recovery of liver GSH levels and improved the detoxification of reactive oxygen species but did not prevent the APAP-induced oxidant stress. In contrast, the JNK inhibitor SP600125 did not only promote the faster recovery of the hepatic GSH content, it completely prevented the increase in GSSG levels and the change in the GSSG-to-GSH ratio (Figure 6.9). These data are consistent with the conclusion that the JNK inhibitor completely prevented the APAP-induced oxidant stress.

Late treatment with GSH inhibits JNK activation

It was previously shown that delayed treatment with GSH up to 2.5 h protects against APAP hepatotoxicity by stimulating hepatic GSH synthesis and replenishing mitochondrial GSH levels, which scavenge reactive oxygen and peroxynitrite, as well as support the mitochondrial energy metabolism (Knight *et al.*, 2002; Saito *et al.*, 2009). Treatment with GSH 4 h after APAP enhanced hepatic GSH levels (Figure 6.10C) and strongly reduced JNK activation at 6 h in the APAP and the APAP/DMSO group (Figure 6.10A). SP600125 treatment alone prevented JNK activation and GSH administration did not affect these results despite inducing the highest GSH levels (Figure 6.10). Interestingly, DMSO did not affect JNK activation but reduced plasma ALT values by 71% (Figure 6.10B). In addition, delayed GSH treatment significantly reduced liver injury in the APAP group by 62% and in the APAP/DMSO group by 60% (Figure 6.10B). Despite a similar degree of low P-JNK expression in 4 groups, there were substantial differences in injury between the groups. These data suggest that scavenging mitochondrial reactive oxygen and peroxynitrite attenuates JNK activation and reduces APAP-induced liver injury.

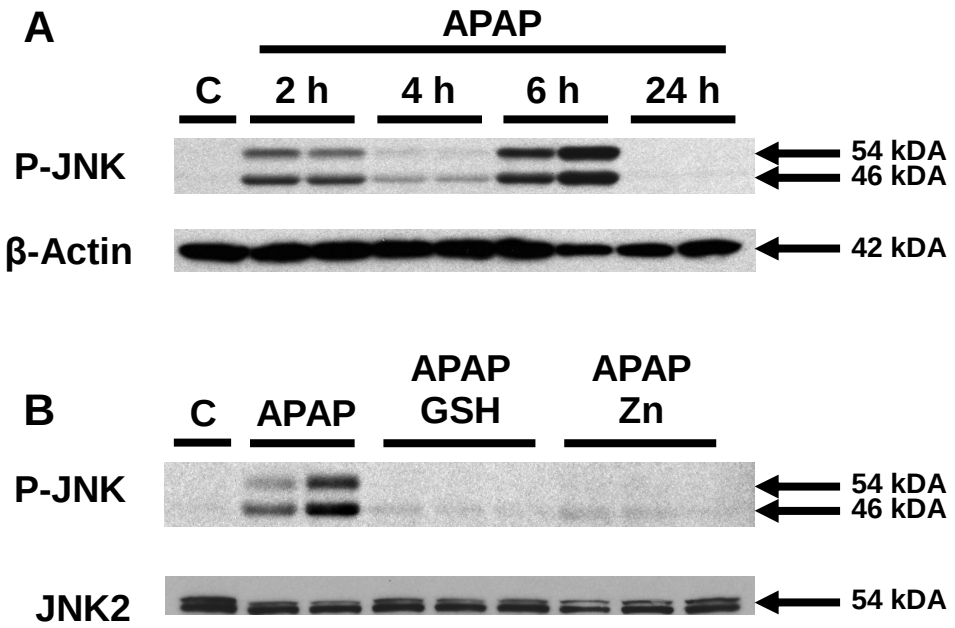
A
APAP
C
2 h
4 h
6 h
24 h
P-JNK
54 kDA
46 kDA
β-Actin
42 kDA
B
C
APAP
APAP
GSH
APAP
Zn
P-JNK
54 kDA
46 kDA
JNK2
54 kDA

Figure 6.1

Figure 6.1

JNK activation in response to treatment with 300 mg/kg acetaminophen (APAP). A. Time course of P-JNK formation as indicator of JNK activation in response to APAP treatment. β-actin protein expression is shown as loading control. B. Total JNK and P-JNK protein expression were measured in untreated controls (C) and in animals treated with 300 mg/kg APAP alone or together with either 0.65 mmol/kg GSH (i.v.) administered at 1.5 h after APAP or 100 µmol/kg $ZnCl_2$ administered for 3 days as described in details in the methods section.

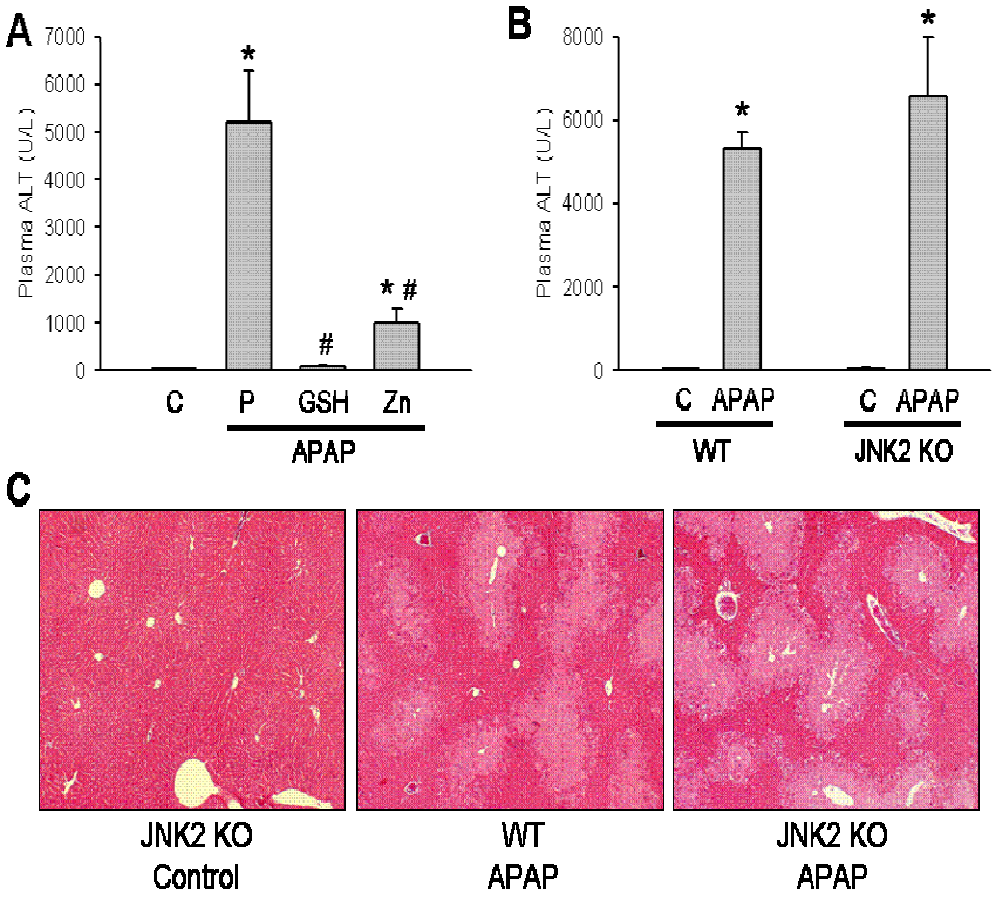
A
Plasma ALT (U/L)
7000
6000
5000
4000
3000
2000
1000
0
*
#
* #
C
P
GSH
Zn
APAP
B
Plasma ALT (U/L)
8000
6000
4000
2000
0
*
*
C
APAP
C
APAP
WT
JNK2 KO
C
JNK2 KO
Control
WT
APAP
JNK2 KO
APAP

Figure 6.2

Plasma alanine aminotransferase (ALT) activities as an indicator for APAP-induced hepatotoxicity were measured in C57BL/6 mice 6 h after 300 mg/kg APAP administration. A. Animals were either untreated (C) or received APAP alone or together with GSH at 1.5 h after APAP or with 100 µmol/kg $ZnCl_2$. Data represent means $\pm$ SE of n = 4 animals per group. *P<0.05 (compared to C), $^{\#}$P<0.05 (compared to APAP). B. Plasma ALT activities were measured in wild type and JNK2-deficient (JNK2 KO) mice 6 h after injection of 300 mg/kg APAP. Data represent means $\pm$ SE of n = 4 animals per group. *P<0.05 (compared to untreated controls). C. Representative liver sections of animals treated for 6 h with 300 mg/kg APAP were stained with H&E (assess area of necrosis) (C). (x50 for all panels).

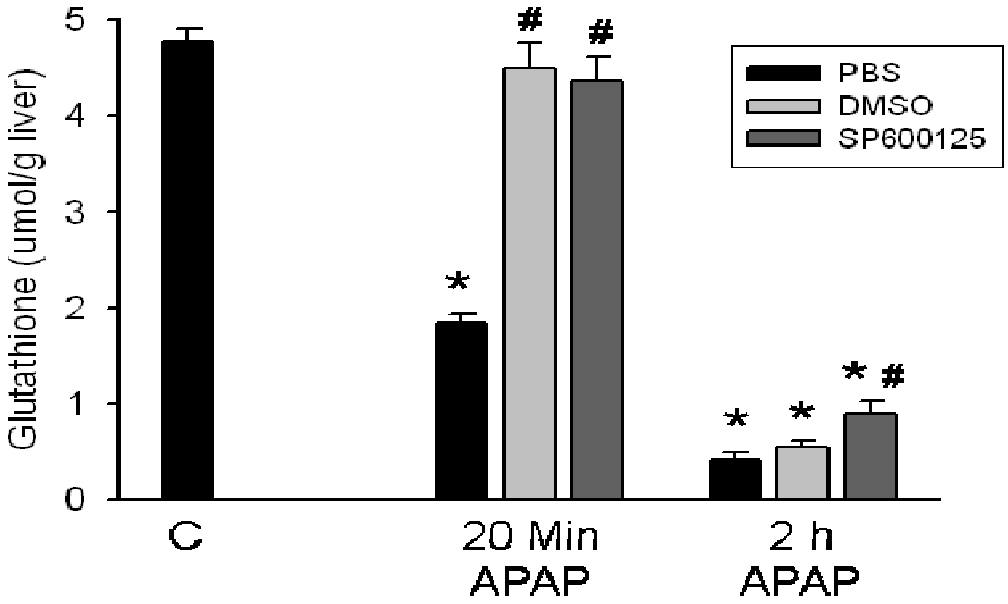
Glutathione (umol/g liver)
5
4
3
2
1
0
C
20 Min APAP
2 h APAP
PBS
DMSO
SP600125
*
#
#
*
*
*
#

Figure 6.3

Figure 6.3

The liver content of total glutathione (GSH + GSSG) was determined in untreated controls (C) or 20 min or 2 h after injection of APAP (600 mg/kg, ip). Some of the animals were pretreated with either 15ml/kg PBS, 15 ml/kg DMSO (8.3% in PBS) or SP600125 (10 mg/kg in DMSO/PBS). Data represent means ± SE of n = 4 animals per group. *P<0.05 (compared to C) #P<0.05 (compared to APAP- PBS).

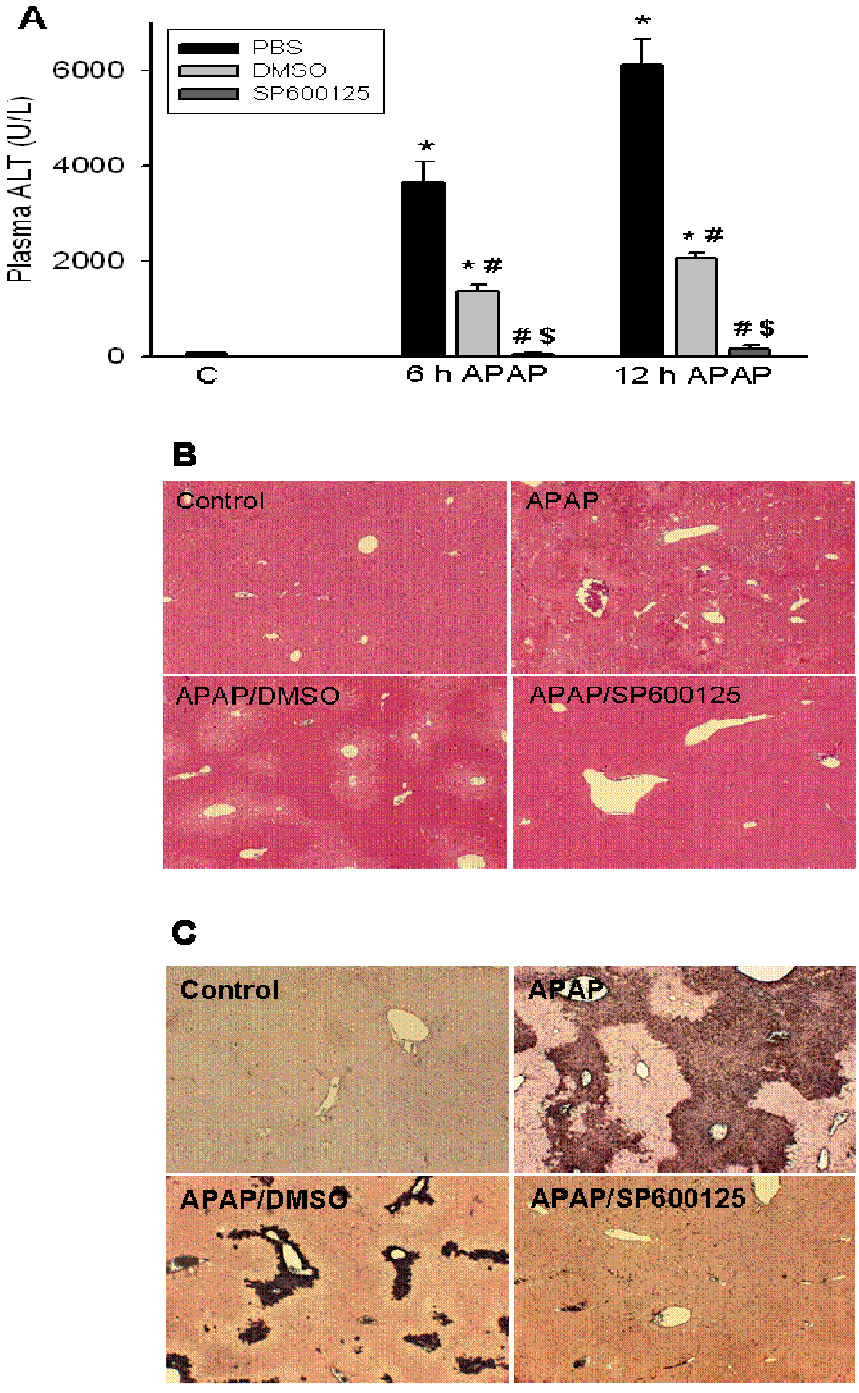
A
PBS
DMSO
SP600125
Plasma ALT (U/L)
6000
4000
2000
0
C
6 h APAP
12 h APAP
B
Control
APAP
APAP/DMSO
APAP/SP600125
C
Control
APAP
APAP/DMSO
APAP/SP600125

Figure 6.4

Figure 6.4

A. Plasma ALT activities were measured in untreated controls (C) and at 6 or 12 h after administration of 600 mg/kg APAP in mice with either 15 ml/kg PBS, 15 ml/kg DMSO in PBS or 10 mg/kg of the JNK inhibitor SP600125 at 1 h before APAP. Data represent means ± SE of n= 4-6 animals per group. *P<0.05 (compared to C), $^{\#}$P<0.05 (compared to APAP-PBS) and $^{\$}$P<0.05 (compared to DMSO). B. Histological assessment of liver injury in representative H&E-stained tissue sections obtained 12 h after APAP administration. C. DNA fragmentation was evaluated by the TUNEL assay in animals treated with 600 mg/kg APAP for 12h. (x50 for all panels).

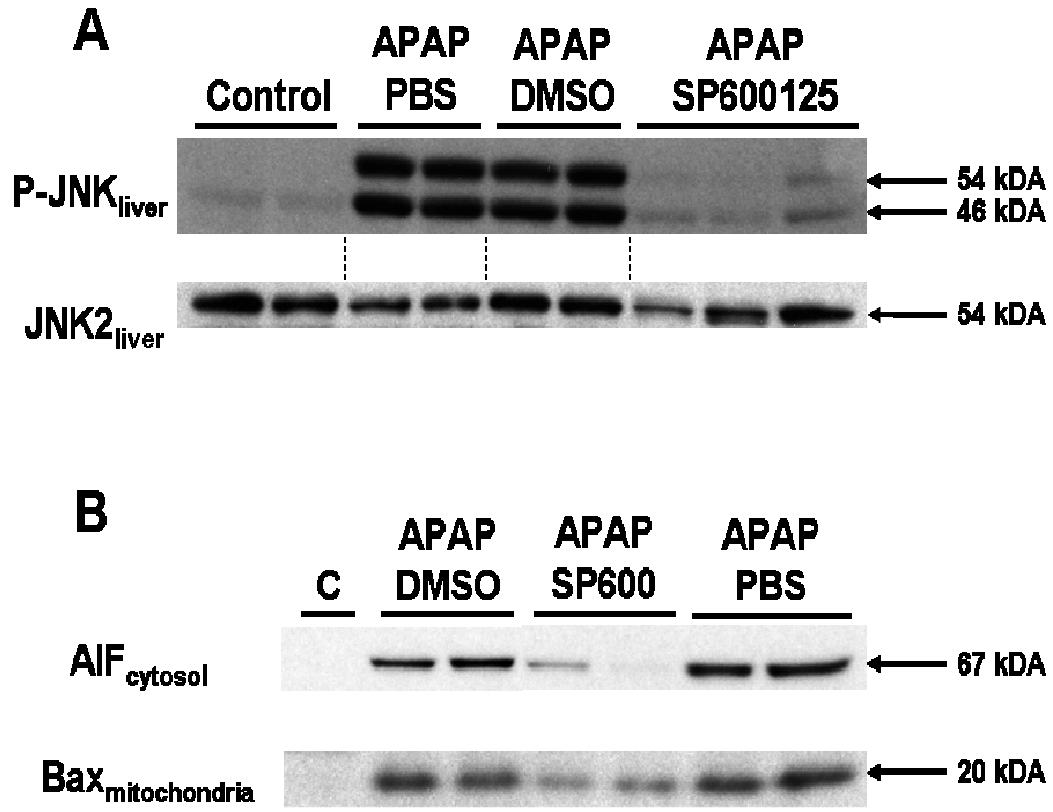
A
Control
APAP PBS
APAP DMSO
APAP SP600125
P-JNK liver
54 kDA
46 kDA
JNK2 liver
54 kDA
B
C
APAP DMSO
APAP SP600
APAP PBS
AIF cytosol
67 kDA
Bax mitochondria
20 kDA

Figure 6.5

Figure 6.5

P-JNK and JNK protein expression were determined in whole liver homogenates by Western blot analysis in untreated controls or at 12 h after APAP (600 mg/kg). The APAP-treated animals received either15 ml/kg PBS, 15 ml/kg DMSO/PBS or 10 mg/kg of the JNK inhibitor SP600125 in DMSO/PBS. B. Apoptosis-induced factor (AIF) and Bax protein levels were determined by Western blot analysis in the cytosol and mitochondria, respectively, from animals treated with APAP and PBS, DMSO or SP600125 as described under A.

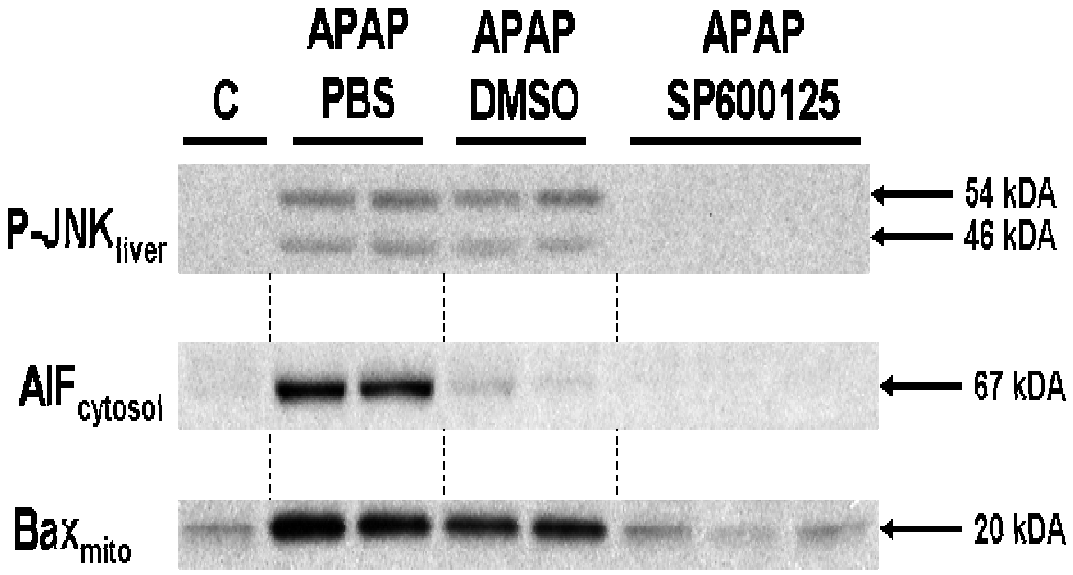
C
APAP PBS
APAP DMSO
APAP SP600125
P-JNK liver
AIF cytosol
Bax mito
54 kDA
46 kDA
67 kDA
20 kDA

Figure 6.6

Figure 6.6

P-JNK in whole liver, AIF in cytosol and Bax in mitochondria were measured by Western blot analysis at 4 h after APAP (600 mg/kg). Some animals received PBS, DMSO or SP600125 1 h before APAP administration.

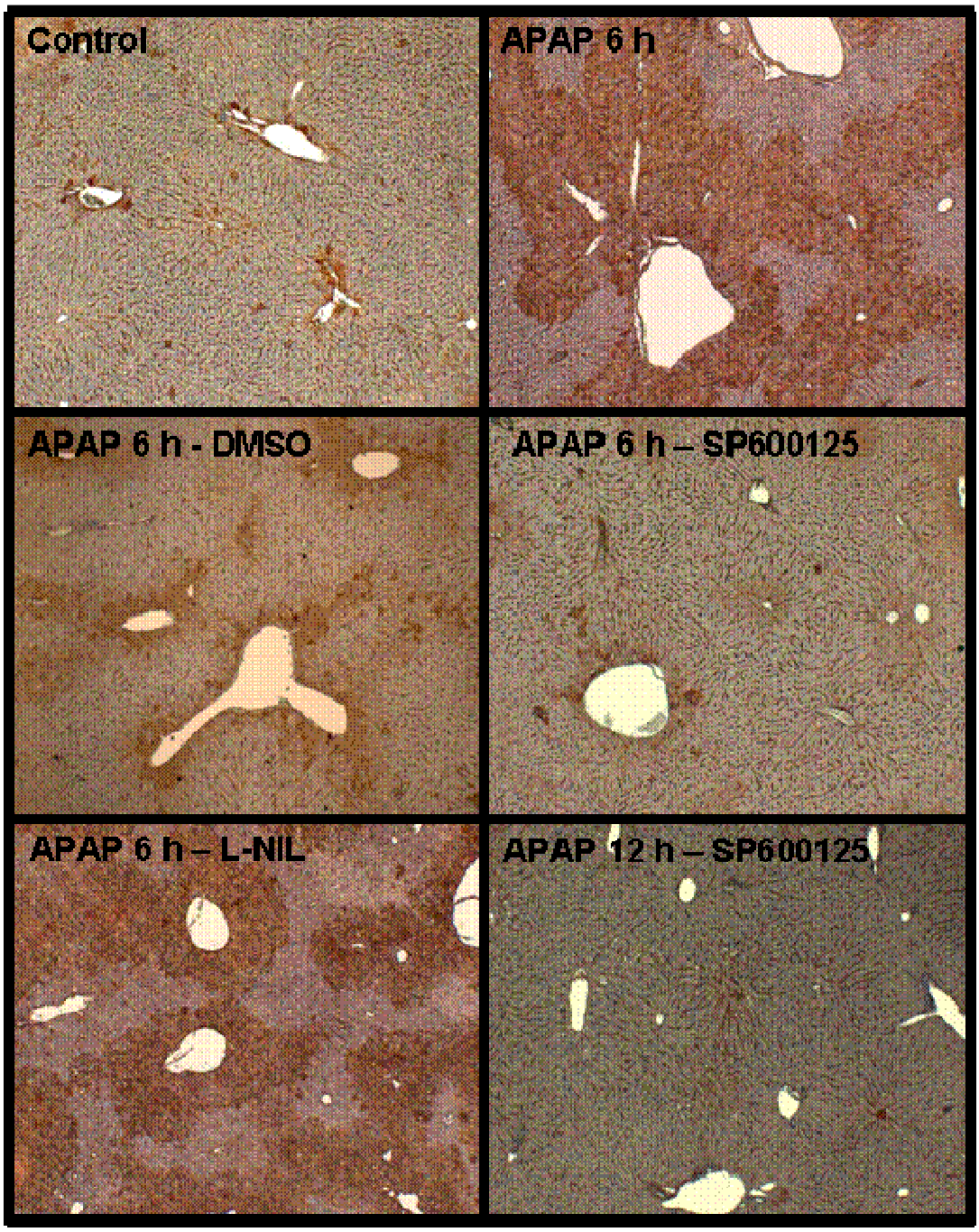
Control
APAP 6 h
APAP 6 h - DMSO
APAP 6 h – SP600125
APAP 6 h – L-NIL
APAP 12 h – SP600125

Figure 6.7

Figure 6.7

Nitrotyrosine staining as indicator of peroxynitrite formation in mice treated with 600 mg/kg APAP for 6 h or 12 h. Some of the animals received PBS, DMSO or the JNK inhibitor SP600125 at 1 h before APAP administration. One group of animals was treated with the iNOS inhibitor L-N-(1-iminoethyl)lysine (L-Nil; 3.3 mg/kg) at 0 and 3 h after APAP.

-

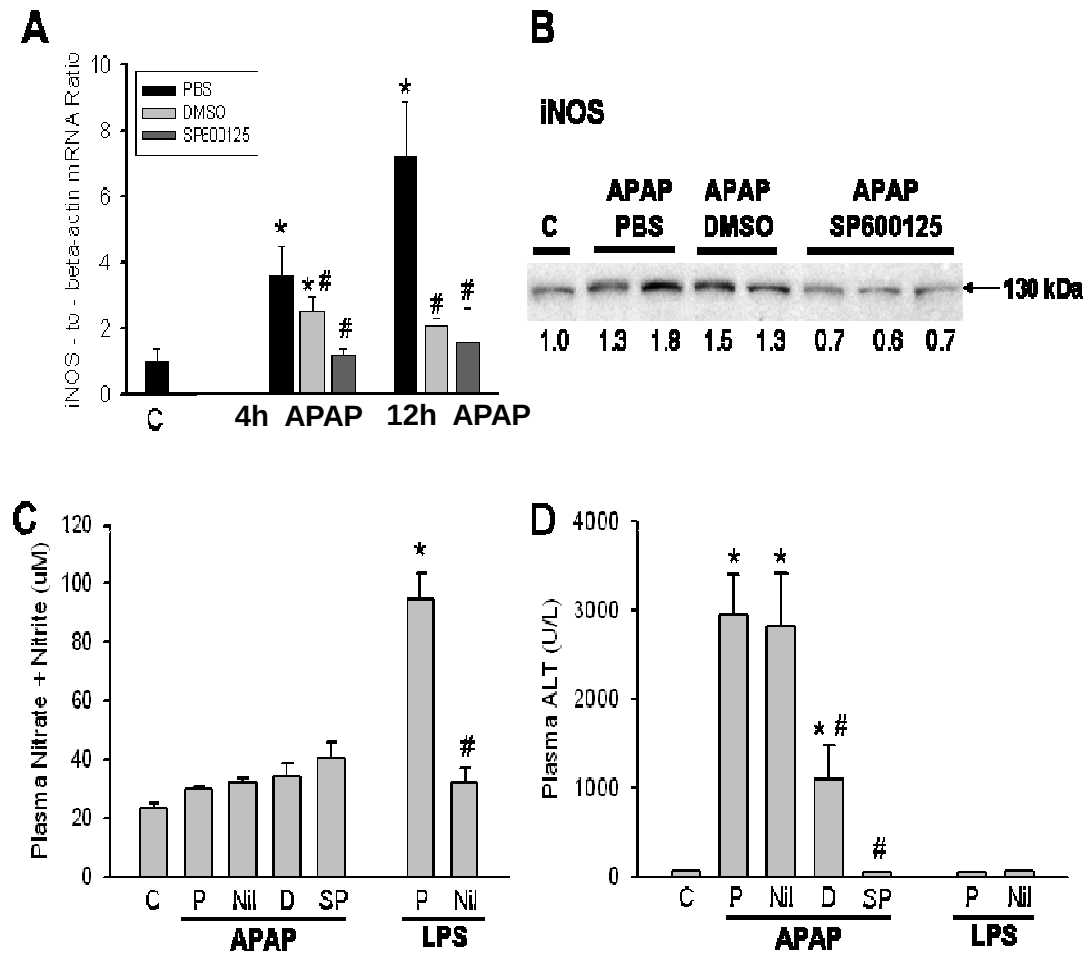
A
iNOS - to - beta-actin mRNA Ratio
PBS
DMSO
SP600125
C
4h APAP
12h APAP
B
iNOS
C
APAP PBS
APAP DMSO
APAP SP600125
130 kDa
1.0 1.3 1.8 1.5 1.3 0.7 0.6 0.7
C
Plasma Nitrate + Nitrite (uM)
C P Nil D SP P Nil
APAP
LPS
D
Plasma ALT (U/L)
C P Nil D SP P Nil
APAP
LPS

Figure 6.8

Figure 6.8

A. Hepatic iNOS mRNA expression was measured by real time RT-PCR in mice at 4 h and 12 h after 600 mg/kg APAP treatment. Data are expressed as the iNOS-to-actin mRNA ratio; the value of untreated control animals was set as 1. Some of the animals received 15 ml/kg PBS, 15 ml/kg DMSO/PBS or 10 mg/kg SP600125 in DMSO/PBS at 1 h before APAP administration. Data represent means ± SE of n = 3 animals per group. *P<0.05 (compared to C), #P<0.05 (compared to APAP/PBS). B. Western blot analysis of iNOS expression in livers of controls or animals treated with 600 mg/kg APAP for 6 h. One to three representative samples are shown from each group. The numbers under the blot show the results of the densitometric analysis. Data of control animals were set as 1. C. Plasma nitrate plus nitrite, which were used as a marker of NO production, and D. plasma ALT activities were measured at 6 h after 600 mg/kg APAP or 2 mg/kg lipopolysaccharide (LPS). Some of the animals received 15 ml/kg PBS (P), 15 ml/kg DMSO (8.3% in PBS) (D) or 10 mg/kg SP600125 in DMSO/PBS (SP) at 1 h before APAP administration. An additional group was treated with 3.3 mg/kg of the iNOS inhibitor L-N-(1-iminoethyl)lysine (NIL) at 0 and 3 h after APAP or LPS administration. Data represent means ± SE of n= 3-4 animals per group. *P<0.05 (compared to C), #P<0.05 (compared to P).

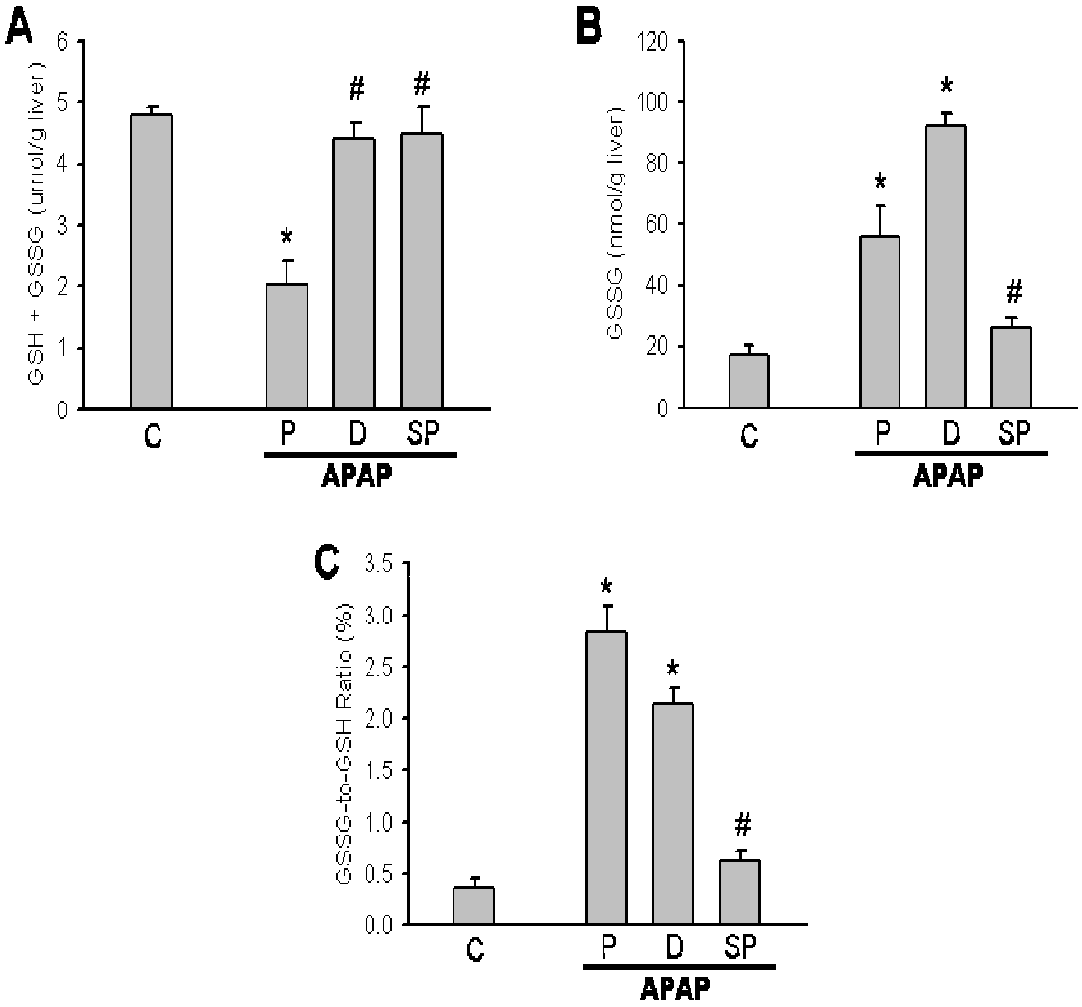
A
GSH + GSSG (umol/g liver)
0
1
2
3
4
5
6
*
#
#
C
P
D
SP
APAP
B
GSSG (nmol/g liver)
0
20
40
60
80
100
120
*
*
#
C
P
D
SP
APAP
C
GSSG-to-GSH Ratio (%)
0.0
0.5
1.0
1.5
2.0
2.5
3.0
3.5
*
*
#
C
P
D
SP
APAP

Figure 6.9

Figure 6.9

Hepatic content of total GSH (GSH + GSSG) (Panel A) and GSSG (Panel B) were measured in untreated controls (C) and in animals treated with 600 mg/kg APAP for 12 h. In addition, the GSSG-to-GSH ratio (Panel C) was calculated from each animal. Some of the animals received 15 ml/kg PBS (P), 15 ml/kg DMSO (8.3% in PBS) (D) or 10 mg/kg SP600125 in DMSO/PBS (SP) at 1 h before APAP administration. Data represent means ± SE of n = 4 animals per group. *P<0.05 (compared to C), #P<0.05 (compared to P).

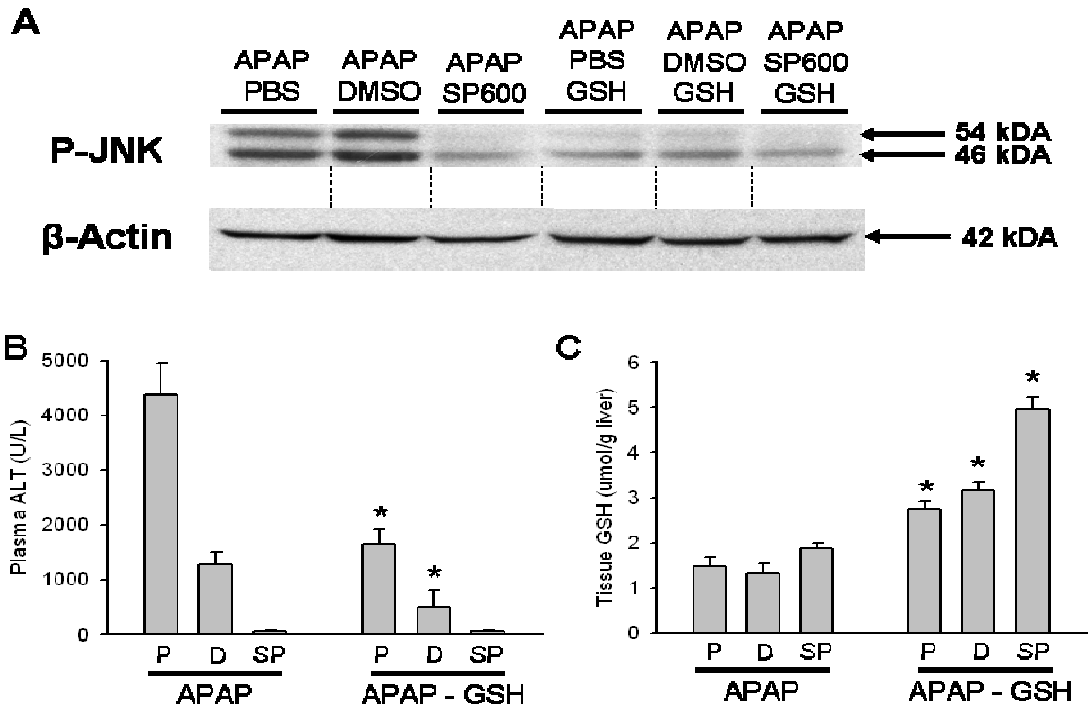
A
APAP PBS
APAP DMSO
APAP SP600
APAP PBS GSH
APAP DMSO GSH
APAP SP600 GSH
P-JNK
β-Actin
54 kDA
46 kDA
42 kDA
B
Plasma ALT (U/L)
5000
4000
3000
2000
1000
0
P D SP
APAP
P D SP
APAP - GSH
C
Tissue GSH (umol/g liver)
6
5
4
3
2
1
0
P D SP
APAP
P D SP
APAP - GSH

Figure 6.10

Figure 6.10

P-JNK and β-actin protein expression (Panel A), plasma ALT activities (Panel B), and hepatic total glutathione content (GSH+GSSG) (Panel C) were measured at 6 h after 600 mg/kg APAP. Some of the animals received 15 ml/kg PBS (P), 15 ml/kg DMSO (8.3% in PBS) (D) or 10 mg/kg SP600125 in DMSO/PBS (SP) at 1 h before APAP administration. Additionally, some animals received 0.65 mmol/kg GSH (i.v.) 4 h after APAP administration.

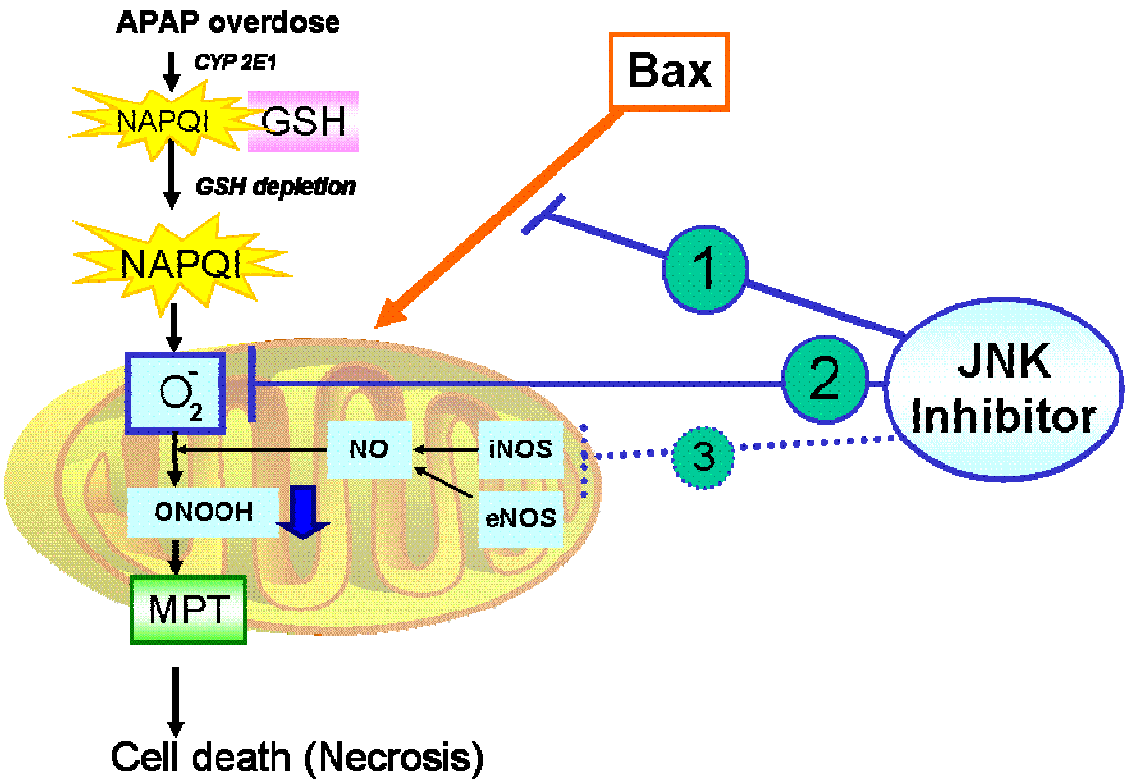
APAP overdose
CYP 2E1
NAPQI
GSH
GSH depletion
NAPQI
Bax
1
2
JNK
Inhibitor
O_2^-
NO
iNOS
3
ONOOH
eNOS
MPT
Cell death (Necrosis)

Figure 6.11

Figure 6.11

Mechanisms of protection by JNK inhibitor against APAP-induced hepatotoxicity.

6.4 Discussion

Protection against APAP hepatotoxicity by JNK inhibition.

The main goal of this study was to evaluate the relative importance of several potential mechanisms of the involvement of JNK signaling in APAP-induced liver injury. JNK activation was monitored by formation of P-JNK due to the autophosphorylation of JNK during activation and the fact that JNK can phosphorylate a variety of downstream proteins not always to the same degree (Wicovsky *et al.*, 2007). Overall, our data showing JNK activation after APAP overdose and a protective effect with the specific JNK inhibitor SP600125 are in agreement with several previous studies (Gunawan *et al.*, 2006; Hanawa *et al.*, 2008; Henderson *et al.*, 2007; Latchoumycandane *et al.*, 2007). Furthermore, the importance of JNK in APAP-induced liver injury was demonstrated by the elimination of ASK, an upstream activator of JNK (Nakagawa *et al.*, 2008b). Our studies also support the conclusion that in contrast to the earlier report (Gunawan *et al.*, 2006) inhibition of JNK2 alone is not effective in reducing APAP hepatotoxicity (Bourdi *et al.*, 2008; Hanawa *et al.*, 2008; Henderson *et al.*, 2007). In addition, selective elimination of JNK1 was also ineffective (Bourdi *et al.*, 2008; Gunawan *et al.*, 2006; Henderson *et al.*, 2007). However, we did not observe an increase in APAP-induced liver injury at the 6 h time point using JNK2-/- mice as was reported by Bourdi et al. for 12 -32 h after APAP (Bourdi *et al.*, 2008). Another important observation in our study is the fact that the solvent used to administer SP600125 (DMSO in

PBS) clearly inhibits the early metabolic activation of APAP and accounts for a substantial protection in this model. Although the inhibitor provides a significant additional effect, it cannot be excluded that the high efficacy of SP600125 may involve some solvent effect. However, since a peptide inhibitor of JNK in the absence of DMSO showed similar efficacy as SP600125 (Henderson *et al.*, 2007), the effect is predominantly caused by inhibition of JNK rather than the initial inhibition of the metabolism.

JNK activation and Bax translocation. Our data indicate that inhibition of JNK reduces the mitochondrial translocation of Bax and the release of AIF from the mitochondria at early and late time points after APAP administration. The effect of JNK on Bax is in agreement with previous reports (Gunawan *et al.*, 2006; Hanawa *et al.*, 2008). We have previously shown that mitochondrial Bax translocation is an early event (beginning at 1 h) after APAP overdose, which is responsible for the early release of intermembrane proteins (Bajt *et al.*, 2008; Jaeschke and Bajt, 2006). Although the release of cytochrome c and Smac does not result in activation of caspases (Knight and Jaeschke, 2002), the nuclear translocation of AIF and endonuclease G appears to be mainly responsible for the characteristic nuclear DNA fragmentation observed after APAP (Bajt *et al.*, 2006). Since Bax-deficient mice show a strong reduction of intermembrane protein release, nuclear DNA damage and cell injury, it can be concluded that these Bax-mediated events contribute to cell

death at these early time-points (Bajt *et al.*, 2008). However, mitochondrial Bax translocation does not affect the mitochondrial oxidant stress and peroxynitrite formation, which subsequently will trigger MPT resulting in mitochondrial swelling and rupture of the outer membrane (Bajt *et al.*, 2008). At this later time-point, intermembrane proteins are released independent of Bax. Thus, even complete elimination of Bax results only in a temporary protection against APAP overdose. This means that the protective effect of JNK inhibition, which lasts during the first 12-24 h, can at best be mediated in part by inhibiting mitochondrial Bax translocation.

The possibility that JNK activation leads to inactivation of the protective Bcl-2 family members Bcl-2 and Bcl-x_L by phosphorylation could also contribute to the mitochondrial dysfunction (Latchoumycandane *et al.*, 2007). However, the protective role of Bcl-2 in APAP hepatotoxicity has been questioned as Bcl-2 overexpressing mice show actually higher injury compared to wild type animals (Adams *et al.*, 2001). Other mechanisms suggested by which inhibition of JNK activation could be protective include the inhibition of Bid processing by caspase-8 inactivation (Wang *et al.*, 2006) and downregulation of Bad expression (Takamura *et al.*, 2007). However, this appears to be a mechanism mainly relevant for TNF-mediated apoptosis. Although not all of the individual Bcl-2 family members have been assessed in the APAP model, Bid-deficient mice are not protected (H. Jaeschke and X.M. Yin, unpublished)

and pancaspase inhibitors do not prevent mitochondrial dysfunction and liver injury after APAP (Jaeschke *et al.*, 2006; Lawson *et al.*, 1999) suggesting that potential effects of JNK on caspase-8 activation and Bid may not be relevant for the injury process.

JNK activation and iNOS induction.

Peroxynitrite, which is formed by the combination of the two radical species superoxide and nitric oxide (NO), is generated in cells undergoing necrosis during APAP hepatotoxicity (Hinson *et al.*, 1998). Scavenging of this aggressive oxidant and nitrating agent by GSH resulted in a profound protection and improved regeneration (Bajt *et al.*, 2003; Knight *et al.*, 2002). However, the source of NO is still controversial. An induction of iNOS during APAP-induced liver injury has been reported (Gardner *et al.*, 2002; Latchoumycandane *et al.*, 2007) but peroxynitrite formation in the absence of iNOS induction was also observed (Knight *et al.*, 2001). In the current study we found a relevant increase of iNOS mRNA but only a moderate increase in iNOS protein expression. Furthermore, no significant elevation of plasma nitrite+nitrate levels as indicator of actual NO formation was found. The potent iNOS inhibitor L-Nil (Zhang *et al.*, 2000a), which completely prevented the endotoxin-induced increase in plasma nitrite+nitrate levels, had no effect on the formation of NO or peroxynitrite during APAP hepatotoxicity and did not affect liver injury. These data do not support the hypothesis that iNOS-derived

NO is critical for APAP-induced peroxynitrite formation and liver injury under our present conditions. A potential reason for the limited importance of iNOS during APAP-induced liver injury may be the formation of IL-10, which can suppress pro-inflammatory gene expression including iNOS thereby reducing a potential contribution of iNOS to the pathophysiology (Bourdi *et al.*, 2002). Although SP600125 attenuated iNOS mRNA and also the minor increase in protein expression, there was no effect on plasma nitrite+nitrate levels. Together these data suggest that JNK activation may contribute to a limited iNOS induction during APAP hepatotoxicity. However, consistent with previous data of us and others (Hinson *et al.*, 2002; Knight *et al.*, 2001), iNOS did not play a relevant role and therefore it is unlikely that the profound protective effect of JNK inhibition was mediated by effects on iNOS. These conclusions are different than those of Latchoumycandane et al. (Latchoumycandane *et al.*, 2007). However, these investigators used leflonamide, which may have additional effects beyond just inhibiting JNK.

JNK activation and oxidant stress.

Our previous studies with APAP hepatotoxicity documented the presence of a mitochondrial oxidant stress (Jaeschke, 1990; Knight *et al.*, 2001) and mitochondrial peroxynitrite formation (Cover *et al.*, 2005b), which preceded cell death and occurred as soon as GSH was depleted (Bajt *et al.*, 2004). Furthermore, when peroxynitrite was being scavenged and more ROS was

detoxified by accelerated recovery of mitochondrial GSH levels initiated by treatment with GSH (Knight *et al.*, 2002), JNK activation was prevented (Figure 6.1). Likewise, when the mitochondrial oxidant stress is inhibited by scavenging of NAPQI by metallothionein induction (Saito *et al.*), JNK activation was prevented (Figure 6.1). These findings suggest that in agreement with previous findings (Hanawa et al., 2008), an oxidant stress was the main trigger of JNK activation after APAP overdose. The oxidant stress most likely does not activate JNK directly but targets upstream events such promoting the dissociation of thioredoxin and apoptosis signal-regulating kinase 1 (ASK1) (Nakagawa *et al.*, 2008a) or the Ras pathway (Saha and Nandi, 2009). Alternatively, JNK can be released from a complex with GST-Pi by binding of NAPQI to GST (Elsby *et al.*, 2003). This would be in agreement with AMAP treatment not activating JNK (Hanawa *et al.*, 2008) and the fact that JNK activation occurs in the cytosol and oxidant stress occurs mainly in mitochondria.

Although JNK appears to be activated by the initial oxidant stress, given the fact that nitrotyrosine staining of the tissue was eliminated by the JNK inhibitor at 6 and 12 h after APAP and that there was no increase of tissue GSSG or the GSSG-to-GSH ratio, it can be concluded that SP600125 effectively prevented the formation of reactive oxygen species. Since ROS and peroxynitrite are mainly formed in mitochondria, this suggested that JNK

activation promotes the formation of ROS in this cell organelle. Interestingly, the solvent of the JNK inhibitor (DMSO in PBS) did not prevent the oxidant stress (judged by GSSG formation) but appears to allow a faster recovery of hepatic GSH levels, which seem to scavenge most of the ROS and peroxynitrite and thus reduce tissue injury. The effect of DMSO is attributed to its inhibitory effect on APAP activation, which limits the injury and promotes recovery. Nevertheless, the JNK inhibitor clearly has additional effects that prevent the mitochondrial oxidant stress. Hanawa et al proposed that translocation of activated JNK may induce MPT (Hanawa *et al.*, 2008). Given the time sequence of rapid GSH depletion and mitochondrial dysfunction followed by oxidant stress, eventually MPT and then cell necrosis (Bajt *et al.*, 2004; Kon *et al.*, 2004), it appears that JNK activation enhances the oxidant stress and peroxynitrite formation, which subsequently induces MPT. Mitochondrial oxidant stress is a potent inducer of MPT (Nieminen *et al.*, 1997). This does not exclude that JNK can synergistically promote MPT through acting directly on proteins involved in MPT (Hanawa *et al.*, 2008). However, it appears highly unlikely that JNK inhibition can prevent MPT in the presence of a substantial mitochondrial oxidant stress and peroxynitrite formation. Further studies are necessary to identify the various targets of JNK in the mitochondria.

In summary, JNK activation seems to control, at least in part, the early release

of intermembrane proteins and DNA fragmentation through mitochondrial Bax translocation. However, the most important effect of JNK activation was a profound suppression of peroxynitrite formation, which was not caused by inhibition of iNOS induction. In contrast, there was clearly a complete elimination of the mitochondrial oxidant stress. Although the exact target of JNK in the mitochondria has to be identified, it appears to be upstream of MPT. Because of the critical role of oxidant stress and peroxynitrite for the propagation of the cell injury mechanisms, especially mitochondrial viability, (Figure 6.11) these data demonstrate that JNK could be an important target to limit cell injury and liver failure at least during the first 24 h after APAP overdose.

CHAPTER 7: CONCLUSION and CLINICAL RELEVANCY

APAP-induced hepatotoxicity in patients undergoes

In England and Wales, there are over 30,000 hospital admissions and about 150 deaths because of APAP overdose each year (Morgan *et al.*, 2007). In the USA, acetaminophen-associated overdoses result in 56,000 emergency room visits, 26,000 hospital admissions, and about 450 deaths annually (Nourjah *et al.*, 2006). Clinically, there are two causes of APAP overdose in patients including unintentional overdose and attempted suicide. In many cases of unintentional APAP ingestion, people are using alcohol, hypnotics, or illicit drugs in combination with APAP and often are unaware of the risk of delaying hospitalization. On the other hand, most intentional overdose patients receive medical care within 24 hours of APAP overdose. Unintentional overdoses are more frequent than intentional overdoses with the median dose being 34 g versus 20 g respectively, but these large doses are consumed over an average of 3 days. Once acute liver failure develops, the outcome for suicidal or unintentional APAP ingestion is similar (Lee, 2004).

The antidote for APAP poising is *N*-acetylcysteine (NAC), which is a cysteine prodrug, and a GSH precursor. Although NAC and cysteine are very similar in terms of chemical structure, NAC is less toxic, because it is less susceptible to oxidation and it is more soluble in water, which makes it a better source of cysteine than administration of cysteine itself (Atkuri *et al.*, 2007). In the clinic,

NAC is injected as follows: one loading dose of 150 mg/kg followed by maintenance doses of 50 mg/kg every 4 h (Polson and Lee, 2005). Oral NAC administration frequently exacerbates the nausea and vomiting associated with APAP poisoning itself since the sulfur moiety of NAC gives a “rotten egg” smell. In 2004, the Food and Drug Administration approved an intravenous NAC administration, Acetadote® which is manufactured by Cumberland Pharmaceuticals in Nashville, Tennessee (Whyte *et al.*, 2008). Intravenous administration of NAC was associated with reduction of antiemetic effects and cost saving (Miller *et al.*, 2007).

Summary and Conclusion

We investigated three mechanisms of protection against APAP-induced hepatotoxicity in this thesis (Figure 7.1) and the following discussion focuses on the relevance of the conclusions to the clinical situation.

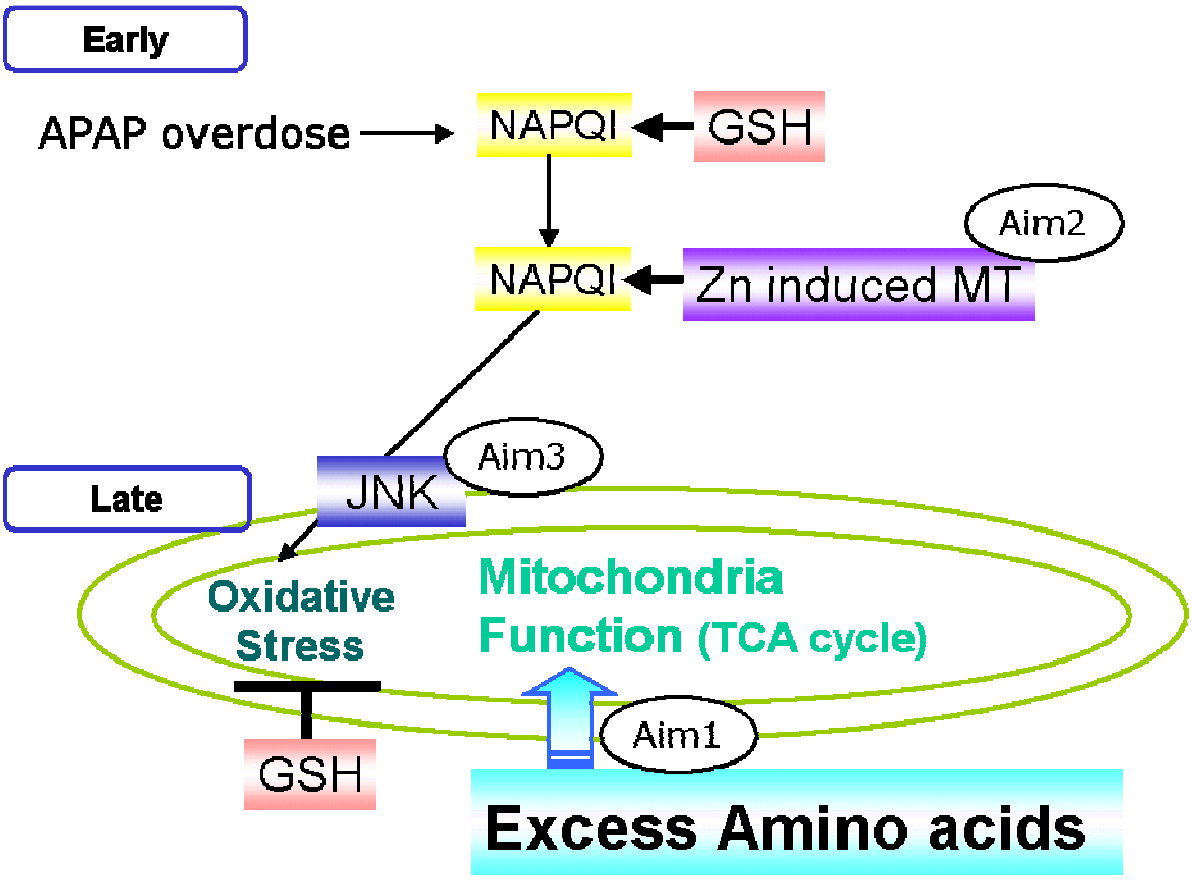

Figure 7.1
Mechanisms of protection in APAP-induced hepatotoxicity

a) Mechanism of protection A: preventing NAPQI binding to proteins

It is well known that the most effective mechanism of protection by GSH or NAC is to enhance the scavenging capacity for NAPQI in hepatocytes. This prevents modification of mitochondrial proteins and thereby blocks the

initiation of APAP toxicity. However, a limitation of this approach in the clinical scenario is that GSH or NAC must be administered during the time when APAP is being metabolized to NAPQI. By the time APAP overdose patients arrive at the emergency room, the metabolism of APAP is over in most cases. In aim 2, we demonstrated that zinc induced metallothionein (MT) can scavenge some of the excess NAPQI after GSH depletion thereby preventing covalent binding to cellular proteins. There are various stimuli to induce MT, such as restriction of food intake (Bremner and Davies, 1975), exercise (Oh *et al.*, 1978; Shiraishi *et al.*, 1983) in addition to heavy metal, and chemical induced MT. Therefore, a non-toxic intervention that induces MT might be beneficial for APAP overdose patients.

b) Mechanism of protection B: scavenging of reactive oxygen and peroxynitirite

Covalent binding of NAPQI to mitochondrial proteins leads to inhibition of mitochondrial respiration with increased mitochondrial synthesis of reactive oxygen species and peroxynitrite formation in mitochondria (Cover *et al.*, 2005b; Jaeschke, 1990; Knight *et al.*, 2001; Tirmenstein and Nelson, 1990). The resulting oxidant stress can activate the c-jun N-terminal kinase, which translocates to the mitochondria and may be involved in the further aggregation of ROS formation and induction of the mitochondrial membrane permeability transition pore opening (Hanawa *et al.*, 2008).

In aim 3, we found that a JNK inhibitor suppressed peroxynitrite formation, which was not caused by inhibition of iNOS induction. However, there was clearly a complete elimination of the mitochondrial oxidant stress. It is probable that JNK could phosphorylate some of the proteins that are important for respiration in the mitochondria and inhibit mitochondrial function. This might also lead to accumulation of electrons and cause oxidative stress in mitochondria. In fact, it has been reported that JNK phosphorylated proteins have been implicated in the induction of mitochondrial membrane permeability pore in the rat brain (Schroeter *et al.*, 2003). In addition, JNK inhibition can protect against APAP-induced disturbance of state III respiration (Hanawa *et al.*, 2008). Although further research is required to determine the detailed mechanisms, JNK inhibitor may be a promising approach because it targets a critical toxic mechanism (ROS formation). In our experience, only interventions that target the mitochondria oxidative stress can be successful in preventing cell death. In addition, SP600125 was shown to be effective even several hours after APAP overdose (Gunawan *et al.*, 2006; Hanawa *et al.*, 2008; Henderson *et al.*, 2007; Latchoumycandane *et al.*, 2007).

c) Mechanism of protection C: Mitochondrial energy substrates

In the 1970s, NAC was used to treat patients with APAP overdose (Prescott *et al.*, 1977). Even today, NAC therapy is thought to be the best treatment for overdose patients (Polson and Lee, 2005). However, our data from aim 1

indicates that GSH confers more efficient protection when compared to an equimolar dose of NAC. This effect is clearly caused by the 3-fold higher amount of amino acids in GSH compared to NAC, and we demonstrated that excess amino acids for metabolism in the Krebs cycle provide the most effective reduction of APAP-induced liver injury. Therefore, in addition to NAC to promote GSH synthesis, the administration of substrates to support the mitochondrial energy metabolism could be a promising supportive strategy to limit APAP-induced cell death and liver failure.

CHAPTER 8: REFERENCES CITED

Adams, M. L., Pierce, R. H., Vail, M. E., White, C. C., Tonge, R. P., Kavanagh, T. J., Fausto, N., Nelson, S. D., and Bruschi, S. A. (2001). Enhanced acetaminophen hepatotoxicity in transgenic mice overexpressing BCL-2. *Mol. Pharmacol.* **60**, 907-15.

Agostini, L., Martinon, F., Burns, K., McDermott, M. F., Hawkins, P. N., and Tschopp, J. (2004). NALP3 forms an IL-1beta-processing inflammasome with increased activity in Muckle-Wells autoinflammatory disorder. *Immunity* **20**, 319-25.

Anderson, S., Bankier, A. T., Barrell, B. G., de Bruijn, M. H., Coulson, A. R., Drouin, J., Eperon, I. C., Nierlich, D. P., Roe, B. A., Sanger, F., Schreier, P. H., Smith, A. J., Staden, R., and Young, I. G. (1981). Sequence and organization of the human mitochondrial genome. *Nature* **290**, 457-65.

Antonsson, B., Montessuit, S., Lauper, S., Eskes, R., and Martinou, J. C. (2000). Bax oligomerization is required for channel-forming activity in liposomes and to trigger cytochrome c release from mitochondria. *Biochem. J.* ***345 Pt 2****, 271-8.*

Atkuri, K. R., Mantovani, J. J., Herzenberg, L. A., and Herzenberg, L. A. (2007). N-Acetylcysteine--a safe antidote for cysteine/glutathione deficiency. *Curr Opin Pharmacol* **7**, 355-9.

Baines, C. P., Kaiser, R. A., Sheiko, T., Craigen, W. J., and Molkentin, J. D. (2007). Voltage-dependent anion channels are dispensable for mitochondrial-dependent cell death. *Nat. Cell Biol.* **9**, 550-5.

Bajt, M. L., Cover, C., Lemasters, J. J., and Jaeschke, H. (2006). Nuclear translocation of endonuclease G and apoptosis-inducing factor during acetaminophen-induced liver cell injury. *Toxicol Sci* **94**, 217-25.

Bajt, M. L., Farhood, A., and Jaeschke, H. (2001). Effects of CXC chemokines on neutrophil activation and sequestration in hepatic vasculature. *Am. J. Physiol.* **281**, G1188-95.

Bajt, M. L., Farhood, A., Lemasters, J. J., and Jaeschke, H. (2008). Mitochondrial bax translocation accelerates DNA fragmentation and cell necrosis in a murine model of acetaminophen hepatotoxicity. *J. Pharmacol. Exp. Ther.* **324**, 8-14.

Bajt, M. L., Knight, T. R., Farhood, A., and Jaeschke, H. (2003). Scavenging peroxynitrite with glutathione promotes regeneration and enhances survival during acetaminophen-induced liver injury in mice. *J. Pharmacol. Exp. Ther.* **307**, 67-73.

Bajt, M. L., Knight, T. R., Lemasters, J. J., and Jaeschke, H. (2004). Acetaminophen-induced oxidant stress and cell injury in cultured mouse hepatocytes: protection by N-acetyl cysteine. *Toxicol Sci* **80**, 343-9.

Bautista, A. P., Meszaros, K., Bojta, J., and Spitzer, J. J. (1990). Superoxide anion generation in the liver during the early stage of endotoxemia in rats. *J. Leukoc. Biol* **48**, 123-8.

Belizario, J. E., Alves, J., Occhiucci, J. M., Garay-Malpartida, M., and Sesso, A. (2007). A mechanistic view of mitochondrial death decision pores. *Braz. J. Med. Biol. Res.* **40**, 1011-24.

Bellot, G., Cartron, P. F., Er, E., Oliver, L., Juin, P., Armstrong, L. C., Bornstein, P., Mihara, K., Manon, S., and Vallette, F. M. (2007). TOM22, a core component of the mitochondria outer membrane protein translocation pore, is a mitochondrial receptor for the proapoptotic protein Bax. *Cell Death Differ.* **14**, 785-94.

Bilzer, M., and Lauterburg, B. H. (1991). Effects of hypochlorous acid and chloramines on vascular resistance, cell integrity, and biliary glutathione disulfide in the perfused rat liver: modulation by glutathione. *J. Hepatol.* **13**, 84-9.

Boess, F., Bopst, M., Althaus, R., Polsky, S., Cohen, S. D., Eugster, H. P., and Boelsterli, U. A. (1998). Acetaminophen hepatotoxicity in tumor necrosis factor/lymphotoxin-alpha gene knockout mice. *Hepatology* **27**, 1021-9.

Bourdi, M., Eiras, D. P., Holt, M. P., Webster, M. R., Reilly, T. P., Welch, K. D., and Pohl, L. R. (2007). Role of IL-6 in an IL-10 and IL-4 double knockout mouse model uniquely susceptible to acetaminophen-induced liver injury. *Chem. Res. Toxicol.* **20**, 208-16.

Bourdi, M., Korrapati, M. C., Chakraborty, M., Yee, S. B., and Pohl, L. R. (2008). Protective role of c-Jun N-terminal kinase 2 in acetaminophen-induced liver injury. *Biochem. Biophys. Res. Commun*. **374**, 6-10.

Bourdi, M., Masubuchi, Y., Reilly, T. P., Amouzadeh, H. R., Martin, J. L.,

George, J. W., Shah, A. G., and Pohl, L. R. (2002). Protection against acetaminophen-induced liver injury and lethality by interleukin 10: role of inducible nitric oxide synthase. *Hepatology* **35**, 289-98.

Bremner, I., and Davies, N. T. (1975). The induction of metallothionein in rat liver by zinc injection and restriction of food intake. *Biochem. J.* **149**, 733-8.

Brenner, C., Cadiou, H., Vieira, H. L., Zamzami, N., Marzo, I., Xie, Z., Leber, B., Andrews, D., Duclohier, H., Reed, J. C., and Kroemer, G. (2000). Bcl-2 and Bax regulate the channel activity of the mitochondrial adenine nucleotide translocator. *Oncogene* **19**, 329-36.

Brigelius-Flohe, R. (1999). Tissue-specific functions of individual glutathione peroxidases. *Free Radic. Biol. Med.* **27**, 951-65.

Brok, J., Buckley, N., and Gluud, C. (2006). Interventions for paracetamol (acetaminophen) overdose. *Cochrane Database Syst Rev*, CD003328.

Burcham, P. C., and Harman, A. W. (1991). Acetaminophen toxicity results in site-specific mitochondrial damage in isolated mouse hepatocytes. *J. Biol. Chem.* **266**, 5049-54.

Cadenas, E., and Davies, K. J. (2000). Mitochondrial free radical generation, oxidative stress, and aging. *Free Radic. Biol. Med.* **29**, 222-30.

Cagen, S. Z., and Klaassen, C. D. (1980). Binding of glutathione-depleting agents to metallothionein. *Toxicol. Appl. Pharmacol.* **54**, 229-37.

Cao, Z., Tanaka, M., Regnier, C., Rothe, M., Yamit-hezi, A., Woronicz, J. D., Fuentes, M. E., Durnin, M. H., Dalrymple, S. A., and Goeddel, D. V. (1999). NF-kappa B activation by tumor necrosis factor and interleukin-1. *Cold Spring Harb. Symp. Quant. Biol.* **64**, 473-83.

Carini, R., Bellomo, G., Benedetti, A., Fulceri, R., Gamberucci, A., Parola, M., Dianzani, M. U., and Albano, E. (1995). Alteration of Na+ homeostasis as a critical step in the development of irreversible hepatocyte injury after adenosine triphosphate depletion. *Hepatology* **21**, 1089-98.

Cartron, P. F., Bellot, G., Oliver, L., Grandier-Vazeille, X., Manon, S., and Vallette, F. M. (2008). Bax inserts into the mitochondrial outer membrane by different mechanisms. *FEBS Lett.* **582**, 3045-51.

Charron, M. J., and Bonner-Weir, S. (1999). Implicating PARP and NAD+ depletion in type I diabetes. *Nat. Med.* **5**, 269-70.

Chen, C., Hennig, G. E., Whiteley, H. E., and Manautou, J. E. (2002). Protection against acetaminophen hepatotoxicity by clofibrate pretreatment: role of catalase induction. *J. Biochem. Mol. Toxicol.* **16**, 227-34.

Chen, C. J., Kono, H., Golenbock, D., Reed, G., Akira, S., and Rock, K. L. (2007). Identification of a key pathway required for the sterile inflammatory response triggered by dying cells. *Nat. Med.* **13**, 851-6.

Cheng, W. H., Zheng, X., Quimby, F. R., Roneker, C. A., and Lei, X. G. (2003). Low levels of glutathione peroxidase 1 activity in selenium-deficient mouse liver affect c-Jun N-terminal kinase activation and p53 phosphorylation on Ser-15 in pro-oxidant-induced aponecrosis. *Biochem. J.* **370**, 927-34.

Chengelis, C. P., Dodd, D. C., Means, J. R., and Kotsonis, F. N. (1986). Protection by zinc against acetaminophen induced hepatotoxicity in mice. *Fundam Appl Toxicol* **6**, 278-84.

Chiu, H., Brittingham, J. A., and Laskin, D. L. (2002). Differential induction of heme oxygenase-1 in macrophages and hepatocytes during acetaminophen-induced hepatotoxicity in the rat: effects of hemin and biliverdin. *Toxicol. Appl. Pharmacol.* **181**, 106-15.

Chosay, J. G., Essani, N. A., Dunn, C. J., and Jaeschke, H. (1997). Neutrophil margination and extravasation in sinusoids and venules of liver during endotoxin-induced injury. *Am. J. Physiol.* **272**, G1195-200.

Cohen, S. D., and Khairallah, E. A. (1997). Selective protein arylation and acetaminophen-induced hepatotoxicity. D*rug Metab. Rev.* **29**, 59-77.

Cohen, S. D., Pumford, N. R., Khairallah, E. A., Boekelheide, K., Pohl, L. R., Amouzadeh, H. R., and Hinson, J. A. (1997). Selective protein covalent binding and target organ toxicity. *Toxicol. Appl. Pharmacol.* **143**, 1-12.

Coles, B., Wilson, I., Wardman, P., Hinson, J. A., Nelson, S. D., and Ketterer, B. (1988). The spontaneous and enzymatic reaction of N-acetyl-p-benzoquinonimine with glutathione: a stopped-flow kinetic study. *Arch. Biochem. Biophys*. **264**, 253-60.

Colletti, L. M., Kunkel, S. L., Walz, A., Burdick, M. D., Kunkel, R. G., Wilke, C. A., and Strieter, R. M. (1996). The role of cytokine networks in the local liver

injury following hepatic ischemia/reperfusion in the rat. *Hepatology* **23**, 506-14.

Corcoran, G. B., Racz, W. J., Smith, C. V., and Mitchell, J. R. (1985). Effects of N-acetylcysteine on acetaminophen covalent binding and hepatic necrosis in mice. *J. Pharmacol. Exp. Ther.* **232**, 864-72.

Corcoran, G. B., and Wong, B. K. (1986). Role of glutathione in prevention of acetaminophen-induced hepatotoxicity by N-acetyl-L-cysteine in vivo: studies with N-acetyl-D-cysteine in mice. *J. Pharmacol. Exp. Ther.* **238**, 54-61.

Costantini, P., Belzacq, A. S., Vieira, H. L., Larochette, N., de Pablo, M. A., Zamzami, N., Susin, S. A., Brenner, C., and Kroemer, G. (2000). Oxidation of a critical thiol residue of the adenine nucleotide translocator enforces Bcl-2-independent permeability transition pore opening and apoptosis. *Oncogene* **19**, 307-14.

Cover, C., Fickert, P., Knight, T. R., Fuchsbichler, A., Farhood, A., Trauner, M., and Jaeschke, H. (2005a). Pathophysiological role of poly(ADP-ribose) polymerase (PARP) activation during acetaminophen-induced liver cell necrosis in mice. *Toxicol Sci* **84**, 201-8.

Cover, C., Liu, J., Farhood, A., Malle, E., Waalkes, M. P., Bajt, M. L., and Jaeschke, H. (2006). Pathophysiological role of the acute inflammatory response during acetaminophen hepatotoxicity. *Toxicol. Appl. Pharmacol.* **216**, 98-107.

Cover, C., Mansouri, A., Knight, T. R., Bajt, M. L., Lemasters, J. J., Pessayre, D., and Jaeschke, H. (2005b). Peroxynitrite-induced mitochondrial and endonuclease-mediated nuclear DNA damage in acetaminophen hepatotoxicity. *J. Pharmacol. Exp. Ther.* **315**, 879-87.

Crompton, M. (1999). The mitochondrial permeability transition pore and its role in cell death. *Biochem. J.* **341 (Pt 2)**, 233-49.

de Kroon, A. I., Dolis, D., Mayer, A., Lill, R., and de Kruijff, B. (1997). Phospholipid composition of highly purified mitochondrial outer membranes of rat liver and Neurospora crassa. Is cardiolipin present in the mitochondrial outer membrane? *Biochim. Biophys. Acta* **1325**, 108-16.

Decker, K. (1990). Biologically active products of stimulated liver macrophages (Kupffer cells). *Eur. J. Biochem.* **192**, 245-61.

Dinarello, C. A. (1996). Biologic basis for interleukin-1 in disease. *Blood* **87**, 2095-147.

Dorman, R. B., Gujral, J. S., Bajt, M. L., Farhood, A., and Jaeschke, H. (2005). Generation and functional significance of CXC chemokines for neutrophil-induced liver injury during endotoxemia. *Am. J. Physiol.* **288**, G880-6.

Dripps, D. J., Brandhuber, B. J., Thompson, R. C., and Eisenberg, S. P. (1991). Interleukin-1 (IL-1) receptor antagonist binds to the 80-kDa IL-1 receptor but does not initiate IL-1 signal transduction. *J. Biol. Chem.* **266**, 10331-6.

El-Benna, J., Dang, P. M., Gougerot-Pocidalo, M. A., and Elbim, C. (2005). Phagocyte NADPH oxidase: a multicomponent enzyme essential for host defenses. *Arch. Immunol. Ther. Exp.* **53**, 199-206.

El-Hassan, H., Anwar, K., Macanas-Pirard, P., Crabtree, M., Chow, S. C., Johnson, V. L., Lee, P. C., Hinton, R. H., Price, S. C., and Kass, G. E. (2003). Involvement of mitochondria in acetaminophen-induced apoptosis and hepatic injury: roles of cytochrome c, Bax, Bid, and caspases. *Toxicol. Appl. Pharmacol.* **191**, 118-29.

Elsby, R., Kitteringham, N. R., Goldring, C. E., Lovatt, C. A., Chamberlain, M., Henderson, C. J., Wolf, C. R., and Park, B. K. (2003). Increased constitutive c-Jun N-terminal kinase signaling in mice lacking glutathione S-transferase Pi. *J. Biol. Chem.* **278**, 22243-9.

Er, E., Oliver, L., Cartron, P. F., Juin, P., Manon, S., and Vallette, F. M. (2006). Mitochondria as the target of the pro-apoptotic protein Bax. *Biochim. Biophys. Acta* **1757**, 1301-11.

Eskes, R., Desagher, S., Antonsson, B., and Martinou, J. C. (2000). Bid induces the oligomerization and insertion of Bax into the outer mitochondrial membrane. *Mol. Cell. Biol.* **20**, 929-35.

Essani, N. A., Bajt, M. L., Farhood, A., Vonderfecht, S. L., and Jaeschke, H. (1997). Transcriptional activation of vascular cell adhesion molecule-1 gene in vivo and its role in the pathophysiology of neutrophil-induced liver injury in murine endotoxin shock. *J Immunol* **158**, 5941-8.

Essani, N. A., Fisher, M. A., Farhood, A., Manning, A. M., Smith, C. W., and Jaeschke, H. (1995). Cytokine-induced upregulation of hepatic intercellular

adhesion molecule-1 messenger RNA expression and its role in the pathophysiology of murine endotoxin shock and acute liver failure. *Hepatology* **21**, 1632-9.

Esterline, R. L., Ray, S. D., and Ji, S. (1989). Reversible and irreversible inhibition of hepatic mitochondrial respiration by acetaminophen and its toxic metabolite, N-acetyl-p-benzoquinoneimine (NAPQI). *Biochem. Pharmacol.* **38**, 2387-90.

Farhood, A., McGuire, G. M., Manning, A. M., Miyasaka, M., Smith, C. W., and Jaeschke, H. (1995). Intercellular adhesion molecule 1 (ICAM-1) expression and its role in neutrophil-induced ischemia-reperfusion injury in rat liver. *J. Leukoc. Biol.* **57**, 368-74.

Fernandez-Checa, J. C., and Kaplowitz, N. (2005). Hepatic mitochondrial glutathione: transport and role in disease and toxicity. *Toxicol. Appl. Pharmacol.* **204**, 263-73.

Ferret, P. J., Hammoud, R., Tulliez, M., Tran, A., Trebeden, H., Jaffray, P., Malassagne, B., Calmus, Y., Weill, B., and Batteux, F. (2001). Detoxification of reactive oxygen species by a nonpeptidyl mimic of superoxide dismutase cures acetaminophen-induced acute liver failure in the mouse. *Hepatology* **33**, 1173-80.

Fujimoto, K., Kumagai, K., Ito, K., Arakawa, S., Ando, Y., Oda, S., Yamoto, T., and Manabe, S. (2009). Sensitivity of liver injury in heterozygous Sod2 knockout mice treated with troglitazone or acetaminophen. *Toxicol Pathol* **37**, 193-200.

Gao, B., Jeong, W. I., and Tian, Z. (2008). Liver: An organ with predominant innate immunity. *Hepatology* **47**, 729-36.

Gao, B., Radaeva, S., and Park, O. (2009). Liver natural killer and natural killer T cells: immunobiology and emerging roles in liver diseases. J*. Leukoc. Biol.* **86,** 513-28.

Gardner, C. R., Laskin, J. D., Dambach, D. M., Chiu, H., Durham, S. K., Zhou, P., Bruno, M., Gerecke, D. R., Gordon, M. K., and Laskin, D. L. (2003). Exaggerated hepatotoxicity of acetaminophen in mice lacking tumor necrosis factor receptor-1. Potential role of inflammatory mediators. *Toxicol. Appl. Pharmacol.* **192**, 119-30.

Gardner, C. R., Laskin, J. D., Dambach, D. M., Sacco, M., Durham, S. K.,

Bruno, M. K., Cohen, S. D., Gordon, M. K., Gerecke, D. R., Zhou, P., and Laskin, D. L. (2002). Reduced hepatotoxicity of acetaminophen in mice lacking inducible nitric oxide synthase: potential role of tumor necrosis factor-alpha and interleukin-10. *Toxicol. Appl. Pharmacol.* **184**, 27-36.

Gottlieb, R. A. (2000). Mitochondria: execution central. *FEBS Lett.* **482**, 6-12.

Gross, A., McDonnell, J. M., and Korsmeyer, S. J. (1999). BCL-2 family members and the mitochondria in apoptosis. *Genes Dev.* **13**, 1899-911.

Gujral, J. S., Knight, T. R., Farhood, A., Bajt, M. L., and Jaeschke, H. (2002). Mode of cell death after acetaminophen overdose in mice: apoptosis or oncotic necrosis? *Toxicol Sci* **67**, 322-8.

Gunawan, B. K., Liu, Z. X., Han, D., Hanawa, N., Gaarde, W. A., and Kaplowitz, N. (2006). c-Jun N-terminal kinase plays a major role in murine acetaminophen hepatotoxicity. *Gastroenterology* **131**, 165-78.

Gupta, S., Rogers, L. K., Taylor, S. K., and Smith, C. V. (1997). Inhibition of carbamyl phosphate synthetase-I and glutamine synthetase by hepatotoxic doses of acetaminophen in mice. *Toxicol. Appl. Pharmacol.* **146**, 317-27.

Ha, H. C., and Snyder, S. H. (1999). Poly(ADP-ribose) polymerase is a mediator of necrotic cell death by ATP depletion. P*roc. Natl. Acad. Sci. U.S.A*. **96**, 13978-82.

Hanawa, N., Shinohara, M., Saberi, B., Gaarde, W. A., Han, D., and Kaplowitz, N. (2008). Role of JNK translocation to mitochondria leading to inhibition of mitochondria bioenergetics in acetaminophen-induced liver injury. *J. Biol. Chem*. **283**, 13565-77.

Harrison, P. M., Keays, R., Bray, G. P., Alexander, G. J., and Williams, R. (1990). Improved outcome of paracetamol-induced fulminant hepatic failure by late administration of acetylcysteine. *Lancet* **335**, 1572-3.

Hayakawa, J., Depatie, C., Ohmichi, M., and Mercola, D. (2003). The activation of c-Jun NH2-terminal kinase (JNK) by DNA-damaging agents serves to promote drug resistance via activating transcription factor 2 (ATF2)-dependent enhanced DNA repair. *J. Biol. Chem* **278**, 20582-92.

Henderson, N. C., Pollock, K. J., Frew, J., Mackinnon, A. C., Flavell, R. A., Davis, R. J., Sethi, T., and Simpson, K. J. (2007). Critical role of c-jun (NH2) terminal kinase in paracetamol- induced acute liver failure. *Gut* **56**, 982-90.

Hibi, M., Lin, A., Smeal, T., Minden, A., and Karin, M. (1993). Identification of an oncoprotein- and UV-responsive protein kinase that binds and potentiates the c-Jun activation domain. *Genes Dev* **7**, 2135-48.

Hinson, J. A., Bucci, T. J., Irwin, L. K., Michael, S. L., and Mayeux, P. R. (2002). Effect of inhibitors of nitric oxide synthase on acetaminophen-induced hepatotoxicity in mice. *Nitric Oxide* **6**, 160-7.

Hinson, J. A., Pike, S. L., Pumford, N. R., and Mayeux, P. R. (1998). Nitrotyrosine-protein adducts in hepatic centrilobular areas following toxic doses of acetaminophen in mice. *Chem. Res. Toxicol.* **11**, 604-7.

Hoos, J. S., Damsten, M. C., de Vlieger, J. S., Commandeur, J. N., Vermeulen, N. P., Niessen, W. M., Lingeman, H., and Irth, H. (2007). Automated detection of covalent adducts to human serum albumin by immunoaffinity chromatography, on-line solution phase digestion and liquid chromatography-mass spectrometry. *J Chromatogr B Analyt Technol Biomed Life Sci* **859**, 147-56.

Horbach, M., Gerber, E., and Kahl, R. (1997). Influence of acetaminophen treatment and hydrogen peroxide treatment on the release of a CINC-related protein and TNF-alpha from rat hepatocyte cultures. *Toxicology* **121**, 117-26.

Hunter, D. R., and Haworth, R. A. (1979). The Ca2+-induced membrane transition in mitochondria. I. The protective mechanisms. *Arch. Biochem. Biophys.* **195**, 453-9.

Imaeda, A. B., Watanabe, A., Sohail, M. A., Mahmood, S., Mohamadnejad, M., Sutterwala, F. S., Flavell, R. A., and Mehal, W. Z. (2009). Acetaminophen-induced hepatotoxicity in mice is dependent on Tlr9 and the Nalp3 inflammasome. *J. Clin. Invest.* **119**, 305-14.

Ishibe, T., Kimura, A., Ishida, Y., Takayasu, T., Hayashi, T., Tsuneyama, K., Matsushima, K., Sakata, I., Mukaida, N., and Kondo, T. (2009). Reduced acetaminophen-induced liver injury in mice by genetic disruption of IL-1 receptor antagonist. *Lab. Invest.* **89**, 68-79.

Ishida, Y., Kondo, T., Ohshima, T., Fujiwara, H., Iwakura, Y., and Mukaida, N. (2002). A pivotal involvement of IFN-gamma in the pathogenesis of acetaminophen-induced acute liver injury. *Faseb J* **16**, 1227-36.

Ishida, Y., Kondo, T., Tsuneyama, K., Lu, P., Takayasu, T., and Mukaida, N.

(2004). The pathogenic roles of tumor necrosis factor receptor p55 in acetaminophen-induced liver injury in mice. *J. Leukoc. Biol.* **75**, 59-67.

Ito, Y., Abril, E. R., Bethea, N. W., and McCuskey, R. S. (2004). Role of nitric oxide in hepatic microvascular injury elicited by acetaminophen in mice. *Am. J. Physiol.* **286**, G60-7.

Jacob, M., Mannherz, H. G., and Napirei, M. (2007). Chromatin breakdown by deoxyribonuclease1 promotes acetaminophen-induced liver necrosis: an ultrastructural and histochemical study on male CD-1 mice. *Histochem. Cell Biol.* **128**, 19-33.

Jaeschke, H. (1990). Glutathione disulfide formation and oxidant stress during acetaminophen-induced hepatotoxicity in mice in vivo: the protective effect of allopurinol. *J. Pharmacol. Exp. Ther.* **255**, 935-41.

Jaeschke, H. (2000). Reactive oxygen and mechanisms of inflammatory liver injury. *J. Gastroenterol. Hepatol.* **15**, 718-24.

Jaeschke, H. (2005). Role of inflammation in the mechanism of acetaminophen-induced hepatotoxicity. *Expert Opin Drug Metab Toxicol* **1**, 389-97.

Jaeschke, H. (2006). Mechanisms of Liver Injury. II. Mechanisms of neutrophil-induced liver cell injury during hepatic ischemia-reperfusion and other acute inflammatory conditions. *Am. J. Physiol.* **290**, G1083-8.

Jaeschke, H. (2008). Innate immunity and acetaminophen-induced liver injury: why so many controversies? *Hepatology* **48**, 699-701.

Jaeschke, H., and Bajt, M. L. (2006). Intracellular signaling mechanisms of acetaminophen-induced liver cell death. *Toxicol Sci* **89**, 31-41.

Jaeschke, H., Bautista, A. P., Spolarics, Z., and Spitzer, J. J. (1991). Superoxide generation by Kupffer cells and priming of neutrophils during reperfusion after hepatic ischemia. *Free Radic. Res. Commun.* **15**, 277-84.

Jaeschke, H., Cover, C., and Bajt, M. L. (2006). Role of caspases in acetaminophen-induced liver injury. *Life Sci.* **78**, 1670-6.

Jaeschke, H., and Farhood, A. (1991). Neutrophil and Kupffer cell-induced oxidant stress and ischemia-reperfusion injury in rat liver. *Am. J. Physiol.* **260**, G355-62.

Jaeschke, H., and Hasegawa, T. (2006). Role of neutrophils in acute inflammatory liver injury. *Liver Int* **26**, 912-9.

Jaeschke, H., Knight, T. R., and Bajt, M. L. (2003). The role of oxidant stress and reactive nitrogen species in acetaminophen hepatotoxicity. *Toxicol. Lett.* **144**, 279-88.

Jaeschke, H., Lebofsky, M., Lemasters, J.J., and Bajt, M.L. (2007). Apoptosis-inducing factor causes mitochondrial oxidant stress and nuclear DNA fragmentation in acetaminophen-induced liver injury. *Hepatology* **46**, 253A.

Jaeschke, H., and Liu, J. (2007). Neutrophil depletion protects against murine acetaminophen hepatotoxicity: another perspective. *Hepatology* **45**, 1588-9; author reply 1589.

Jaeschke, H., and Mitchell, J. R. (1990). Use of isolated perfused organs in hypoxia and ischemia/reperfusion oxidant stress. *Meth. Enzymol.* **186**, 752-9.

Jaeschke, H., and Smith, C. W. (1997a). Cell adhesion and migration. III. Leukocyte adhesion and transmigration in the liver vasculature. *Am. J. Physiol.* **273**, G1169-73.

Jaeschke, H., and Smith, C. W. (1997b). Mechanisms of neutrophil-induced parenchymal cell injury. *J. Leukoc. Biol.* **61**, 647-53.

James, L. P., Mayeux, P. R., and Hinson, J. A. (2003a). Acetaminophen-induced hepatotoxicity. *Drug Metab. Dispos.* **31**, 1499-506.

James, L. P., McCullough, S. S., Knight, T. R., Jaeschke, H., and Hinson, J. A. (2003b). Acetaminophen toxicity in mice lacking NADPH oxidase activity: role of peroxynitrite formation and mitochondrial oxidant stress. *Free Radic Res* **37**, 1289-97.

James, L. P., McCullough, S. S., Lamps, L. W., and Hinson, J. A. (2003c). Effect of N-acetylcysteine on acetaminophen toxicity in mice: relationship to reactive nitrogen and cytokine formation. *Toxicol Sci* **75**, 458-67.

Janeway, C. A., Jr., and Medzhitov, R. (2002). Innate immune recognition. *Annu. Rev. Immunol.* **20**, 197-216.

Jollow, D. J., Mitchell, J. R., Potter, W. Z., Davis, D. C., Gillette, J. R., and

Brodie, B. B. (1973). Acetaminophen-induced hepatic necrosis. II. Role of covalent binding in vivo. *J. Pharmacol. Exp.* **187**, 195-202.

Ju, C., Reilly, T. P., Bourdi, M., Radonovich, M. F., Brady, J. N., George, J. W., and Pohl, L. R. (2002). Protective role of Kupffer cells in acetaminophen-induced hepatic injury in mice. *Chem. Res. Toxicol.* **15**, 1504-13.

Jurkowitz, M. S., Geisbuhler, T., Jung, D. W., and Brierley, G. P. (1983). Ruthenium red-sensitive and -insensitive release of Ca2+ from uncoupled heart mitochondria. *Arch. Biochem. Biophys.* **223**, 120-8.

Klaassen, C. D., Liu, J., and Choudhuri, S. (1999). Metallothionein: an intracellular protein to protect against cadmium toxicity. A*nnu. Rev. Pharmacol. Toxicol.* **39**, 267-94.

Klingenberg, M. (1980). The ADP-ATP translocation in mitochondria, a membrane potential controlled transport. *J. Membr. Biol.* **56**, 97-105.

Knight, T. R., Fariss, M. W., Farhood, A., and Jaeschke, H. (2003). Role of lipid peroxidation as a mechanism of liver injury after acetaminophen overdose in mice. *Toxicol Sci* **76**, 229-36.

Knight, T. R., Ho, Y. S., Farhood, A., and Jaeschke, H. (2002). Peroxynitrite is a critical mediator of acetaminophen hepatotoxicity in murine livers: protection by glutathione. *J. Pharmacol. Exp. Ther.* **303**, 468-75.

Knight, T. R., and Jaeschke, H. (2002). Acetaminophen-induced inhibition of Fas receptor-mediated liver cell apoptosis: mitochondrial dysfunction versus glutathione depletion. *Toxicol. Appl. Pharmacol.* **181**, 133-41.

Knight, T. R., and Jaeschke, H. (2004). Peroxynitrite formation and sinusoidal endothelial cell injury during acetaminophen-induced hepatotoxicity in mice. *Comp Hepatol* **3 Suppl 1**, S46.

Knight, T. R., Kurtz, A., Bajt, M. L., Hinson, J. A., and Jaeschke, H. (2001). Vascular and hepatocellular peroxynitrite formation during acetaminophen toxicity: role of mitochondrial oxidant stress. *Toxicol Sci* **62**, 212-20.

Kokoszka, J. E., Waymire, K. G., Levy, S. E., Sligh, J. E., Cai, J., Jones, D. P., MacGregor, G. R., and Wallace, D. C. (2004). The ADP/ATP translocator is not essential for the mitochondrial permeability transition pore. *Nature* **427**, 461-5.

Kon, K., Kim, J. S., Jaeschke, H., and Lemasters, J. J. (2004). Mitochondrial permeability transition in acetaminophen-induced necrosis and apoptosis of cultured mouse hepatocytes. *Hepatology* **40**, 1170-9.

Koppenol, W. H. (1998). The basic chemistry of nitrogen monoxide and peroxynitrite. *Free Radic. Biol. Med.* **25**, 385-91.

Kowaltowski, A. J., Castilho, R. F., and Vercesi, A. E. (2001). Mitochondrial permeability transition and oxidative stress. *FEBS Lett.* **495**, 12-5.

Kowaltowski, A. J., Vercesi, A. E., and Fiskum, G. (2000). Bcl-2 prevents mitochondrial permeability transition and cytochrome c release via maintenance of reduced pyridine nucleotides. *Cell Death Differ.* **7**, 903-10.

Kroemer, G., Galluzzi, L., and Brenner, C. (2007). Mitochondrial membrane permeabilization in cell death. *Physiol. Rev.* **87**, 99-163.

Kumari, M. V., Hiramatsu, M., and Ebadi, M. (1998). Free radical scavenging actions of metallothionein isoforms I and II. *Free Radic. Res.* **29**, 93-101.

Larson, A. M., Polson, J., Fontana, R. J., Davern, T. J., Lalani, E., Hynan, L. S., Reisch, J. S., Schiodt, F. V., Ostapowicz, G., Shakil, A. O., and Lee, W. M. (2005). Acetaminophen-induced acute liver failure: results of a United States multicenter, prospective study. *Hepatology* **42**, 1364-72.

Lash, L. H. (2006). Mitochondrial glutathione transport: physiological, pathological and toxicological implications. *Chem. Biol. Interact.* **163**, 54-67.

Laskin, D. L., Gardner, C. R., Price, V. F., and Jollow, D. J. (1995). Modulation of macrophage functioning abrogates the acute hepatotoxicity of acetaminophen. *Hepatology* **21**, 1045-50.

Laskin, D. L., and Pilaro, A. M. (1986). Potential role of activated macrophages in acetaminophen hepatotoxicity. I. Isolation and characterization of activated macrophages from rat liver. *Toxicol. Appl. Pharmacol.* **86**, 204-15.

Latchoumycandane, C., Goh, C. W., Ong, M. M., and Boelsterli, U. A. (2007). Mitochondrial protection by the JNK inhibitor leflunomide rescues mice from acetaminophen-induced liver injury. *Hepatology* **45**, 412-21.

Lauterburg, B. H., Corcoran, G. B., and Mitchell, J. R. (1983). Mechanism of

action of N-acetylcysteine in the protection against the hepatotoxicity of acetaminophen in rats in vivo. *J. Clin. Invest.* **71**, 980-91.

Lauterburg, B. H., Smith, C. V., Hughes, H., and Mitchell, J. R. (1984). Biliary excretion of glutathione and glutathione disulfide in the rat. Regulation and response to oxidative stress. *J. Clin. Invest.* **73**, 124-33.

Lawson, J. A., Farhood, A., Hopper, R. D., Bajt, M. L., and Jaeschke, H. (2000). The hepatic inflammatory response after acetaminophen overdose: role of neutrophils. *Toxicol Sci* **54**, 509-16.

Lawson, J. A., Fisher, M. A., Simmons, C. A., Farhood, A., and Jaeschke, H. (1999). Inhibition of Fas receptor (CD95)-induced hepatic caspase activation and apoptosis by acetaminophen in mice. *Toxicol. Appl. Pharmacol.* **156**, 179-86.

Lee, W. M. (2004). Acetaminophen and the U.S. Acute Liver Failure Study Group: lowering the risks of hepatic failure. *Hepatology* **40**, 6-9.

Lentsch, A. B., Yoshidome, H., Cheadle, W. G., Miller, F. N., and Edwards, M. J. (1998). Chemokine involvement in hepatic ischemia/reperfusion injury in mice: roles for macrophage inflammatory protein-2 and Kupffer cells. *Hepatology* **27**, 507-12.

Li, D., Ueta, E., Kimura, T., Yamamoto, T., and Osaki, T. (2004a). Reactive oxygen species (ROS) control the expression of Bcl-2 family proteins by regulating their phosphorylation and ubiquitination. *Cancer Sci.* **95**, 644-50.

Li, L., Feng, Z., and Porter, A. G. (2004b). JNK-dependent phosphorylation of c-Jun on serine 63 mediates nitric oxide-induced apoptosis of neuroblastoma cells. *J. Biol. Chem.* **279**, 4058-65.

Li, L. Y., Luo, X., and Wang, X. (2001). Endonuclease G is an apoptotic DNase when released from mitochondria. *Nature* **412**, 95-9.

Lim, S. Y., Davidson, S. M., Hausenloy, D. J., and Yellon, D. M. (2007). Preconditioning and postconditioning: the essential role of the mitochondrial permeability transition pore. *Cardiovasc. Res.* **75**, 530-5.

Limaye, P. B., Apte, U. M., Shankar, K., Bucci, T. J., Warbritton, A., and Mehendale, H. M. (2003). Calpain released from dying hepatocytes mediates progression of acute liver injury induced by model hepatotoxicants. T*oxicol. Appl. Pharmacol.* **191**, 211-26.

Limaye, P. B., Bhave, V. S., Palkar, P. S., Apte, U. M., Sawant, S. P., Yu, S., Latendresse, J. R., Reddy, J. K., and Mehendale, H. M. (2006). Upregulation of calpastatin in regenerating and developing rat liver: role in resistance against hepatotoxicity. *Hepatology* **44**, 379-88.

Liu, J., Liu, Y., Hartley, D., Klaassen, C. D., Shehin-Johnson, S. E., Lucas, A., and Cohen, S. D. (1999). Metallothionein-I/II knockout mice are sensitive to acetaminophen-induced hepatotoxicity. *J. Pharmacol. Exp. Ther.* **289**, 580-6.

Liu, J., Zhou, Z. X., Zhang, W., Bell, M. W., and Waalkes, M. P. (2009). Changes in hepatic gene expression in response to hepatoprotective levels of zinc. *Liver Int* **29**, 1222-9.

Liu, P., McGuire, G. M., Fisher, M. A., Farhood, A., Smith, C. W., and Jaeschke, H. (1995). Activation of Kupffer cells and neutrophils for reactive oxygen formation is responsible for endotoxin-enhanced liver injury after hepatic ischemia. *Shock* **3**, 56-62.

Liu, Z. X., Govindarajan, S., and Kaplowitz, N. (2004). Innate immune system plays a critical role in determining the progression and severity of acetaminophen hepatotoxicity. *Gastroenterology* **127**, 1760-74.

Liu, Z. X., Han, D., Gunawan, B., and Kaplowitz, N. (2006). Neutrophil depletion protects against murine acetaminophen hepatotoxicity. *Hepatology* **43**, 1220-30.

Lores Arnaiz, S., Llesuy, S., Cutrin, J. C., and Boveris, A. (1995). Oxidative stress by acute acetaminophen administration in mouse liver. F*ree Radic. Biol. Med.* **19**, 303-10.

Lu, S. C. (2009). Regulation of glutathione synthesis. *Mol. Aspects Med.* **30**, 42-59.

Mansouri, A., Gaou, I., De Kerguenec, C., Amsellem, S., Haouzi, D., Berson, A., Moreau, A., Feldmann, G., Letteron, P., Pessayre, D., and Fromenty, B. (1999). An alcoholic binge causes massive degradation of hepatic mitochondrial DNA in mice. *Gastroenterology* **117**, 181-90.

Mansouri, A., Haouzi, D., Descatoire, V., Demeilliers, C., Sutton, A., Vadrot, N., Fromenty, B., Feldmann, G., Pessayre, D., and Berson, A. (2003). Tacrine inhibits topoisomerases and DNA synthesis to cause mitochondrial DNA depletion and apoptosis in mouse liver. *Hepatology* **38**, 715-25.

Mariathasan, S., and Monack, D. M. (2007). Inflammasome adaptors and sensors: intracellular regulators of infection and inflammation. *Nat. Rev.* **7**, 31-40.

Mariathasan, S., Newton, K., Monack, D. M., Vucic, D., French, D. M., Lee, W. P., Roose-Girma, M., Erickson, S., and Dixit, V. M. (2004). Differential activation of the inflammasome by caspase-1 adaptors ASC and Ipaf. *Nature* **430**, 213-8.

Martinon, F., Burns, K., and Tschopp, J. (2002). The inflammasome: a molecular platform triggering activation of inflammatory caspases and processing of proIL-beta. *Mol. Cell* **10**, 417-26.

Marzo, I., Brenner, C., Zamzami, N., Jurgensmeier, J. M., Susin, S. A., Vieira, H. L., Prevost, M. C., Xie, Z., Matsuyama, S., Reed, J. C., and Kroemer, G. (1998). Bax and adenine nucleotide translocator cooperate in the mitochondrial control of apoptosis. *Science* **281**, 2027-31.

Masson, M. J., Carpenter, L. D., Graf, M. L., and Pohl, L. R. (2008). Pathogenic role of natural killer T and natural killer cells in acetaminophen-induced liver injury in mice is dependent on the presence of dimethyl sulfoxide. *Hepatology* **48**, 889-97.

Mathupala, S. P., Ko, Y. H., and Pedersen, P. L. (2006). Hexokinase II: cancer's double-edged sword acting as both facilitator and gatekeeper of malignancy when bound to mitochondria. *Oncogene* **25**, 4777-86.

McConnachie, L. A., Mohar, I., Hudson, F. N., Ware, C. B., Ladiges, W. C., Fernandez, C., Chatterton-Kirchmeier, S., White, C. C., Pierce, R. H., and Kavanagh, T. J. (2007). Glutamate cysteine ligase modifier subunit deficiency and gender as determinants of acetaminophen-induced hepatotoxicity in mice. *Toxicol Sci* **99**, 628-36.

Michael, S. L., Mayeux, P. R., Bucci, T. J., Warbritton, A. R., Irwin, L. K., Pumford, N. R., and Hinson, J. A. (2001). Acetaminophen-induced hepatotoxicity in mice lacking inducible nitric oxide synthase activity. *Nitric Oxide* **5**, 432-41.

Michael, S. L., Pumford, N. R., Mayeux, P. R., Niesman, M. R., and Hinson, J. A. (1999). Pretreatment of mice with macrophage inactivators decreases acetaminophen hepatotoxicity and the formation of reactive oxygen and nitrogen species. *Hepatology* **30**, 186-95.

Miller, M. A., Navarro, M., Bird, S. B., and Donovan, J. L. (2007). Antiemetic use in acetaminophen poisoning: how does the route of N-acetylcysteine administration affect utilization? *J Med Toxicol* **3**, 152-6.

Mitchell, J. R., Jollow, D. J., Potter, W. Z., Davis, D. C., Gillette, J. R., and Brodie, B. B. (1973a). Acetaminophen-induced hepatic necrosis. I. Role of drug metabolism. *J. Pharmacol. Exp. Ther.* **187**, 185-94.

Mitchell, J. R., Jollow, D. J., Potter, W. Z., Gillette, J. R., and Brodie, B. B. (1973b). Acetaminophen-induced hepatic necrosis. IV. Protective role of glutathione. *J. Pharmacol. Exp. Ther.* **187**, 211-7.

Mitchell, P., and Moyle, J. (1965a). Evidence discriminating between the chemical and the chemiosmotic mechanisms of electron transport phosphorylation. *Nature* **208**, 1205-6.

Mitchell, P., and Moyle, J. (1965b). Stoichiometry of proton translocation through the respiratory chain and adenosine triphosphatase systems of rat liver mitochondria. *Nature* **208**, 147-51.

Morgan, O. W., Griffiths, C., and Majeed, A. (2007). Interrupted time-series analysis of regulations to reduce paracetamol (acetaminophen) poisoning. *PLoS Med.* **4**, e105.

Muriel, P. (2000). Regulation of nitric oxide synthesis in the liver. *J Appl Toxicol* **20**, 189-95.

Nakagawa, H., Maeda, S., Hikiba, Y., Ohmae, T., Shibata, W., Yanai, A., Sakamoto, K., Ogura, K., Noguchi, T., Karin, M., Ichijo, H., and Omata, M. (2008a). Deletion of apoptosis signal-regulating kinase 1 attenuates acetaminophen-induced liver injury by inhibiting c-Jun N-terminal kinase activation. *Gastroenterology* **135**, 1311-21.

Napirei, M., Basnakian, A. G., Apostolov, E. O., and Mannherz, H. G. (2006). Deoxyribonuclease 1 aggravates acetaminophen-induced liver necrosis in male CD-1 mice. *Hepatology* **43**, 297-305.

Napirei, M., Ricken, A., Eulitz, D., Knoop, H., and Mannherz, H. G. (2004a). Expression pattern of the deoxyribonuclease 1 gene: lessons from the Dnase1 knockout mouse. *Biochem. J.* **380**, 929-37.

Napirei, M., Wulf, S., Eulitz, D., Mannherz, H. G., and Kloeckl, T. (2005).

Comparative characterization of rat deoxyribonuclease 1 (Dnase1) and murine deoxyribonuclease 1-like 3 (Dnase1l3). *Biochem. J.* **389**, 355-64.

Napirei, M., Wulf, S., and Mannherz, H. G. (2004b). Chromatin breakdown during necrosis by serum Dnase1 and the plasminogen system. *Arthritis Rheum.* **50**, 1873-83.

Nelson, S. D. (1990). Molecular mechanisms of the hepatotoxicity caused by acetaminophen. *Semin. Liver Dis.* **10**, 267-78.

Nelson, S. D. (1995). Mechanisms of the formation and disposition of reactive metabolites that can cause acute liver injury. *Drug Metab. Rev.* **27**, 147-77.

Nieminen, A. L., Byrne, A. M., Herman, B., and Lemasters, J. J. (1997). Mitochondrial permeability transition in hepatocytes induced by t-BuOOH: NAD(P)H and reactive oxygen species. *Am. J. Physiol.* **272**, C1286-94.

Nieminen, A. L., Saylor, A. K., Tesfai, S. A., Herman, B., and Lemasters, J. J. (1995). Contribution of the mitochondrial permeability transition to lethal injury after exposure of hepatocytes to t-butylhydroperoxide. *Biochem. J.* **307 (Pt 1)**, 99-106.

Nourjah, P., Ahmad, S. R., Karwoski, C., and Willy, M. (2006). Estimates of acetaminophen (Paracetomal)-associated overdoses in the United States. *Pharmacoepidemiol Drug Saf* **15**, 398-405.

Ogura, Y., Sutterwala, F. S., and Flavell, R. A. (2006). The inflammasome: first line of the immune response to cell stress. *Cell* **126**, 659-62.

Oh, S. H., Deagen, J. T., Whanger, P. D., and Weswig, P. H. (1978). Biological function of metallothionein-IV. Biosynthesis and degradation of liver and kidney metallothionein in rats fed diets containing zinc or cadmium. *Bioinorg Chem* **8**, 245-54.

Okaya, T., and Lentsch, A. B. (2003). Cytokine cascades and the hepatic inflammatory response to ischemia and reperfusion. *J Invest Surg* **16**, 141-7.

Olafsdottir, K., and Reed, D. J. (1988). Retention of oxidized glutathione by isolated rat liver mitochondria during hydroperoxide treatment. *Biochim. Biophys. Acta* **964**, 377-82.

Orrenius, S., Gogvadze, V., and Zhivotovsky, B. (2007). Mitochondrial oxidative stress: implications for cell death. *Annu. Rev. Pharmacol. Toxicol.* **47**,

143-83.

Oswald, I. P., Gazzinelli, R. T., Sher, A., and James, S. L. (1992). IL-10 synergizes with IL-4 and transforming growth factor-beta to inhibit macrophage cytotoxic activity. *J Immunol* **148**, 3578-82.

Ott, M., Gogvadze, V., Orrenius, S., and Zhivotovsky, B. (2007a). Mitochondria, oxidative stress and cell death. *Apoptosis* **12**, 913-22.

Ott, M., Norberg, E., Walter, K. M., Schreiner, P., Kemper, C., Rapaport, D., Zhivotovsky, B., and Orrenius, S. (2007b). The mitochondrial TOM complex is required for tBid/Bax-induced cytochrome c release. *J. Biol. Chem.* **282**, 27633-9.

Ott, M., Robertson, J. D., Gogvadze, V., Zhivotovsky, B., and Orrenius, S. (2002). Cytochrome c release from mitochondria proceeds by a two-step process. *Proc. Natl. Acad. Sci. U.S.A.* **99**, 1259-63.

Pastorino, J. G., Hoek, J. B., and Shulga, N. (2005). Activation of glycogen synthase kinase 3beta disrupts the binding of hexokinase II to mitochondria by phosphorylating voltage-dependent anion channel and potentiates chemotherapy-induced cytotoxicity. *Cancer Res.* **65**, 10545-54.

Polson, J., and Lee, W. M. (2005). AASLD position paper: the management of acute liver failure. *Hepatology* **41**, 1179-97.

Polster, B. M., Basanez, G., Etxebarria, A., Hardwick, J. M., and Nicholls, D. G. (2005). Calpain I induces cleavage and release of apoptosis-inducing factor from isolated mitochondria. *J. Biol. Chem.* **280**, 6447-54.

Prescott, L. F., Park, J., Ballantyne, A., Adriaenssens, P., and Proudfoot, A. T. (1977). Treatment of paracetamol (acetaminophen) poisoning with N-acetylcysteine. *Lancet* **2**, 432-4.

Pumford, N. R., Roberts, D. W., Benson, R. W., and Hinson, J. A. (1990). Immunochemical quantitation of 3-(cystein-S-yl)acetaminophen protein adducts in subcellular liver fractions following a hepatotoxic dose of acetaminophen. *Biochem. Pharmacol.* **40**, 573-9.

Qiu, Y., Benet, L. Z., and Burlingame, A. L. (1998). Identification of the hepatic protein targets of reactive metabolites of acetaminophen in vivo in mice using two-dimensional gel electrophoresis and mass spectrometry. *J. Biol. Chem.* **273**, 17940-53.

Qiu, Y., Benet, L. Z., and Burlingame, A. L. (2001). Identification of hepatic protein targets of the reactive metabolites of the non-hepatotoxic regioisomer of acetaminophen, 3'-hydroxyacetanilide, in the mouse in vivo using two-dimensional gel electrophoresis and mass spectrometry. *Adv. Exp. Med. Biol.* **500**, 663-73.

Ramaiah, S. K., and Jaeschke, H. (2007). Role of neutrophils in the pathogenesis of acute inflammatory liver injury. *Toxicol Pathol* **35**, 757-66.

Ramsay, R. R., Rashed, M. S., and Nelson, S. D. (1989). In vitro effects of acetaminophen metabolites and analogs on the respiration of mouse liver mitochondria. *Arch. Biochem. Biophys.* **273**, 449-57.

Ranger, A. M., Malynn, B. A., and Korsmeyer, S. J. (2001). Mouse models of cell death. *Nat. Genet.* **28**, 113-8.

Ray, S. D., Balasubramanian, G., Bagchi, D., and Reddy, C. S. (2001). Ca(2+)-calmodulin antagonist chlorpromazine and poly(ADP-ribose) polymerase modulators 4-aminobenzamide and nicotinamide influence hepatic expression of BCL-XL and P53 and protect against acetaminophen-induced programmed and unprogrammed cell death in mice. *Free Radic. Biol. Med.* **31**, 277-91.

Ray, S. D., Kamendulis, L. M., Gurule, M. W., Yorkin, R. D., and Corcoran, G. B. (1993). Ca2+ antagonists inhibit DNA fragmentation and toxic cell death induced by acetaminophen. *Faseb J* **7**, 453-63.

Ray, S. D., Sorge, C. L., Raucy, J. L., and Corcoran, G. B. (1990). Early loss of large genomic DNA in vivo with accumulation of Ca2+ in the nucleus during acetaminophen-induced liver injury. *Toxicol. Appl. Pharmacol.***106**, 346-51.

Resnick, L., and Fennell, M. (2004). Targeting JNK3 for the treatment of neurodegenerative disorders. *Drug Discov. Today* **9**, 932-9.

Riddick, D. S., Lee, C., Bhathena, A., Timsit, Y. E., Cheng, P. Y., Morgan, E. T., Prough, R. A., Ripp, S. L., Miller, K. K., Jahan, A., and Chiang, J. Y. (2004). Transcriptional suppression of cytochrome P450 genes by endogenous and exogenous chemicals. *Drug Metab. Dispos.* **32**, 367-75.

Roberts, D. W., Pumford, N. R., Potter, D. W., Benson, R. W., and Hinson, J. A. (1987). A sensitive immunochemical assay for acetaminophen-protein adducts. *J. Pharmacol. Exp. Ther.* **241**, 527-33.

Rofe, A. M., Barry, E. F., Shelton, T. L., Philcox, J. C., and Coyle, P. (1998). Paracetamol hepatotoxicity in metallothionein-null mice. *Toxicology* **125**, 131-40.

Sabapathy, K., Hochedlinger, K., Nam, S. Y., Bauer, A., Karin, M., and Wagner, E. F. (2004). Distinct roles for JNK1 and JNK2 in regulating JNK activity and c-Jun-dependent cell proliferation. *Mol. Cell* **15**, 713-25.

Saha, B., and Nandi, D. (2009). Farnesyltransferase inhibitors reduce Ras activation and ameliorate acetaminophen-induced liver injury in mice. *Hepatology* **50**, 1547-57.

Saito, C., Yan, H. M., Artigues, A., Villar, M. T., Farhood, A., and Jaeschke, H. Mechanism of protection by metallothionein against acetaminophen hepatotoxicity. *Toxicol. Appl. Pharmacol.* **242**, 182-90.

Saito, C., Zwingmann, C., and Jaeschke, H. (2009). Novel mechanisms of protection against acetaminophen hepatotoxicity in mice by glutathione and N-acetylcysteine. *Hepatology* **51**, 246-54.

Salhanick, S. D., Orlow, D., Holt, D. E., Pavlides, S., Reenstra, W., and Buras, J. A. (2006). Endothelially derived nitric oxide affects the severity of early acetaminophen-induced hepatic injury in mice. *Acad Emerg Med* **13**, 479-85.

Salminen, W. F., Jr., Voellmy, R., and Roberts, S. M. (1998). Effect of N-acetylcysteine on heat shock protein induction by acetaminophen in mouse liver. *J. Pharmacol. Exp. Ther.* **286**, 519-24.

Salvi, M., Battaglia, V., Brunati, A. M., La Rocca, N., Tibaldi, E., Pietrangeli, P., Marcocci, L., Mondovi, B., Rossi, C. A., and Toninello, A. (2007). Catalase takes part in rat liver mitochondria oxidative stress defense. *J. Biol. Chem.* **282**, 24407-15.

Sato, M., and Bremner, I. (1993). Oxygen free radicals and metallothionein. *Free Radic. Biol. Med.* **14**, 325-37.

Schroeter, H., Boyd, C. S., Ahmed, R., Spencer, J. P., Duncan, R. F., Rice-Evans, C., and Cadenas, E. (2003). c-Jun N-terminal kinase (JNK)-mediated modulation of brain mitochondria function: new target proteins for JNK signalling in mitochondrion-dependent apoptosis. *Biochem. J.* **372**, 359-69.

Shen, W., Kamendulis, L. M., Ray, S. D., and Corcoran, G. B. (1991). Acetaminophen-induced cytotoxicity in cultured mouse hepatocytes: correlation of nuclear Ca2+ accumulation and early DNA fragmentation with cell death. *Toxicol. Appl. Pharmacol.* **111**, 242-54.

Shen, W., Kamendulis, L. M., Ray, S. D., and Corcoran, G. B. (1992). Acetaminophen-induced cytotoxicity in cultured mouse hepatocytes: effects of Ca(2+)-endonuclease, DNA repair, and glutathione depletion inhibitors on DNA fragmentation and cell death. *Toxicol. Appl. Pharmacol.* **112**, 32-40.

Shimizu, S., Narita, M., and Tsujimoto, Y. (1999). Bcl-2 family proteins regulate the release of apoptogenic cytochrome c by the mitochondrial channel VDAC. *Nature* **399**, 483-7.

Shiraishi, N., Aono, K., and Utsumi, K. (1983). Increased metallothionein content in rat liver induced by X irradiation and exposure to high oxygen tension. *Radiat. Res.* **95**, 298-302.

Sies, H., Sharov, V. S., Klotz, L. O., and Briviba, K. (1997). Glutathione peroxidase protects against peroxynitrite-mediated oxidations. A new function for selenoproteins as peroxynitrite reductase. *J. Biol. Chem*. **272**, 27812-7.

Simpson, K. J., Lukacs, N. W., McGregor, A. H., Harrison, D. J., Strieter, R. M., and Kunkel, S. L. (2000). Inhibition of tumour necrosis factor alpha does not prevent experimental paracetamol-induced hepatic necrosis. *J. Pathol.* **190**, 489-94.

Slot, J. W., Geuze, H. J., Freeman, B. A., and Crapo, J. D. (1986). Intracellular localization of the copper-zinc and manganese superoxide dismutases in rat liver parenchymal cells. *Lab. Invest.* **55**, 363-71.

Smilkstein, M. J., Knapp, G. L., Kulig, K. W., and Rumack, B. H. (1988). Efficacy of oral N-acetylcysteine in the treatment of acetaminophen overdose. Analysis of the national multicenter study (1976 to 1985). *N. Engl. J. Med.* **319**, 1557-62.

Squadrito, G. L., and Pryor, W. A. (1998). Oxidative chemistry of nitric oxide: the roles of superoxide, peroxynitrite, and carbon dioxide. *Free Radic. Biol. Med.* **25**, 392-403.

Susin, S. A., Lorenzo, H. K., Zamzami, N., Marzo, I., Snow, B. E., Brothers, G. M., Mangion, J., Jacotot, E., Costantini, P., Loeffler, M., Larochette, N., Goodlett, D. R., Aebersold, R., Siderovski, D. P., Penninger, J. M., and

Kroemer, G. (1999). Molecular characterization of mitochondrial apoptosis-inducing factor. *Nature* **397**, 441-6.

Szabo, C., and Dawson, V. L. (1998). Role of poly(ADP-ribose) synthetase in inflammation and ischaemia-reperfusion. T*rends Pharmacol. Sci.* **19**, 287-98.

Szymanska, J. A., Swietlicka, E. A., and Piotrowski, J. K. (1991). Protective effect of zinc in the hepatotoxicity of bromobenzene and acetaminophen. *Toxicology* **66**, 81-91.

Takada, H., Mawet, E., Shiratori, Y., Hikiba, Y., Nakata, R., Yoshida, H., Okano, K., Kamii, K., and Omata, M. (1995). Chemotactic factors released from hepatocytes exposed to acetaminophen. *Dig. Dis. Sci.* **40**, 1831-6.

Takamura, M., Matsuda, Y., Yamagiwa, S., Tamura, Y., Honda, Y., Suzuki, K., Ichida, T., and Aoyagi, Y. (2007). An inhibitor of c-Jun NH2-terminal kinase, SP600125, protects mice from D-galactosamine/lipopolysaccharide-induced hepatic failure by modulating BH3-only proteins. *Life Sci.* **80**, 1335-44.

Thornalley, P. J., and Vasak, M. (1985). Possible role for metallothionein in protection against radiation-induced oxidative stress. Kinetics and mechanism of its reaction with superoxide and hydroxyl radicals. *Biochim. Biophys. Acta* **827**, 36-44.

Tirmenstein, M. A., and Nelson, S. D. (1989). Subcellular binding and effects on calcium homeostasis produced by acetaminophen and a nonhepatotoxic regioisomer, 3'-hydroxyacetanilide, in mouse liver. *J. Biol. Chem.* **264**, 9814-9.

Tirmenstein, M. A., and Nelson, S. D. (1990). Acetaminophen-induced oxidation of protein thiols. Contribution of impaired thiol-metabolizing enzymes and the breakdown of adenine nucleotides. *J. Biol. Chem.* **265**, 3059-65.

Tolson, J. K., Dix, D. J., Voellmy, R. W., and Roberts, S. M. (2006). Increased hepatotoxicity of acetaminophen in Hsp70i knockout mice. *Toxicol. Appl. Pharmacol.* **210**, 157-62.

Trendelenburg, G. (2008). Acute neurodegeneration and the inflammasome: central processor for danger signals and the inflammatory response? *J Cereb Blood Flow Metab* **28**, 867-81.

Tsokos-Kuhn, J. O., Hughes, H., Smith, C. V., and Mitchell, J. R. (1988). Alkylation of the liver plasma membrane and inhibition of the Ca2+ ATPase by

acetaminophen. *Biochem. Pharmacol. Biochemical pharmacology* **37**, 125-31.

Uchiyama, A., Kim, J. S., Kon, K., Jaeschke, H., Ikejima, K., Watanabe, S., and Lemasters, J. J. (2008). Translocation of iron from lysosomes into mitochondria is a key event during oxidative stress-induced hepatocellular injury. *Hepatology* **48**, 1644-54.

Vandenabeele, P., Declercq, W., Beyaert, R., and Fiers, W. (1995). Two tumour necrosis factor receptors: structure and function. *Trends Cell Biol.* **5**, 392-9.

Vercesi, A. E. (1987). The participation of NADP, the transmembrane potential and the energy-linked NAD(P) transhydrogenase in the process of Ca2+ efflux from rat liver mitochondria. *Arch. Biochem. Biophys.* **252**, 171-8.

Vieira, H. L., Belzacq, A. S., Haouzi, D., Bernassola, F., Cohen, I., Jacotot, E., Ferri, K. F., El Hamel, C., Bartle, L. M., Melino, G., Brenner, C., Goldmacher, V., and Kroemer, G. (2001). The adenine nucleotide translocator: a target of nitric oxide, peroxynitrite, and 4-hydroxynonenal. *Oncogene* **20**, 4305-16.

Virag, L., and Szabo, C. (2002). The therapeutic potential of poly(ADP-ribose) polymerase inhibitors. *Pharmacol. Rev.* **54**, 375-429.

Waldmeier, P. C., Zimmermann, K., Qian, T., Tintelnot-Blomley, M., and Lemasters, J. J. (2003). Cyclophilin D as a drug target. *Curr. Med. Chem.* **10**, 1485-506.

Wang, X. (2001). The expanding role of mitochondria in apoptosis. *Genes Dev.* **15**, 2922-33.

Wang, Y., Singh, R., Lefkowitch, J. H., Rigoli, R. M., and Czaja, M. J. (2006). Tumor necrosis factor-induced toxic liver injury results from JNK2-dependent activation of caspase-8 and the mitochondrial death pathway. *J. Biol. Chem.* **281**, 15258-67.

Wendel, A., and Feuerstein, S. (1981). Drug-induced lipid peroxidation in mice--I. Modulation by monooxygenase activity, glutathione and selenium status. *Biochem. Pharmacol.* **30**, 2513-20.

Wendel, A., Feuerstein, S., and Konz, K. H. (1979). Acute paracetamol intoxication of starved mice leads to lipid peroxidation in vivo. *Biochem. Pharmacol.* **28**, 2051-5.

Wendel, A., and Jaeschke, H. (1982). Drug-induced lipid peroxidation in mice--III. Glutathione content of liver, kidney and spleen after intravenous administration of free and liposomally entrapped glutathione. *Biochem. Pharmacol.* **31**, 3607-11.

Whitehouse, L. W., Wong, L. T., Paul, C. J., Pakuts, A., and Solomonraj, G. (1985). Postabsorption antidotal effects of N-acetylcysteine on acetaminophen-induced hepatotoxicity in the mouse. *Can. J. Physiol. Pharmacol.* **63**, 431-7.

Whyte, A. J., Kehrl, T., Brooks, D. E., Katz, K. D., and Sokolowski, D. (2008). Safety and Effectiveness of Acetadote for Acetaminophen Toxicity. *J Emerg Me*d [Epub ahead of print]

Wicovsky, A., Muller, N., Daryab, N., Marienfeld, R., Kneitz, C., Kavuri, S., Leverkus, M., Baumann, B., and Wajant, H. (2007). Sustained JNK activation in response to tumor necrosis factor is mediated by caspases in a cell type-specific manner. *J. Biol. Chem.* **282**, 2174-83.

Widlak, P., Li, L. Y., Wang, X., and Garrard, W. T. (2001). Action of recombinant human apoptotic endonuclease G on naked DNA and chromatin substrates: cooperation with exonuclease and DNase I. *J. Biol. Chem.* **276**, 48404-9.

Woodfield, K., Ruck, A., Brdiczka, D., and Halestrap, A. P. (1998). Direct demonstration of a specific interaction between cyclophilin-D and the adenine nucleotide translocase confirms their role in the mitochondrial permeability transition. *Biochem. J.* **336 (Pt 2)**, 287-90.

Xiong, H., Turner, K. C., Ward, E. S., Jansen, P. L., and Brouwer, K. L. (2000). Altered hepatobiliary disposition of acetaminophen glucuronide in isolated perfused livers from multidrug resistance-associated protein 2-deficient TR(-) rats. *J. Pharmacol. Exp. Ther.* **295**, 512-8.

Yang, E., and Korsmeyer, S. J. (1996). Molecular thanatopsis: a discourse on the BCL2 family and cell death. *Blood* **88**, 386-401.

Yee, S. B., Bourdi, M., Masson, M. J., and Pohl, L. R. (2007). Hepatoprotective role of endogenous interleukin-13 in a murine model of acetaminophen-induced liver disease. *Chem. Res. Toxicol.* **20**, 734-44.

Yohe, H. C., O'Hara, K. A., Hunt, J. A., Kitzmiller, T. J., Wood, S. G., Bement, J.

L., Bement, W. J., Szakacs, J. G., Wrighton, S. A., Jacobs, J. M., Kostrubsky, V., Sinclair, P. R., and Sinclair, J. F. (2006). Involvement of Toll-like receptor 4 in acetaminophen hepatotoxicity. *Am. J. Physiol.* **290**, G1269-79.

Zago, E. B., Castilho, R. F., and Vercesi, A. E. (2000). The redox state of endogenous pyridine nucleotides can determine both the degree of mitochondrial oxidative stress and the solute selectivity of the permeability transition pore. *FEBS Lett.* **478**, 29-33.

Zaid, H., Abu-Hamad, S., Israelson, A., Nathan, I., and Shoshan-Barmatz, V. (2005). The voltage-dependent anion channel-1 modulates apoptotic cell death. *Cell Death Differ.* **12**, 751-60.

Zamek-Gliszczynski, M. J., Hoffmaster, K. A., Tian, X., Zhao, R., Polli, J. W., Humphreys, J. E., Webster, L. O., Bridges, A. S., Kalvass, J. C., and Brouwer, K. L. (2005). Multiple mechanisms are involved in the biliary excretion of acetaminophen sulfate in the rat: role of Mrp2 and Bcrp1. *Drug Metab. Dispos.* **33**, 1158-65.

Zamzami, N., El Hamel, C., Maisse, C., Brenner, C., Munoz-Pinedo, C., Belzacq, A. S., Costantini, P., Vieira, H., Loeffler, M., Molle, G., and Kroemer, G. (2000). Bid acts on the permeability transition pore complex to induce apoptosis. *Oncogene* **19**, 6342-50.

Zamzami, N., and Kroemer, G. (2001). The mitochondrion in apoptosis: how Pandora's box opens. *Nat. Rev.* **2**, 67-71.

Zhang, C., Walker, L. M., Hinson, J. A., and Mayeux, P. R. (2000a). Oxidant stress in rat liver after lipopolysaccharide administration: effect of inducible nitric-oxide synthase inhibition. *J. Pharmacol. Exp. Ther.* **293**, 968-72.

Zhang, H., Cook, J., Nickel, J., Yu, R., Stecker, K., Myers, K., and Dean, N. M. (2000b). Reduction of liver Fas expression by an antisense oligonucleotide protects mice from fulminant hepatitis. *Nat. Biotechnol.* **18**, 862-7.

Zhong, Q., Putt, D. A., Xu, F., and Lash, L. H. (2008). Hepatic mitochondrial transport of glutathione: studies in isolated rat liver mitochondria and H4IIE rat hepatoma cells. *Arch. Biochem. Biophys.* **474**, 119-27.

Zhou, C., Tabb, M. M., Nelson, E. L., Grun, F., Verma, S., Sadatrafiei, A., Lin, M., Mallick, S., Forman, B. M., Thummel, K. E., and Blumberg, B. (2006). Mutual repression between steroid and xenobiotic receptor and NF-kappaB signaling pathways links xenobiotic metabolism and inflammation. J*. Clin.*

Invest. **116**, 2280-2289.

Zhou, Z., Wang, L., Song, Z., Saari, J. T., McClain, C. J., and Kang, Y. J. (2005). Zinc supplementation prevents alcoholic liver injury in mice through attenuation of oxidative stress. *Am. J. Pathol.* **166**, 1681-90.

Zwingmann, C., and Bilodeau, M. (2006). Metabolic insights into the hepatoprotective role of N-acetylcysteine in mouse liver. *Hepatology* **43**, 454-63.